RADC-TR-62-54
ASTIA DOCUMENT No.

10 DECEMBER 1961

TECHNICAL REPORT

THEORETICAL AND EXPERIMENTAL INVESTIGATION TO DETERMINE THE MICROWAVE CHARACTERISTICS AND APPLICATIONS OF HEXAGONAL MAGNETIC OXIDES TO MICROWAVE CIRCUITRY

Prepared by: G. P. Rodrigue

Approved by: J. E. Pippin

SPERRY MICROWAVE ELECTRONICS COMPANY
DIVISION OF SPERRY RAND CORPORATION
CLEARWATER, FLORIDA

SPERRY REPORT No. SJ220-00012A-8

CONTRACT No. AF30(602)2330

prepared for

ROME AIR DEVELOPMENT CENTER
AIR FORCE SYSTEMS COMMAND
UNITED STATES AIR FORCE

GRIFFISS AIR FORCE BASE
NEW YORK

COPY No. ____

RADC-TR-62-54
ASTIA DOCUMENT No.

10 DECEMBER 1961

TECHNICAL REPORT

THEORETICAL AND EXPERIMENTAL INVESTIGATION TO DETERMINE THE MICROWAVE CHARACTERISTICS AND APPLICATIONS OF HEXAGONAL MAGNETIC OXIDES TO MICROWAVE CIRCUITRY

Prepared by: G. P. Rodrigue

Approved by: J. E. Pippin

SPERRY MICROWAVE ELECTRONICS COMPANY
DIVISION OF SPERRY RAND CORPORATION
CLEARWATER, FLORIDA

SPERRY REPORT No. SJ220-00012A-8

CONTRACT No. AF30(602)2330

PROJECT No. 5578

TASK No. 557801

prepared for

ROME AIR DEVELOPMENT CENTER
AIR FORCE SYSTEMS COMMAND
UNITED STATES AIR FORCE

GRIFFISS AIR FORCE BASE
NEW YORK

COPY No. 2

FOREWORD

1. This program was initiated in an attempt to exploit the unique properties of hexagonal magnetic oxides in microwave devices. Specifically, the objective was to investigate and study the characteristics and applications of the above materials and to accumulate data to obtain a comprehensive set of curves for such components as reciprocal and non-reciprocal phase shifters, isolators and circulators in the microwave region of the spectrum.

2. The approaches taken by the Contractor toward fulfilling the above objective were (1) a materials preparation phase, (2) materials evaluation phase and (3) a device feasibility study phase.

3, Under the first two phases, ceramic samples of nine different planar compounds (Me_2X and Me_2Y), consisting of twenty-seven compositions, were prepared and measured at 25 Kmc and 37.5 Kmc. Initial attention was given to the optimum preparation of nonoriented samples and was primarily concerned with obtaining the firing curves (i. e. density vs firing temperature) for these materials. Eight different compositions of the $(Ni_{1-x}Co_x)_2W$ compounds were prepared as oriented uniaxial materials, where $0.0 \leq x \leq 0.50$. By varying the cobalt content of these materials the effective anisotropy (internal) field can be accurately controlled over a range of 0 to 12,700 oersteds. The measured linewidth was found to be independent of cobalt content but dependent on the degree of crystallite orientation. Optimum alignment exhibited linewidths of 1500 to 1800 oersteds and it was found to improve with grain growth in the sintering process and with the reduction of particle size. Resonance measurements were conducted as a function of temperature from 23 °C to 125 °C. The observed data indicates that as a function of temperature the (1) anisotropy field increases almost linearly, (2) the linewidths are essentially constant and (3) the effective g-factor (Lande' splitting factor) increases and approaches 2.0 near 125° C. Further, the positive slope of the anisotrophy field vs temperature increases with increasing cobalt content of the material.

4. The third phase involved the evaluation of the uniaxial materials in actual device configurations to determine the suitability to practical applications. Appropriate members of the nickel-cobalt W series were evaluated in K and V-band resonance isolators. An optimum K-band isolator was fabricated utilizing a 25% cobalt content having an anisotropy field of 7000 oersteds and an external applied field of 1000 oersteds. It produced a maximum

isolation ratio of 35/1 at a frequency of 23 Kmc and a ratio of 10/1 over a 25% bandwidth. A 10% cobalt content with an anisotropy field of 11,000 oersteds and an applied field of 1000 oersteds was used to fabricate a V-band isolator. This item produced an isolation ratio of 18/1 at a frequency of 36.5 Kmc and a ratio of 10/1 over a 10% bandwidth.

5. This program has demonstrated the feasibility of utilizing hexagonal materials to microwave circuitry and it is worthy to note that the first two isolators mentioned above used the same external fields with different material compositions. In addition, it was possible to obtain isolator operation with no externally applied magnetic field. This device has a maximum isolation ratio of 30/1.5 at 37.5 Kmc with a 10 to 1 bandwidth of 2.2 Kmc.

JOSEPH M. SCHENNA
RADC Project Engineer

ABSTRACT

This final report completes a sixteen month study program on Air Force Contract No. AF30 (602)-2330. The contract period began July, 1960, and four Quarterly Reports have been issued. The work consisted of theoretical and experimental investigation of the properties of hexagonal magnetic oxides and of their application to specific microwave devices.

The work was carried out in the three overlapping phases outlined below.

Preparation of Materials

A procedure was developed for the preparation of good, high density, ceramic samples of nine different Me_2Z and Me_2Y compounds and a series of $(Ni_{1-x}Co_x)_2W$ materials. The Co_2Z, Ni_2Z, Zn_2Z, Mg_2Z, Cu_2Z, Co_2Y, Ni_2Y, Zn_2Y, and Mg_2Y were prepared in unoriented form. The $(Ni_{1-x}Co_x)_2W$ compounds with x = 0.0, 0.05, 0.10, 0.20, 0.25, 0.30, 0.40 and 0.50 were prepared as oriented uniaxial materials. Studies of the degree of orientation of the materials were carried out using x-ray diffraction techniques. It was found that by reducing the particle size of the pressed material the alignment could be improved. Alignment also improved with grain growth in the sintering stage.

Evaluation of Materials

The samples prepared in the laboratory were subjected to both static and microwave evaluation. By varying the cobalt content of the $(Ni_{1-x}Co_x)_2W$ materials the effective anisotropy field of these materials could be accurately controlled over a range of 0 to 12,700 oe. The measured linewidth was found to be independent of cobalt content over this range of substitutions. A strong dependence of linewidth on degree of orientation was noted. Best aligned samples exhibited linewidths in the 1500 oe to 1800 oe range. The temperature dependence of the anisotropy field, linewidth, and effective g-factor of the nickel-cobalt W materials was also studied.

Application of Materials

Appropriate members of the nickel-cobalt W series were evaluated in K- and V-band resonance isolators. At K-band frequencies the twenty-five per cent cobalt substituted nickel W compound with an anisotropy field of 7000 oe was used. A slab of material magnetized in its plane and mounted on a dielectric slab produced a maximum isolation ratio of 35/1 at a frequency of 23 kmc with an applied field of less than 1000 oe supplied by small ceramic magnets. The ten to one bandwidth was greater than 6 kmc, or about a 25 per cent bandwidth.

A ten per cent cobalt substituted nickel W compound with an anisotropy field of approximately 11,000 oe was used in fabricating a V-band resonance isolator. The dielectric loaded configuration

produced maximum isolation ratios of 18 to 1 with 1000 oe applied. A V-band resonance isolator using isotropic ferrite would require on the order of 12,000 oe. This device had a ten to one bandwidth of 3.5 kmc centered at 38.2 kmc.

These and other results of the applications study clearly demonstrate the usefulness of these uniaxial materials with controlled anisotropies in practical devices.

TABLE OF CONTENTS

TABLE OF CONTENTS (Cont'd)

LIST OF ILLUSTRATIONS

LIST OF ILLUSTRATIONS (Cont'd)

LIST OF ILLUSTRATIONS (Cont'd)

LIST OF ILLUSTRATIONS (Cont'd)

LIST OF ILLUSTRATIONS (Cont'd)

LIST OF TABLES

SECTION I

INTRODUCTION

1. PURPOSE OF PROGRAM

1.1 Program Objective

The purpose of this program is to investigate the microwave properties of hexagonal magnetic oxides and to determine their applicability to specific microwave devices.

1.2 Classes of Microwave Devices

The program was initiated with four classes of possible microwave devices utilizing hexagonal materials in view.

1. First there are resonance isolators, phase shifters, and other devices which utilize H_{an} in conjunction with an external magnet to achieve operation. Included are devices which have reduced magnet sizes at ordinary microwave frequencies, millimeter wave ferrite components of all types (perhaps up to 100 kmc/s), and both variable and non-variable devices.

2. Secondly, there are similar devices (except that they are non-variable) which utilize H_{an} to achieve operation without any external magnet. These are placed in a separate category because the materials requirements would be different from those of (1).

3. Thirdly, there are non-variable devices utilizing initial permeability phenomena in both oriented and non-oriented materials. These include antenna rods, harmonic suppressors, and the like. Some devices could be classed in either of the three categories mentioned up to now, depending on their design.

4. Fourthly, there are variable devices, such as phase shifters for antenna arrays, which utilize initial permeability phenomena.

2. SCOPE OF PROGRAM

The program was carried out in three overlapping phases: a materials preparation phase, a materials evaluation phase, and a device feasiblity study phase. The scope of each of these phases is summarized below.

2.1 Materials Preparation

This phase involved the study of the many variables in the ceramic process which must be properly controlled if good ceramic materials are to be obtained. Greatest emphasis was placed on materials with uniaxial anisotropy fields that were controllable over a range of zero to 12,700 oe.

2.2 Materials Evaluation

This phase was concerned primarily with the ferromagnetic resonance studies of these materials to determine their effective anisotropy fields, linewidths, effective g-factors, etc. Also included however are measurements of magnetization curves, degree of alignment, and other measurements aimed at determining the overall material quality.

2.3 Device Feasibility

In this phase materials produced in the laboratory were evaluated in actual device configurations to determine the suitability of various materials to practical applications. These measurements also provided feed-back information as to what improvements were desirable

in materials preparation. Practical devices belonging to each of the first two classes mentioned above were developed during the course of this program.

3. GENERAL BACKGROUND

Highly anisotropic barium ferrite [1] ($BaO \cdot 6Fe_2O_3$) with hexagonal crystal structure has been used for a number of years as a permanent magnet material. Modifications of this compound have appeared under several different trade names.

More recently the anisotropy fields of the barium and strontium ferrite systems have been varied over a range of roughly 17 kilo-oersteds to 40 kilo-oersteds by the substitution of aluminum for iron. [2] This substitution raises the anisotropy field by lowering the saturation magnetization and with a simultaneous reduction in Curie temperature.

In still more recent work the anisotropy field of barium ferrite has been reduced to approximately 15.0, 11.5, and 7.0 kilo-oersteds by the simultaneous substitution of titanium and cobalt for iron. [3, 4] Some of the work on the titanium and cobalt substitutions was done concurrently with the work of this program.

The materials studied under this program are members of three different crystal classes [5] first reported in 1956 and discussed in Subsection B.2. Through proper synthesis of these materials it is possible to obtain any desired value of anisotropy field from 0 to 12.7 kilo-oersteds. Thus the frequency range of application of these materials can be greatly extended.

Substituted barium ferrite materials have been used in fabricating millimeter wave devices requiring minimum externally applied fields.[6] As a result of the present effort, wherein continuous control of the anisotropy field is achieved, application of oriented hexagonal materials is extended to a wider range of frequencies.

SECTION II

GENERAL DISCUSSION

1. HEXAGONAL MATERIALS

All magnetic materials exhibit some degree of magnetocrystalline anisotropy. That is, within individual crystallites of any magnetic material there is a tendency for the magnetic moment vector of the material to be aligned along some particular crystallographic direction. This magnetocrystalline anisotropy energy originates in the coupling between unbalanced electron spins (that give rise to magnetism) and the neighboring ions that make up the crystal lattice. The anisotropy energy of a material always reflects the symmetry of the crystal lattice of the material and can be expressed (for a material with a hexagonal crystal structure) as:

$$f_k = K_1 \sin^2\theta + K_2 \sin^4\theta + \ldots . \qquad (1)$$

where K_1 and K_2 are the first and second order anisotropy constants respectively. Within each single crystal this anisotropy energy exerts a torque on the magnetization tending to align it along some particular crystallographic direction. For convenience this anisotropy energy is often spoken of in terms of an effective anisotropy field defined to have the magnitude and direction required to exert the same torque on the magnetization as is exerted by the anisotropy energy.

While all magnetic materials exhibit magnetocrystalline anisotropy, in the generally encountered case ferromagnetic materials appear to be

quite isotropic. This apparent isotropy arises from the fact that ordinary ferrites and other magnetic oxides are commonly in unoriented polycrystalline form. That is, the materials consist of many thousands of tiny single crystals, called crystallites, randomly oriented with respect to one another. Although each crystallite has an effective anisotropy field located along a preferred direction, the random orientation of crystallites causes the whole polycrystalline sample to be isotropic, i.e., there is no preferred direction for the sample as a whole and no net anisotropy. The possibility of using the anisotropy field to advantage is normally lost in a polycrystal because of the random orientation of crystallites. However, if the individual crystallites were oriented in a polycrystalline material so that the axes of individual crystallites were all parallel, there would be a preferred direction, with its attendant anisotropy field for the polycrystalline material.

In hexagonal materials this effective anisotropy field is generally quite large. While not actually a magnetic field, the action of the effective anisotropy field is, under certain conditions, indistinguishable from an external applied field. This anisotropy field can therefore be used to advantage in augmenting or completely replacing externally applied fields.

In hexagonal materials three different forms of anisotropy can exist.[7] In the first case, called uniaxial, the preferred orientation of magnetization is along the c-axis of the crystal. In this case K_1 is

positive and dominant over K_2. In the second case, called planar, the preferred direction of magnetization is in the basal plane of the crystal. In this case, K_1 is negative and greater than K_2. The third case is that in which the preferred direction of magnetization is in a cone about the c-axis. This third condition occurs when $0 < -K_1 < 2K_2$.

In the first case the anisotropy field is defined as $H_{an} = 2K_1/M_s$ and is directed along the c-axis of the crystal. In the second case the direction of H_{an} is in the basal plane, and the field has a magnitude of $H_{an} = -2(K_1 + 2K_2)/M_s$. For the intermediate case H_{an} is at angle θ with respect to the c-axis where $\sin\theta = \sqrt{\frac{-K_1}{2K_2}}$, and $H_{an} = 2(\frac{K_1}{K_2})(K_1 + 2K_2)/M_s$. The last case occurs only rarely and then only over a fairly narrow temperature range. The third case is therefore not of primary interest in this study. Chief interest is found in the uniaxial and planar materials. The two chief types of hexagonal materials, uniaxial and planar, each have their own unique advantages and possible fields of application.

1.1 Uniaxial Hexagonal Materials

Uniaxial materials with a large anisotropy field acting along the c-axis of the crystal are potentially useful in the first two classes of devices listed in Section I. In the first class of devices the internal anisotropy field augment an external field applied along the c-axis of the material(either single crystal or oriented polycrystal) and thus

greatly reduces the applied field required for operation. In the case of a properly oriented uniaxial material with spherical geometry the equation for ferromagnetic resonance is:

$$\omega_o = \gamma (H_{ap} + H_{an}) \qquad (2)$$

where

γ is the gyromagnetic ratio,

H_{ap} is the external applied field,

H_{an} is the effective anisotropy field.

Equation 2 shows that the applied field required for resonance at a given frequency is reduced by just the anisotropy field. Clearly if H_{an} is large enough, the applied field required for resonance can be made very small. If proper control of H_{an} could be achieved, then resonance isolators, phase shifters, etc., could be made at any desired frequency with only minimal external fields required.

Equation 2 is quantitatively accurate only in the case of a spherically shaped sample. For a practical device using a ferrite slab or rod, this equation would be modified by the effective demagnetizing factors appropriate to the particular geometry.

The discussion thus far holds for so called "soft" magnetic materials with low remanent magnetization and low coercive force. For the applications of Class I devices, and in particular for variable

devices, these would be the type material desired.

For applications involving non-variable devices as discussed in Class 2, "hard" magnetic materials would be needed. These are permanent magnetic materials having large remanent magnetizations and coercive forces and essentially square hysteresis loops. Large values of anisotropy energy are a prerequisite for permanent magnet materials. As will be pointed out later, however, the quality of a highly anisotropic material as a permanent magnet, and therefore its applicability to Class 2 devices, is determined principally by the method of preparation, resultant particle size, and the like.

It is important then in selecting materials for Class 2 applications that one precisely control not only the chemical composition but also the many steps in the preparation process.

1.2 Planar Materials

Planar materials are those whose preferred direction of magnetization is in the basal plane perpendicular to the c-axis of the crystal. In single crystal or oriented planar material the anisotropy field of these compounds can also be used to augment the field required for resonance. While in these materials the applied field is not reduced by the full value of the anisotropy field, the resonance condition for spherical samples does become:

$$\omega_{res} = \bar{\gamma}\sqrt{H_{ap}\,(H_{ap} + H_{an})} \qquad (3)$$

where terms are as defined for equation (2). Obviously some reduction in applied field does take place. The following table[8] shows the reduction in applied field achieved by substituting planar materials with a given value of H_{an} for isotropic ferrites.

TABLE 1

Comparison of Fields Required for Resonance of Planar and Isotropic Ferrites

Frequency	Field for Resonance		H_{an}
	Isotropic	Planar	
mc	oe	oe	oe
3,000	1,070	230	5,000
5,000	1,780	580	5,000
10,000	3,580	1,800	5,000
5,000	1,780	330	10,000
10,000	3,580	1,100	10,000
20,000	7,160	3,700	10,000

The presence of a preferred plane of magnetization in these materials gives rise to one of their most distinctive characteristics - an initial permeability that remains essentially constant up to frequencies as high as 1000 to 2000 Mc/s. This feature makes them attractive for applications based on high magnetic Q and permeability, e. g. variable UHF, and possibly L-band, phase shifters.

Planar materials might also prove useful in harmonic generation because of the basic asymmetry of the precessional motion of the magnetization. That is, in a planar material with the applied field in the basal plane the precessional path is at right angles to this direction and therefore will include both c-axis and basal planes (both hard and easy directions). As the constraining force varies along this path, the precession will be elliptical which, as pointed out by Jepson [9] will enhance the efficiency of harmonic generation.

2. SPECIFIC MATERIAL CLASSES

Highly anisotropic hexagonal materials have been discussed as falling into two groups (uniaxial and planar) based on their magnetic properties. Specific hexagonal materials should probably be discussed in terms of their different crystal classes. This can best be done with the aid of Figs. 1 and 2. Fig. 1 is a compositional diagram of the BaO, Fe_2O_3, MeO system when Me represents one of the divalent transition elements Ni, Fe, Mn, Zn, Mg, Co, etc., or combinations thereof. The point B represents the non-magnetic $BaFe_2O_4$. The composition S is that of the now familiar spinel ferrites of cubic crystal structure and low anisotropy field. These materials have found wide applications as isotropic microwave magnetic materials. The point M represents the composition $BaFe_{12}O_{19}$ (essentially Ferroxdure [1]) which has the hexagonal crystal structure of magnetoplumbite. This highly anisotropic magnetic oxide has been used for many years as a permanent

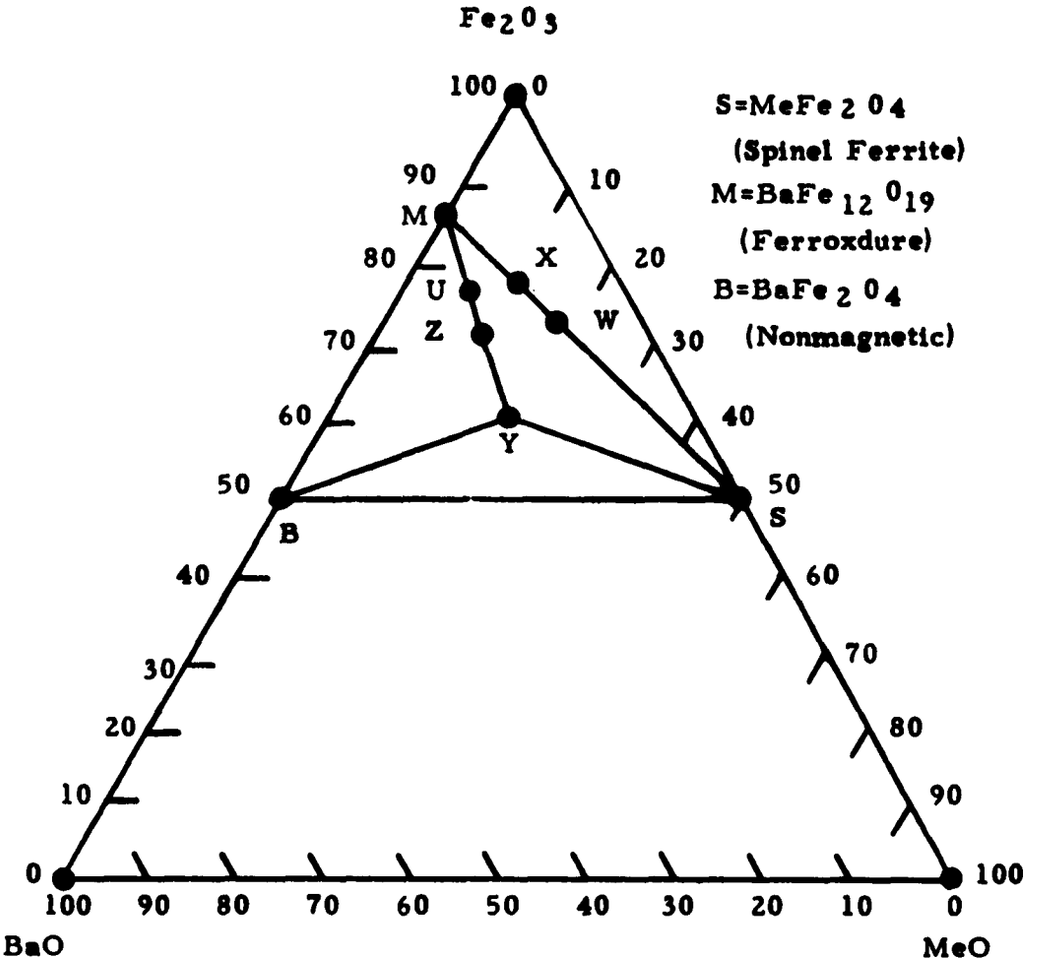

Figure 1. Composition of Various Materials in the BaO - MeO- Fe_2O_3 Complex (After Stuijts and Wijn[12])

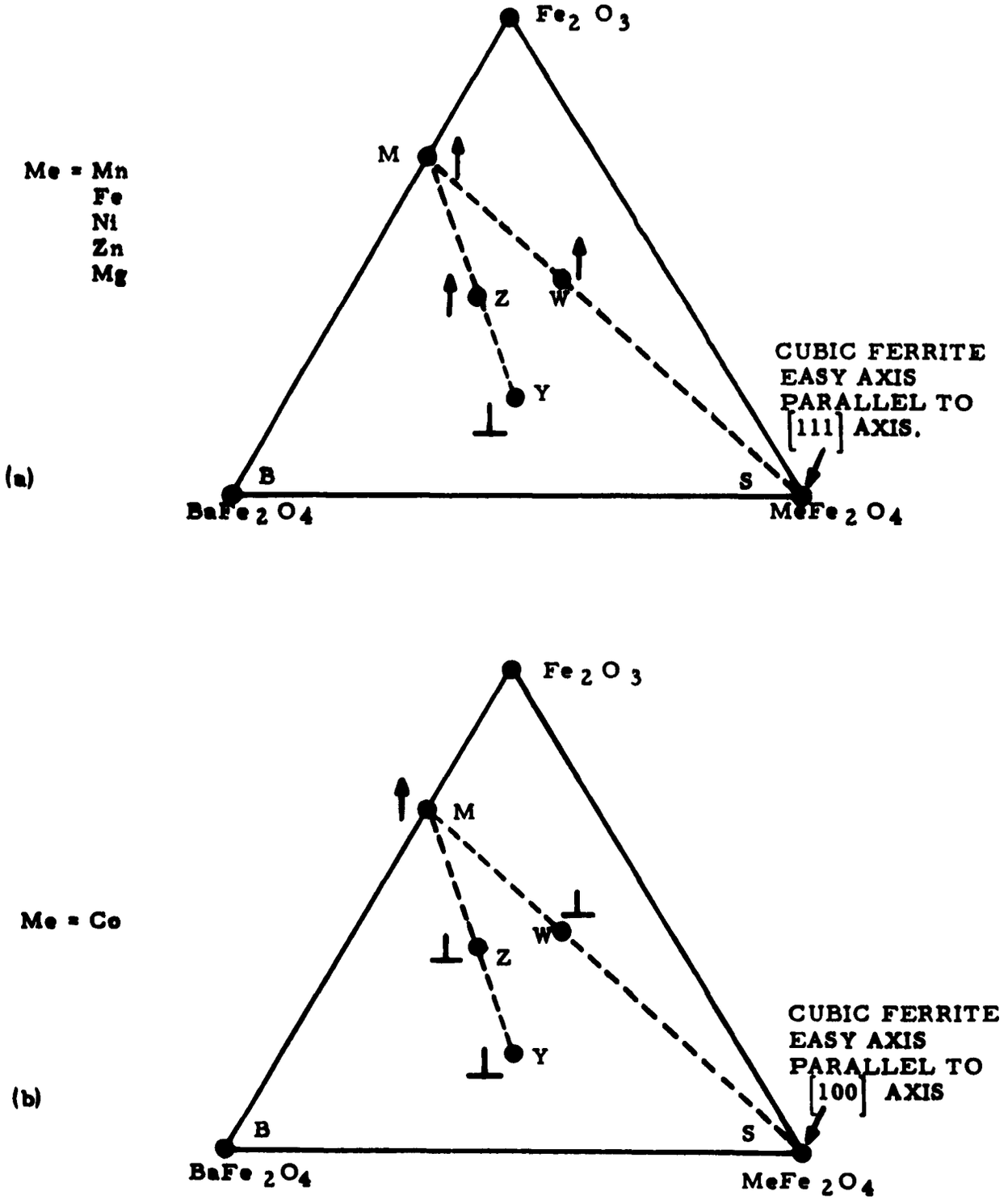

Figure 2. Description of the Magnetocrystalline Anisotropy of the Compounds of Interest. An Arrow Represents a Uniaxial Material, or Positive Anisotropy (Preferred Direction Parallel to C-axis). A Perpendicular Sign Indicates a Planar Material, or Negative Anisotropy (After Jonker, et al.[5]).

magnetic material. This compound has been useful in both oriented and non-oriented polycrystalline form. In recent years several other magnetic oxides containing barium have been discovered at the Philips Laboratories.[5,10,11,12] The new compounds are represented by the symbols W, Z, Y, U and X. The W, Y, Z compounds have thus far received a more thorough investigation than the others, and the discussion will be restricted to these materials. The chemical formulae are as follows:

W: $Ba\,Me_2\,Fe_{16}O_{27}$ or $BaO \cdot 2MeO \cdot 8Fe_2O_3$

Y: $Ba_2Me_2Fe_{12}\,O_{22}$ or $2BaO \cdot 2MeO \cdot 6Fe_2O_3$

Z: $Ba_3Me_2Fe_{24}O_{41}$ or $3BaO \cdot 2MeO \cdot 12Fe_2O_3$

To avoid writing the complicated formulae, the various compounds will usually be denoted by the symbols Me_2W, Me_2Z, etc., where Me represents one or more divalent metals, with subscripts totaling 2.0, e.g., $Ni_{2,0}$ or $Ni_{1.3}Zn_{.7}$.

Some of these materials possess uniaxial (or positive) anisotropy, some planar (or negative) anisotropy. A most interesting property of the W and Z materials is that for some compositions they possess preferential planes of magnetization, or negative K_1[5], while for other compositions they are uniaxial and have positive K_1. This state of affairs is depicted in Fig. 2. Note that the Me_2W and Me_2Z compounds are

uniaxial except when Me is cobalt, in which case they are both planar. All the Me_2Y compounds so far investigated exhibit negative anisotropy (planar materials). The existence of two types of anisotropy in one Crystal system suggests that mixed crystals can be prepared in which the anisotropy can be caused to vary at will between $+ K_1^{max}$ and $-K_1^{max}$ including a zero value of K_1 (the maximum values would be those obtained for the pure W, Y, and Z compounds). This way of controlling K_1 would allow the control of H_{an}

In these materials $4\pi M_s$ and the Curie temperature are roughly comparable to the values for most spinel ferrites, while K_1 is generally quite high and comparable to the value for cobalt ferrite (about 2×10^6 ergs/cc).

Of the materials mentioned, the W, Z, Y series are the most interesting for the applications of this program. It was initially decided that the investigation would be centered on the W, Z, and Y structural types. The field was further narrowed as more facts came to light and the scope of the effort became more clearly defined.

Of primary interest in the study of these hexagonal materials is the effective anisotropy field. The operation of all potential devices that exploit these materials is based on the existence of this field. It was decided therefore that of primary interest in this study would be the control of this field over some desirable range of field values. For devices operating up to 50 kmc the range of fields of interest would be 0 to

approximately 15 kilo-oersteds. Moreover, if these devices are to operate over any specific temperature range, the anisotropy field should not vary excessively over that range of temperatures. This temperature dependence is most important since a change in anisotropy field will affect the device operation just as a change of applied field affects conventional devices using isotropic ferrites. It is unavoidable that the anisotropy field change with temperature. (It must vanish at the Curie temperature!) One can only seek to minimize this change. One way to minimize the temperature sensitivity of the anisotropy field is to have as high a Curie temperaure as possible. As a class of materials the W structure has, in general, higher Curie temperatures than do the Y and Z compounds. The W materials therefore have some advantage over the others for practical device applications. The Ni_2W compound was known to have an anisotropy field of 12.7 koe , a value which is appropriate for use at Q band frequencies, 38 to 50 kmc. In addition, as can be seen from Fig. 2, the anisotropy of Ni_2W is uniaxial ($K_1 = +2.1 \times 10^6 ergs/cm^3$), while the anisotropy of Co_2W is planar. Thus it was thought that ionic substitutions of Co for Ni in the W compound would permit the direct control of K_1 while leaving the saturation magnetization and the Curie temperature essentially unchanged.

It had been shown by many authors[13, 14] that the magnetocrystalline anisotropy of ferromagnetic oxides fits a one-ion description. Each paramagnetic ion exhibits its own anisotropy as determined by the

unbalanced spins of the ion and the crystalline electric field of its immediate environment. The overall or macroscopic anisotropy is then the net result of an algebraic sum of individual-ion anisotropy constants, entirely analogous to the manner in which the saturation magnetization of a ferrimagnet is the net result of the magnetization of individual sublattices. Similar control on the macroscopic anisotropy of spinel ferrites had been achieved by the substitution of cobalt for nickel in $NiFe_2O_4$.[15,16] In the oriented hexagonal materials it should be possible through sufficient cobalt substitution to control the anisotropy constant from + 2.1×10^6 ergs/cm^3 (the value for pure NiW) through zero to a negative value indicating the planar anisotropy characteristic of CoW.

SECTION III
PREPARATION OF MATERIALS

An integral part of this program was the preparation of the materials of interest in our laboratory. In this way the effect of preparation procedures on microwave properties could be carefully studied and controlled, and information obtained from microwave evaluation could be used to perfect synthesis techniques. Initial attention was given to the preparation of the compositions mentioned below. Early work was done on non-oriented samples and was primarily concerned with obtaining firing curves (i.e., density vs. firing temperature) for these materials.

The compositions that were initially studied consist of Me_2Z and Me_2Y compounds. Here Me is an appropriate divalent metallic ion, such as Co^{++}. In some cases the materials were mixed with a deficiency of iron. Table 2 lists the specific compounds that were prepared. One should note, for example, that the symbol Co_2Z may be used when referring to materials of the general composition $3BaO \cdot 2CoO \cdot 12Fe_2O_3$, even when the iron content is not stoichiometric. The NiCoW series is listed last and will be treated as a somewhat separate and special case with modified preparation techniques.

TABLE 2

MATERIALS PREPARED

TYPE OF MATERIAL	STARTING COMPOSITION
Co_2Z	$3BaO \cdot 2CoO\ 12Fe_2O_3$
Co_2Z	$3BaO \cdot 2CoO \cdot 11.8Fe_2O_3$
Co_2Z	$3BaO \cdot 2CoO \cdot 11.6Fe_2O_3$
Ni_2Z	$3BaO \cdot 2NiO \cdot 12Fe_2O_3$
Ni_2Z	$3BaO \cdot 2NiO \cdot 11.8Fe_2O_3$
Ni_2Z	$3BaO \cdot 2NiO \cdot 11.6Fe_2O_3$
Zn_2Z	$3BaO \cdot 2ZnO \cdot 12Fe_2O_3$
Zn_2Z	$3BaO \cdot 2ZnO \cdot 11.8Fe_2O_3$
Zn_2Z	$3BaO \cdot 2ZnO \cdot 11.6Fe_2O_3$
Mg_2Z	$3BaO \cdot 2MgO \cdot 12Fe_2O_3$
Mg_2Z	$3BaO \cdot 2MgO \cdot 11.8Fe_2O_3$
Mg_2Z	$3BaO \cdot 2MgO \cdot 11.6Fe_2O_3$
Cu_2Z	$3BaO \cdot 2CuO \cdot 12Fe_2O_3$
Cu_2Z	$3BaO \cdot 2CuO \cdot 11.8Fe_2O_3$
Cu_2Z	$3BaO \cdot 2CuO \cdot 11.6Fe_2O_3$

TYPE OF MATERIAL	STARTING COMPOSITION
Ni_2Y	$2BaO \cdot 2NiO \cdot 6Fe_2O_3$
Ni_2Y	$2BaO \cdot 2NiO \cdot 5.9Fe_2O_3$
Ni_2Y	$2BaO \cdot 2NiO \cdot 5.8Fe_2O_3$
Co_2Y	$2BaO \cdot 2CoO \cdot 6Fe_2O_3$
Co_2Y	$2BaO \cdot 2CoO \cdot 5.9Fe_2O_3$
Co_2Y	$2BaO \cdot 2CoO \cdot 5.8Fe_2O_3$
Zn_2Y	$2BaO \cdot 2ZnO \cdot 6Fe_2O_3$
Zn_2Y	$2BaO \cdot 2ZnO \cdot 5.9Fe_2O_3$
Zn_2Y	$2BaO \cdot 2ZnO \cdot 5.8Fe_2O_3$
Mg_2Y	$2BaO \cdot 2MgO \cdot 6Fe_2O_3$
Mg_2Y	$2BaO \cdot 2MgO \cdot 5.9Fe_2O_3$
Mg_2Y	$2BaO \cdot 2MgO \cdot 5.8Fe_2O_3$

Ni_2W	$BaO \cdot 2NiO \cdot 7.8Fe_2O_3$
$(Ni_{.95}Co_{.05})_2W$	$BaO \cdot 2(Ni_{.95}Co_{.05}O) \cdot 7.8Fe_2O_3$
$(Ni_{.9}Co_{.1})_2W$	$BaO \cdot 2(Ni_{.9}Co_{.1}O) \cdot 7.8Fe_2O_3$
$(Ni_{.8}Co_{.2})_2W$	$BaO \cdot 2(Ni_{.8}Co_{.2}O) \cdot 7.8Fe_2O_3$
$(Ni_{.75}Co_{.25})_2W$	$BaO \cdot 2(Ni_{.75}Co_{.25}) \cdot 7.8Fe_2O_3$
$(Ni_{.7}Co_{.3})_2W$	$BaO \cdot 2(Ni_{.7}Co_{.3}) \cdot 7.8Fe_2O_3$
$(Ni_{.6}Co_4)_2W$	$BaO \cdot 2(Ni_{.6}Co_{.4}) \cdot 7.8Fe_2O_3$
$(Ni_{.5}Co_{.5})_2W$	$BaO \cdot 2(Ni_{.5}Co_{.5}) \cdot 7.8Fe_2O_3$

1. THE GENERAL PROCEDURE

The general method of preparation is, of course, similar to that for preparing ferrites and other magnetic oxides, and a flow chart for the process is shown in Fig. 3.

The raw materials, e.g., $BaCO_3$, Co_2O_3, and Fe_2O_3, are weighed out (1) in appropriate quantities and placed in a stainless steel ball mill jar containing stainless steel balls and varsol, plus a wetting agent. This mixture is rolled (2) for eight hours, after which the slurry is vacuum filtered and dried (3).

The dried cake is then pulverized so as to pass through a 20-mesh screen, and this powder is presintered (4) at an appropriate temperature, in the range 1050°C to 1200°C. Aluminum oxide or zirconia boats are used here, there being little trouble with reaction between the powder and boat at these temperatures. The presintering operation has been carried out in dead air with a soak-time of 4 to 8 hours. (It has been found that both soak time and temperature influence particle size, but to only a minor degree. The following milling step has a much greater effect.)

After presintering, the powder, along with water and in some cases a binder (approximately 3% Hyform 1205 by weight), is rolled in a ball mill or run in an attritor mill for 2 to 8 hours (5). This accomplishes a thorough blending of the wax with the powder, breaks up the agglomerates, and, if the process continues long enough, reduces average particle size.

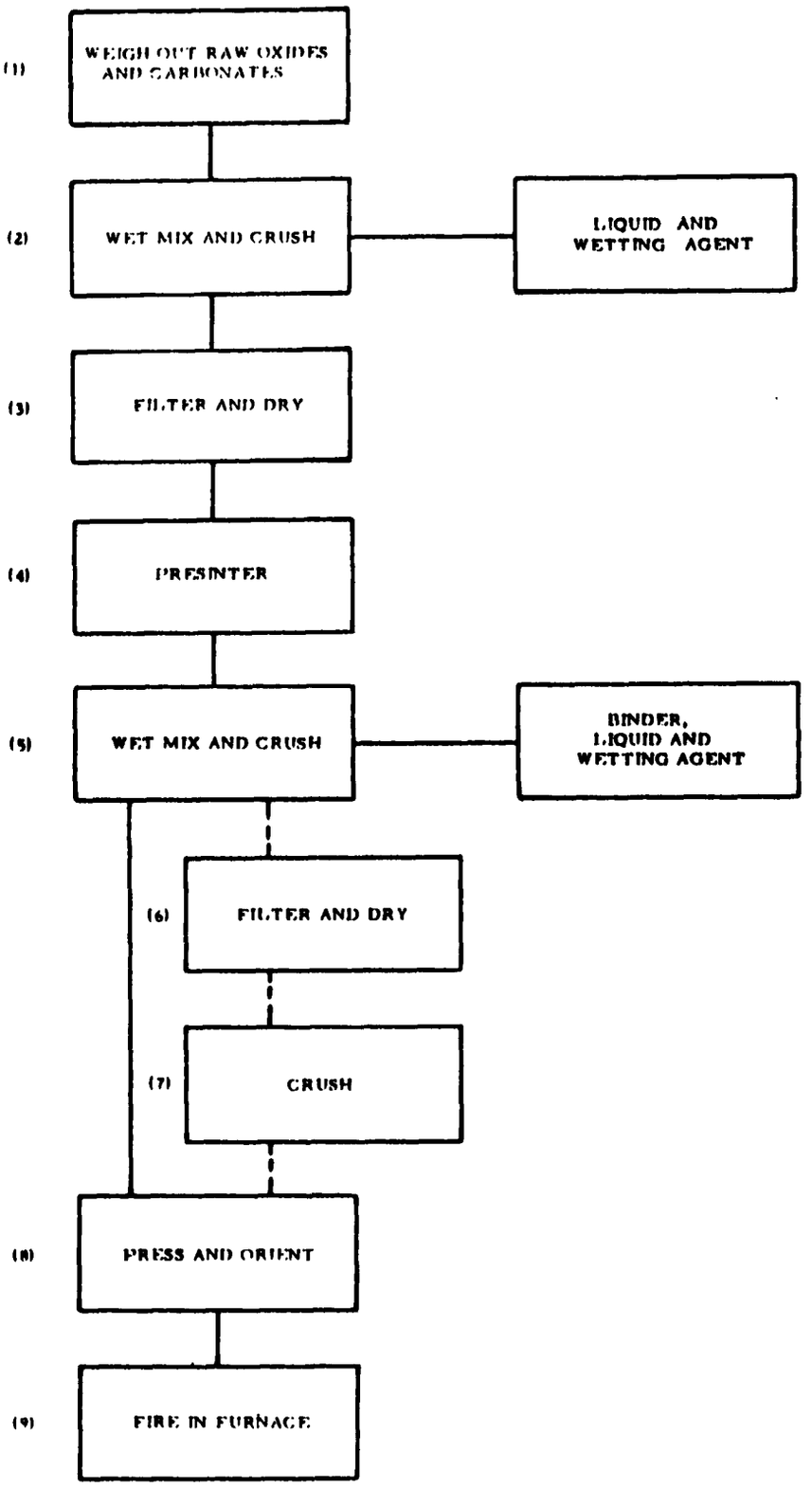

Figure 3. Flow Chart for Preparing Hexagonal Materials

If the material is to be dry pressed, the slurry is again vacuum filtered (6) and dried at 105° C, care being taken not to leave the powder at this temperature for an excessively long time, so as to avoid appreciable loss of the wax. The dried powder is pulverized (7) to pass through a 30-mesh screen, whereupon it is ready for pressing (8).

If the material is to be oriented during pressing, it is sludge pressed (8) and hence not dried subsequent to the vacuum filtering (6). Instead it is placed in sealed jars until the pressing operation is to be performed. The slurry is then pressed in appropriate non-magnetic dies in the presence of a magnetic field. (This technique will be the subject of paragraph 4 below).

First data were taken on dry-pressed samples to determine the appropriate presintering (4) and firing temperatures (9) for a wide range of materials in terms of resultant density. Information was also obtained on the effects of non-stoichiometric mixing to compensate for iron picked up in the preparation process.

After the powder is pulverized and screened (7) as described above, it is mixed with 5% water, by weight, with a mortar and pestle and then pressed (8) at 5 tons/in^2. (The powder is still "dry" after adding this much water, but the result is a more uniform ceramic, free from laminations). The pressed sample is dried overnight at 110 °C, and then fired at the appropriate temperature for 8 hours (later samples were fired for 2 hours and in some cases a few minutes to minimize grain growth.) The temperature is raised slowly (~ 100°C/hr, 5 hrs)

to allow the binder to burn off slowly; after which the temperature is raised to the final firing temperature. The firing is done in oxygen at atmospheric pressure for each of the materials described here.

2. PRESINTERING TEMPERATURE

To obtain a meaningful firing curve, it is necessary that all the samples which are fired at different temperatures be presintered at a common temperature. Like so many of the variables in the preparation process, it is probable that an optimum presintering temperature exists; in principle then, it might be desirable to obtain firing curves for several different presintering temperatures. In practice, however, such thinking, when applied to several variables in the process, results in an excessive number of firings. Thus tentative presintering temperatures were selected for each of the compositions by presintering powder samples at a variety of temperatures, and simply observing their color and texture after reaction. Experience then serves as a guide in the selection. As more knowledge is gained of the various properties of the materials this information is fed back in such a way that optimum presintering temperatures may be decided by more scientific techniques, such as the measurement of particle size and/or saturation magnetization per gram after reaction. This was done in the NiCoW series of materials.

Proceeding in this way, the presintering temperatures listed in Table 3 were selected. There was some noticeable difference in color

and texture for each composition (e. g., Co_2Z) as the iron content was varied as in Table 2; in general, the samples with smallest iron content appeared to have reacted more completely. However, the difference was slight, so that one presintering temperature was selected for each general composition (e. g., Co_2Z).

TABLE 3

Presintering Temperatures for the Various Compositions

Type of Material	Presintering Temperature
Co_2Z	1100 °C
Ni_2Z	1100 °C
Zn_2Z	1000 °C
Mg_2Z	1150 °C
Cu_2Z	900 °C
Co_2Y	1000° C
Ni_2Y	1100 °C
Zn_2Y	1100 °C
Mg_2Y	1200° C
NiCoW	1100° C

The compounds containing magnesium are more refractory, requiring a higher presintering temperature, in line with previous experience with magnesium ferrite. The copper compounds, on the other hand, are highly reactive, and presinter at a much lower temperature. At 1000 °C or higher, for example, these powders form a very hard grained, shrunken agglomerate. This suggests, of course, that small quantities of copper compounds (Cu_2Z or Cu_2Y) may be used as a flux in other similar materials to produce high-density sintering at lower temperatures.

3. DENSITY DATA

Density was measured by calculating the volume of the sintered sample from micrometer measurements and by weighing the dry sample. Thus all the pores, connected or otherwise, reduce measured density. This is the density which one would use in calculating $4\pi M_s$, for example, and is the proper one to consider in microwave applications. In the few cases where the sample was distorted so as to make such a measurement impossible, the density was measured with a mercury volumeter, in which the sample is immersed in mercury. The accuracy of the density determination in such cases is less than for the direct measurement, which is easily within 1%.

The firing temperatures were determined within 5° C except in a few cases where the margin of possible error was somewhat greater. The results of the more complete data are plotted in Figs. 4 through 13. It was thought that a decreased iron content, i. e., an iron

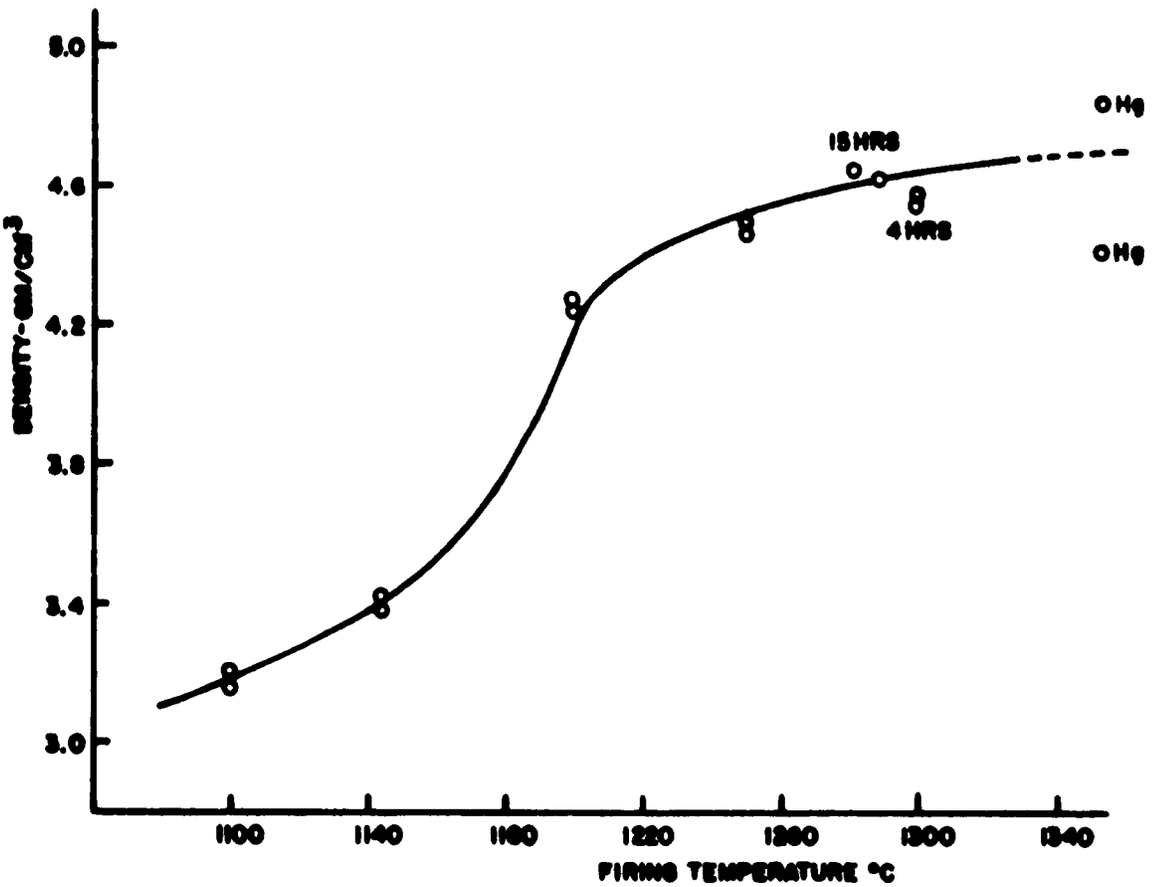

Figure 4. Firing Curve for $3BaO \cdot 2CoO \cdot 12Fe_2O_3$
Time = 8 hours

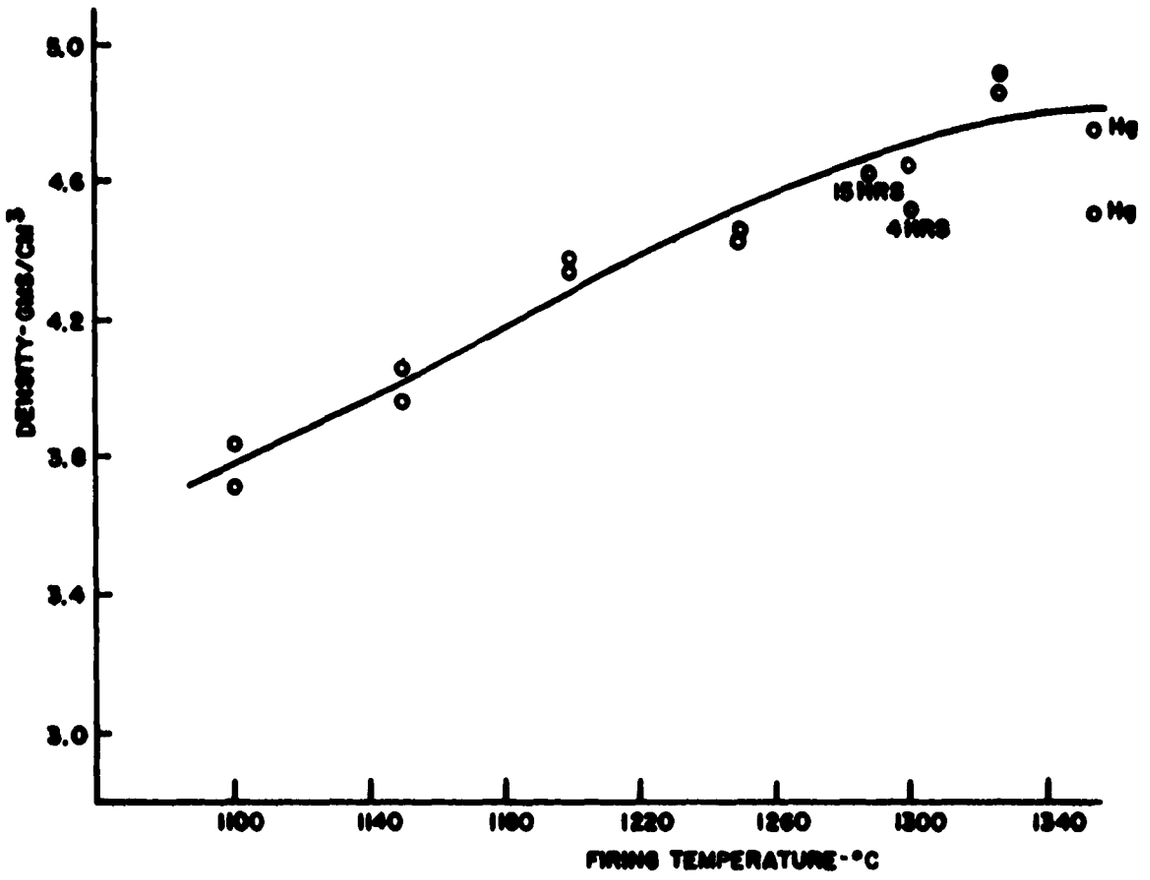

Figure 5. Firing Curve for $3BaO \cdot 2CoO \cdot 11.8Fe_2O_3$
Time = 8 hours

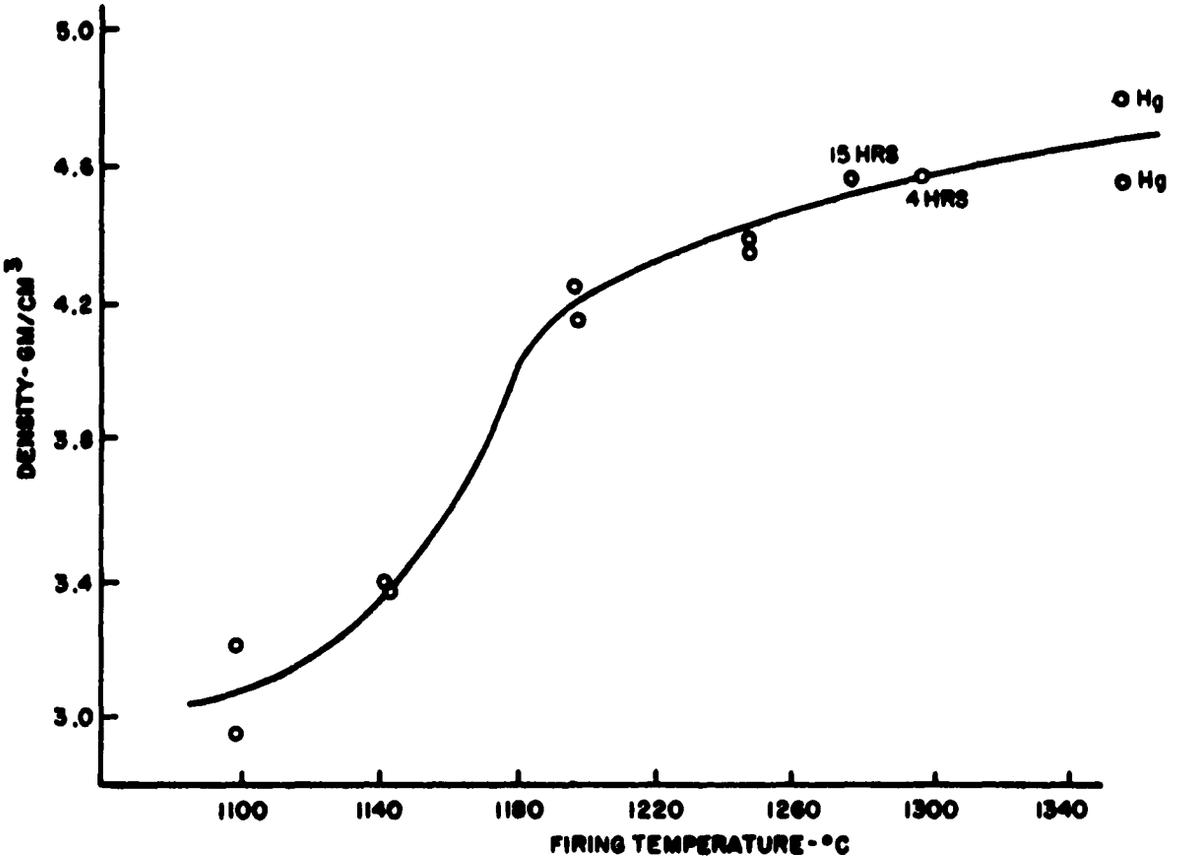

Figure 6. Firing Curve for $3BaO \cdot 2CoO \cdot 11.6Fe_2O_3$
Time = 8 hours

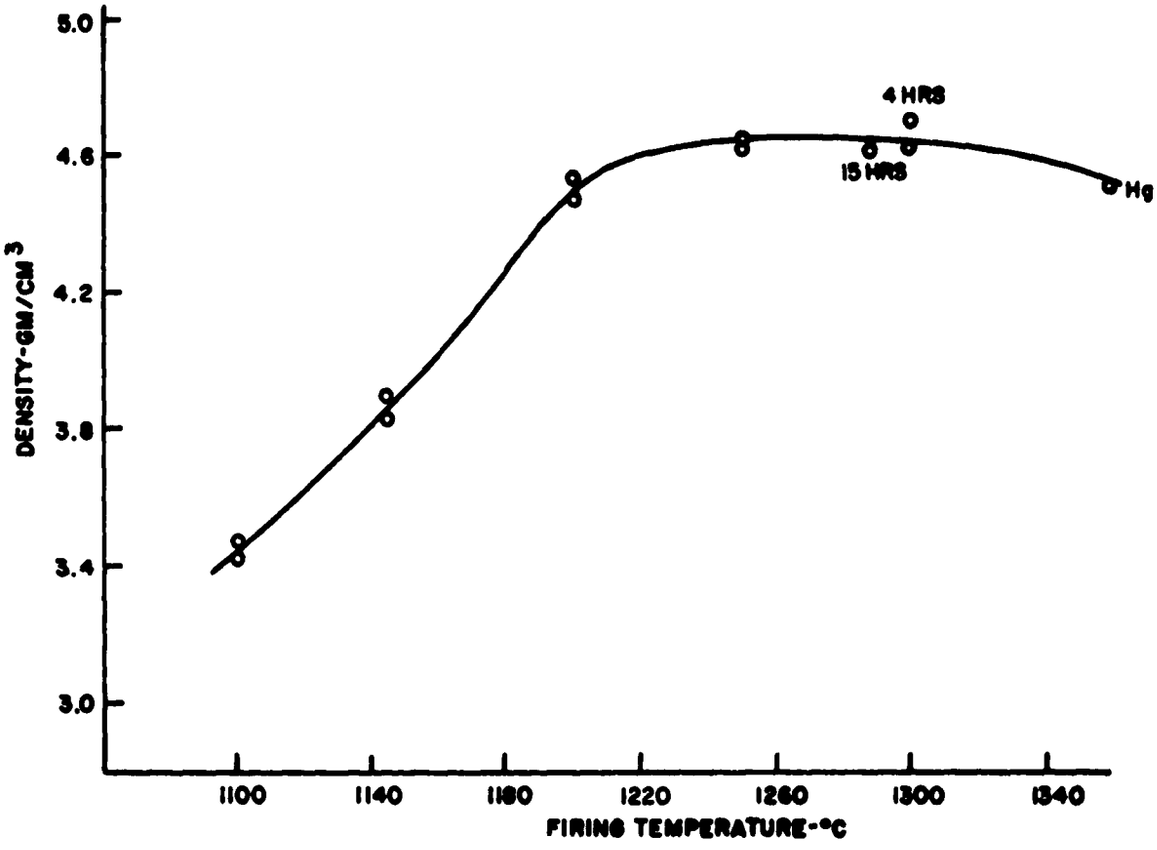

Figure 7. Firing Curve for $3BaO \cdot 2NiO \cdot 12Fe_2O_3$
Time = 8 hours

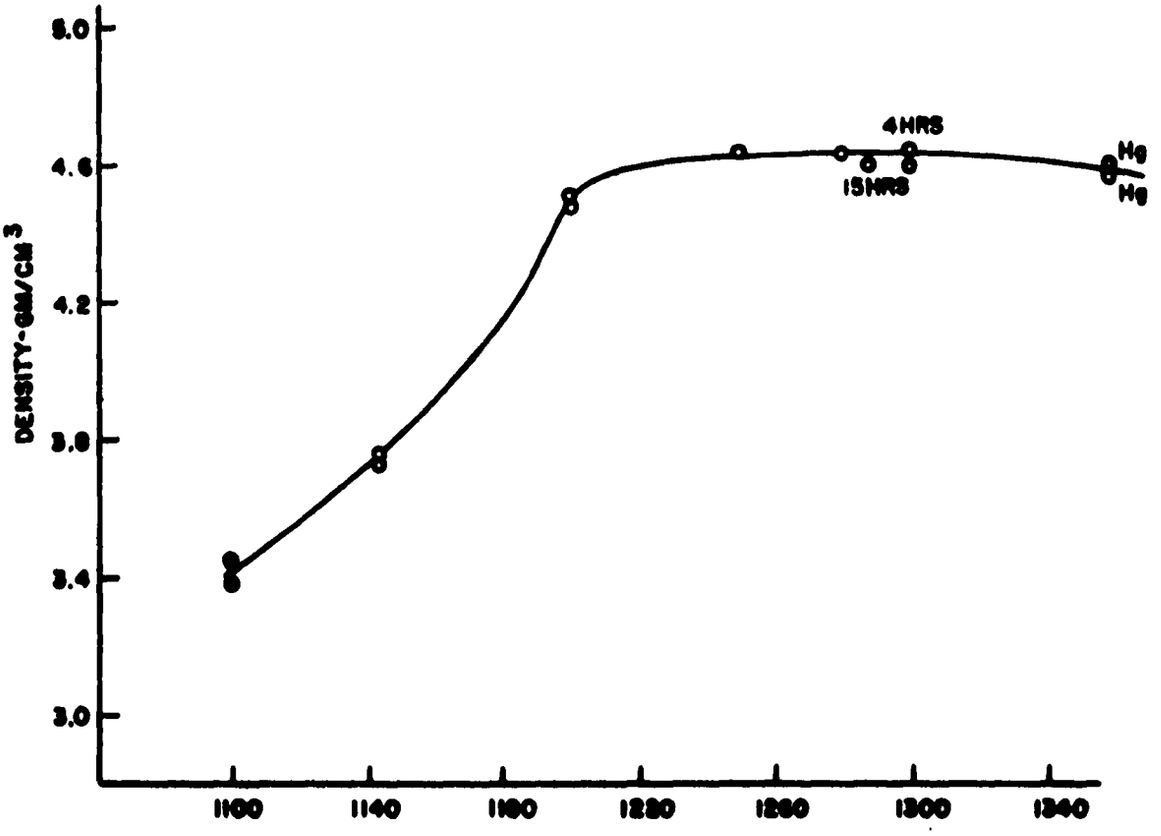

Figure 8. Firing Curve for $3BaO \cdot 2NiO \cdot 11.8Fe_2O_3$
Time = 8 hours

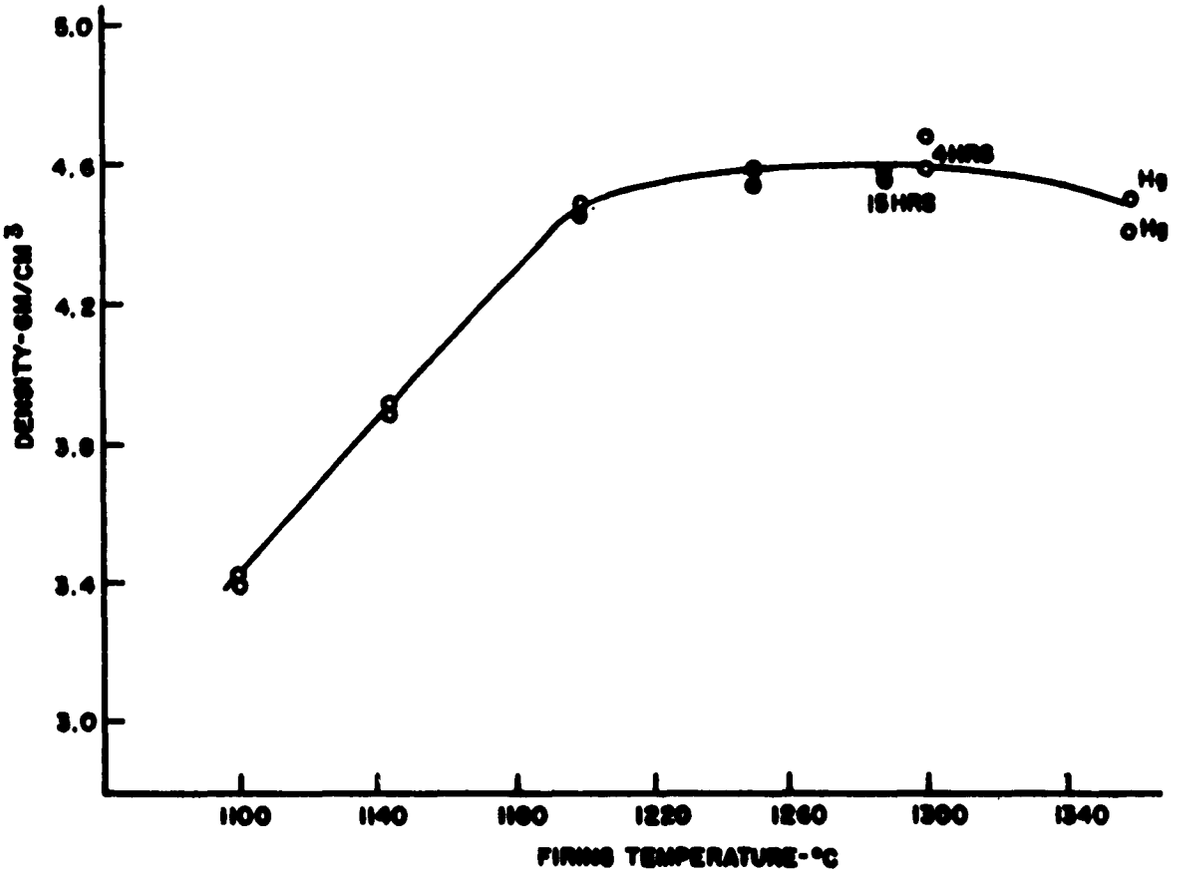

Figure 9. Firing Curve for $3BaO \cdot 2NiO \cdot 11.6Fe_2O_3$

Time = 8 hours

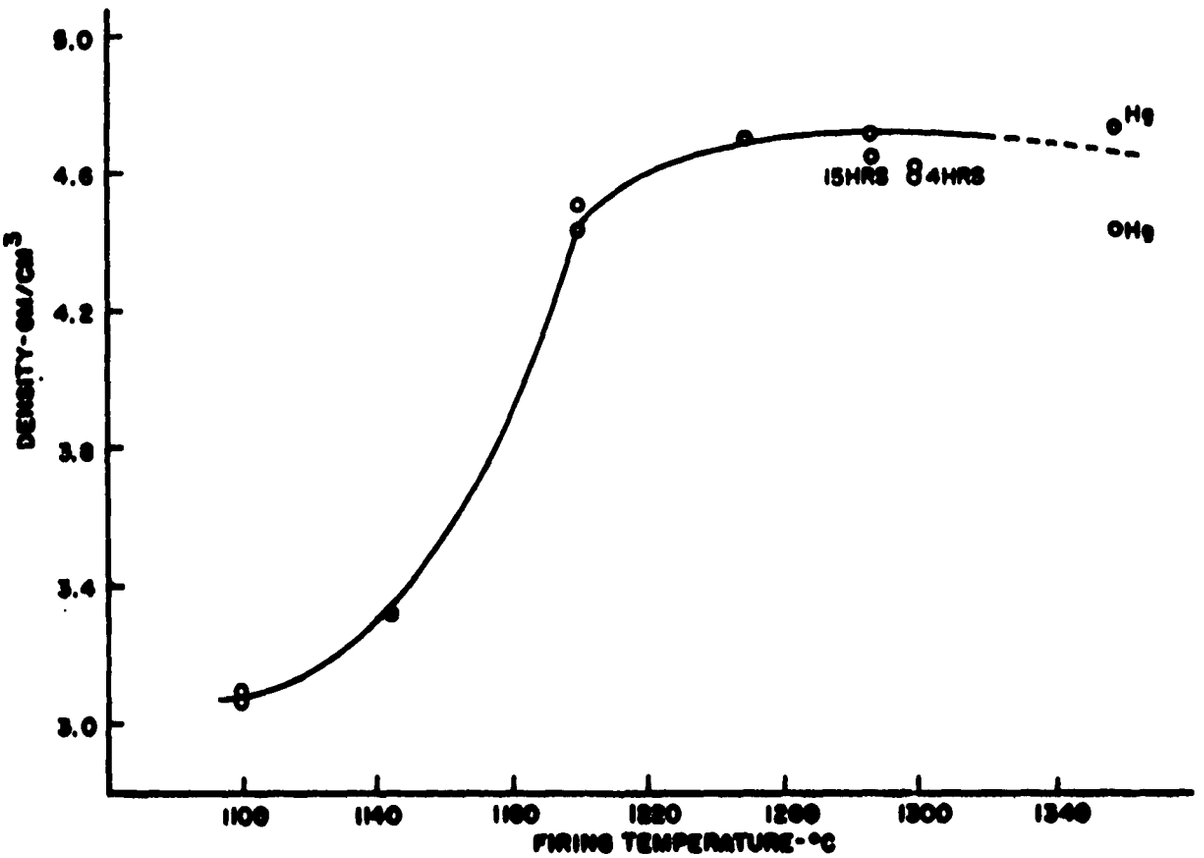

Figure 10. Firing Curve for $3BaO \cdot 2ZnO \cdot 12Fe_2O_3$

Time = 8 hours

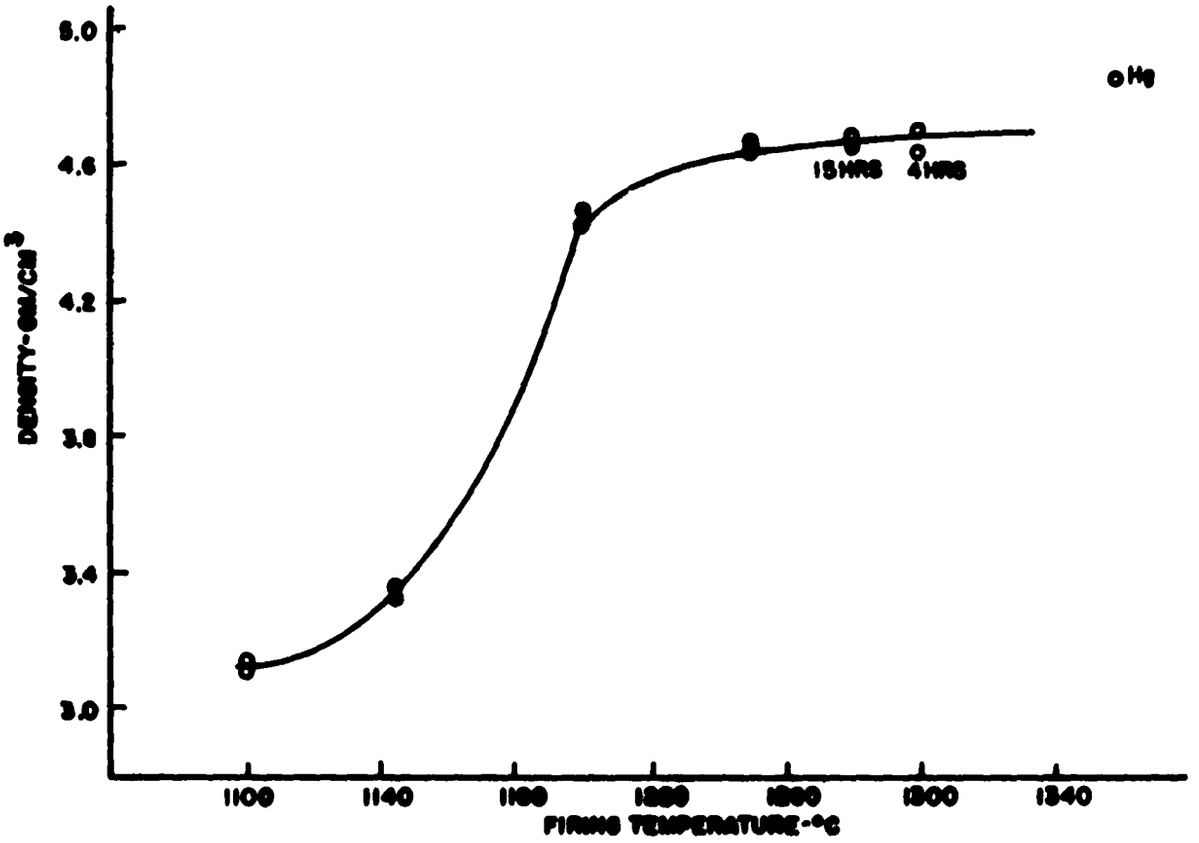

Figure 11. Firing Curve for $3BaO \cdot 2ZnO \cdot 11.8Fe_2O_3$

Time = 8 hours

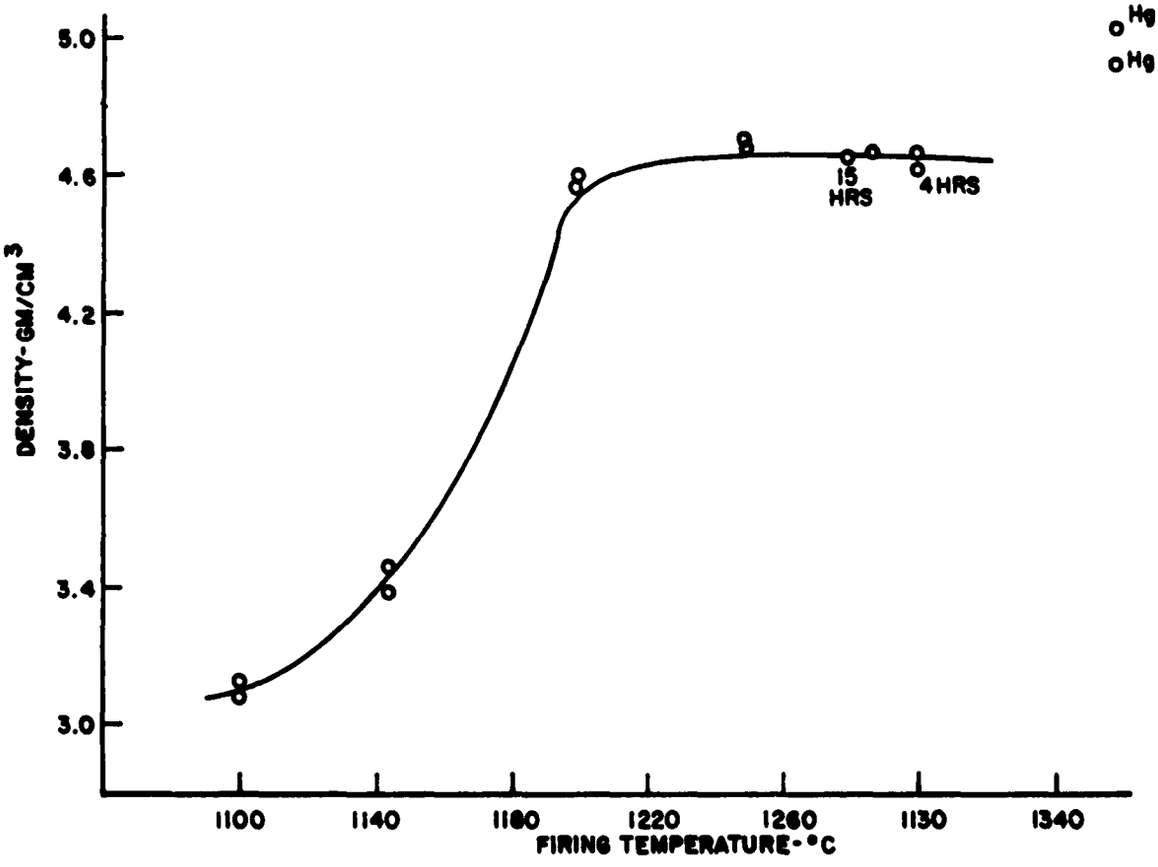

Figure 12. Firing Curve for $3BaO \cdot 2ZnO \cdot 11.6Fe_2O_3$

Time = 8 hours

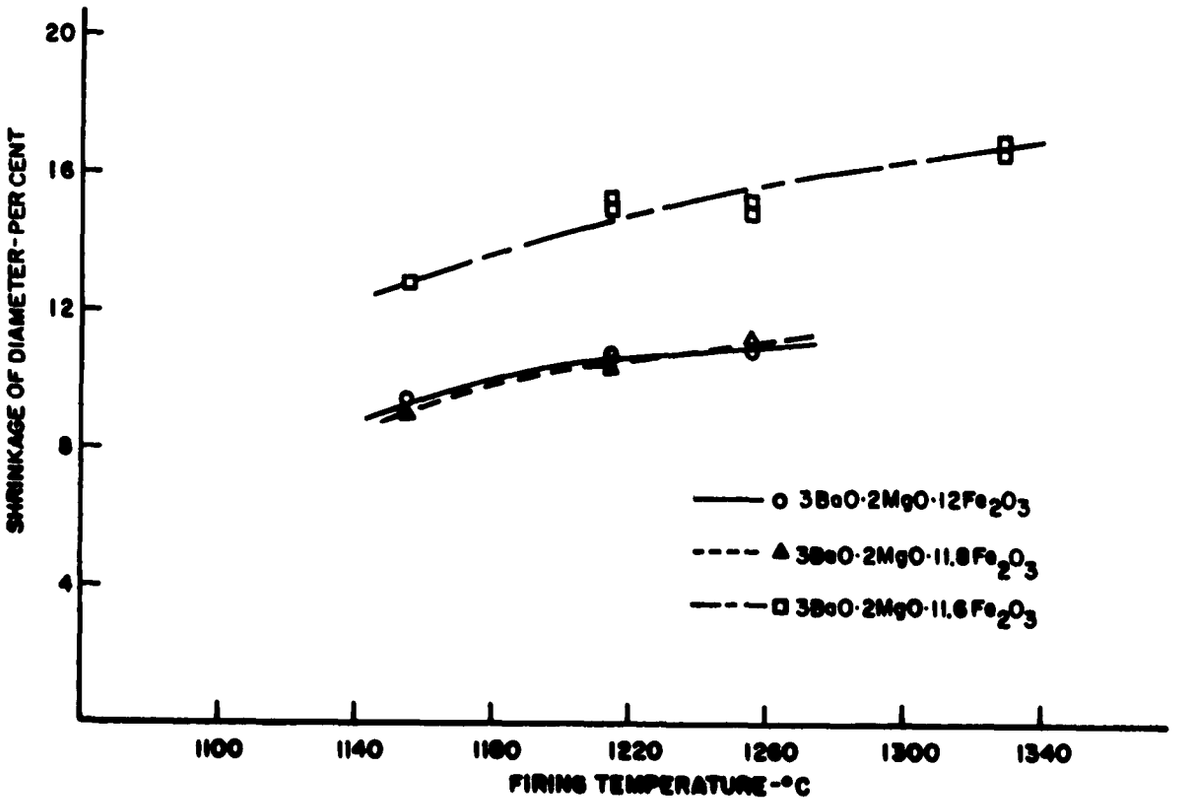

Figure 13. Shrinkage in Mg_2Z Compounds with Variable Iron Contents. Time = 8 hours

content less than the stoichiometric amount, might result in a higher density, i. e., more shrinkage on sintering. Presumably vacancies among the sites would tend to promote diffusion of the ions and more rapid sintering. The results do not show this to be true in a consistent way among most of our samples, at least not to any large extent. In the case of Mg_2Z there is a definite difference, however, as indicated in Fig. 13, the sample with the least iron content does show a pronounced increase in shringkage.

In considering the effect of the variable iron content, it should be kept in mind that the given compositions are starting compositions; no chemical analyses of the final samples were made, so that changes in formula due to volatization of components or iron pick-up in the mills have not been accounted for in writing these formulae. Finally, it may be remarked that the samples with smaller iron content do appear to react more completely in the presintering stage; hence chemical reaction is apparently facilitated by reduced iron content, while the sintering process may not be so strongly affected, perhaps because of increase iron pick up in the granulating step (5).

The data suggest for most materials that a maximum density is obtained for a firing time of about eight hours. A firing time of only two hours generally gives a lower density, while the results for 15 hours are not appreciably different from those for eight hours. For very high temperatures, i. e., above the plateau in the firing curve, this is not

the case, however. The reduction in density at high temperatures may well be due to the loss of certain components through volatization. In that case, longer firing times are detrimental to density. For applications where it is desired to inhibit crystal growth during sintering, it is nevertheless desirable to fire for two hours or less.

The copper compounds sinter to very high density at lower temperatures than do the other material, as in the case for ferrites. Optimum firing temperature for Cu_2Z has not been determined, although it is apparent from the available data that this temperature will lie near 1200°C. It is also apparent that a small quantity of Cu_2Z (or Cu_2Y or Cu_2W) should serve as a flux in other Z, Y, or W compounds to promote high density sintering.

In the early part of this work, some difficulty with cracking of the samples during firing was experienced. Some improvement was achieved by mixing in the binder during the ball milling operation following the presintering step (earlier, a mortar and pestle had been used), and by addition of 5% water as a lubricant just before pressing. (It should also be pointed out that Hyform 1205 apparently "ages" on the shelf, and its use results in sample cracking thereafter. A fresh supply should be maintained at all times).

4. NiW-CoW PREPARATION AND ALIGNMENT

Greatest microwave emphasis was placed on the NiW-CoW materials, and as a result of microwave evaluation certain steps in the preparation process outlined above were modified.

Starting compositions of $BaO \cdot 2\left[1-xNiO \cdot xCoO\right] \cdot 7.8\,Fe_2O_3$ was used, and these iron deficient materials were presintered at temperatures near 1100°C. It was found that the highest degree of alignment of sintered samples was obtained in those that had been run in an attritor mill (step 5) for 2½ hours with water and Hyform 1205 after the presintering stage (4). In general it was found that the higher the degree of dispersion of the material in the slurry, the better the alignment. Best results were obtained with materials pressed directly from the slurry extracted from the attritor mill. This contained approximately 50 per cent solid material, 50 per cent water and 1½ per cent Hyform 1205 (all percentages by weight). The slurry was poured into a non-magnetic die and oriented by an applied field of approximately $H_{ap} = .707\,H_{an}$, where H_{an} is the value of anisotropy field expected for the resultant material. (Further discussion of orienting fields appears in Appendix I.) Fig. 14 shows the press and magnet assembly used. A small motor driven rig was also constructed to permit rotation of the die while pressing in order to facilitate the orientation of planar materials.

The pressed oriented material was dried from 24 to 48 hours at room temperature and 4 to 8 hours at 100°C. Samples were subsequently

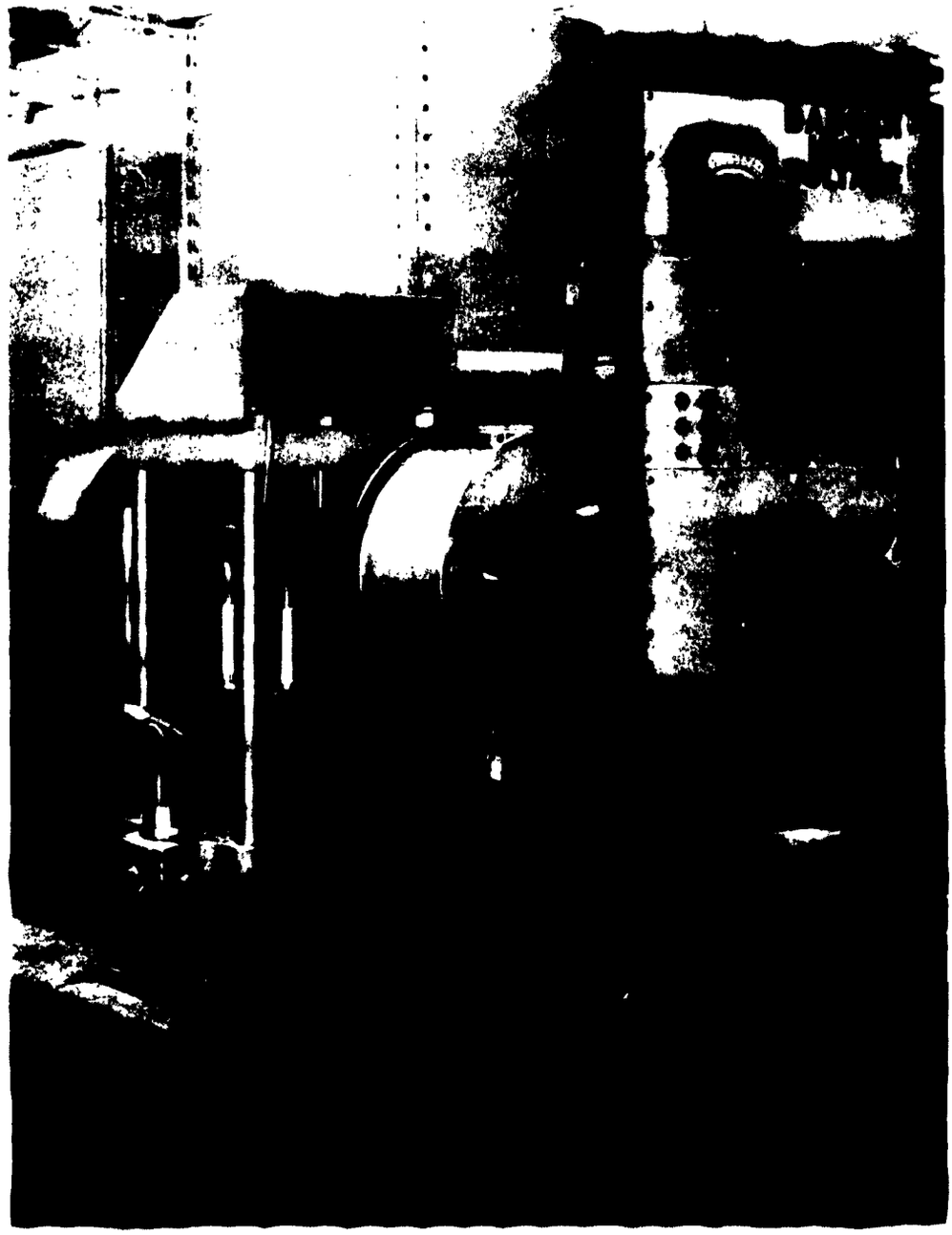

Figure 14. Magnet and Press Assembly for Orienting Materials During the Pressing Operation

fired at 1350°C for 4 hours or less and cooled at furnace cooling rate.

4.1 Effects of Particle Size

The particle size and size distribution at almost every stage in the synthesis process is of considerable importance. Small grains are desirable in the initial ball milling and presintering stages as they will speed both mixing and firing process (the smaller the particles the more reactive the material). From the ceramic standpoint a good particle size distribution is desired at the pressing stage, and absolute particle size is of only secondary importance. A good size distribution facilitates achieving a high packing fraction and hence a higher final density. Size distribution effects are probably of greater importance in spherically shaped grains than in the oriented plate-like grains of hexagonal materials, but a reasonably good distribution is probably still required. The standard ball milling techniques used are known to promote a distribution of particle sizes, and this is felt to suffice for the present case.

In the orienting process absolute particle size is of importance, and the actual requirements are the object of competing demands. The orienting torque per unit volume exerted on a crystallite is given in equation I-3, but the absolute torque varies directly with the volume of the crystallite. Thus the larger the crystallite, the greater the torque. Now the constraints that operate to inhibit orientation must also be considered. Two chief constraints may be considered: (1) mechanical

constraints of neighboring particles and (2) viscosity of the slurry. The second constraint, viscosity, will exert frictional forces on the surface of the crystallite that impede rotation. These frictional forces will vary with the type of slurry used, but in any case will vary directly with the surface area of the crystallite. Since the torque varies with the volume, and the frictional forces with surface area, the net orienting force will vary as the ratio of volume to surface area, and hence directly with mean particle dimensions. Again it appears that orientation should improve with increasing particle size. We must still consider, however, the mechanical constraints from neighboring particles. While these forces cannot be computed, it is reasonable to suppose that the greater the dispersion of particles within the slurry, the less important this factor becomes. (If neighboring particles never come into contact, slurry viscosity will be the overriding factor.) Since small particle sizes yield a higher degree of dispersion (or suspension) in aqueous slurries, this first restraining factor favors small particle sizes.

It is also of great importance to note that equation I-3 was obtained under the assumption that crystallites were <u>single domain</u> particles. The net orienting torque will be appreciably reduced in the case of <u>multi-domain</u> particles. As a result of these considerations it appears that for greatest alignment on pressing one would like to have particles sizes <u>just under</u> the <u>single domain limit</u>. The critical diameter for single domain particles is proportional to $\sqrt{K}/M^2$.[17] Thus the larger the anisotropy field

the larger the single domain particle size limit. If the material to be pressed is to have only single domain particles, the size of these particles must be decreased with decreasing anisotropy field.

If a permanent magnet material is desired with a high coercive force, it is imperative that the grain size of the sintered material be below the critical size for single domain particles. Thus if a permanent magnet material is desired, the particle size of the pressed material must be so small that even after grain growth occurs in firing the particles will still be of single domain size. Since the critical diameter of single domain particles varies with the square root of the anisotropy constant, this size, and hence detailed treatment, will vary from one material to the next. Very weakly anisotropic material would require extremely small particles to achieve any sort of permanent magnet properties.

Our experiments indicated that the degree of orientation continued to improve with reduction in pressed particle size to the limit that our experiments were carried. Best alignment was obtained from material run in an attritor mill for 2½ hours and fired at 1350°C for 4 hours. The particles of the final fired samples were in the form of flat platelets with basal plane diameters of the order of 2 to 3 microns.

The degree of alignment in all cases improved with firing time and grain growth. It has been shown by Stuijts[18] that in the vast majority of cases incorrectly aligned crystals are eliminated in the growth process, and only under the most unusual conditions will an incorrectly aligned

crystal grow at the expense of its more numerous oriented neighbors. Evidence of the improvement in alignment realized through grain growth and the preferred growth of oriented crystals is seen in comparing Figs. 15 and 16. These absorption curves are plotted for two identical samples with only the firing time varied. The data of Fig. 15 were obtained on a sample heated to the final sintering temperature in 8 hours and held there for 2 hours, while the other sample (Fig. 16) was raised to sintering temperature in 15 minutes and held there for only 10 minutes. Both samples were in the form of small pellets, and both appeared to have undergone a complete reaction. It is obvious on comparing these two sets of data that the longer firing time enhances crystallite orientation. Thus in preparing oriented materials with a large coercive force it is advisable that the material to be pressed be constituted of very small particles. In this way one can allow for sufficient grain growth to enhance orientation and at the same time not exceed single domain particle dimensions in the final product.

4.2 Lotgering Alignment.

Studies of alignment indicate that the degree of alignment achieved deteriorates to some extent with decreasing anisotropy field. Since the orienting torque on a crystallite in the slurry is under any circumstances directly proportional to the anisotropy constant (see equation I -3), this is to be expected. The orienting torque approaches zero as the anisotropy field approaches zero. To make matters worse, as the anisotropy

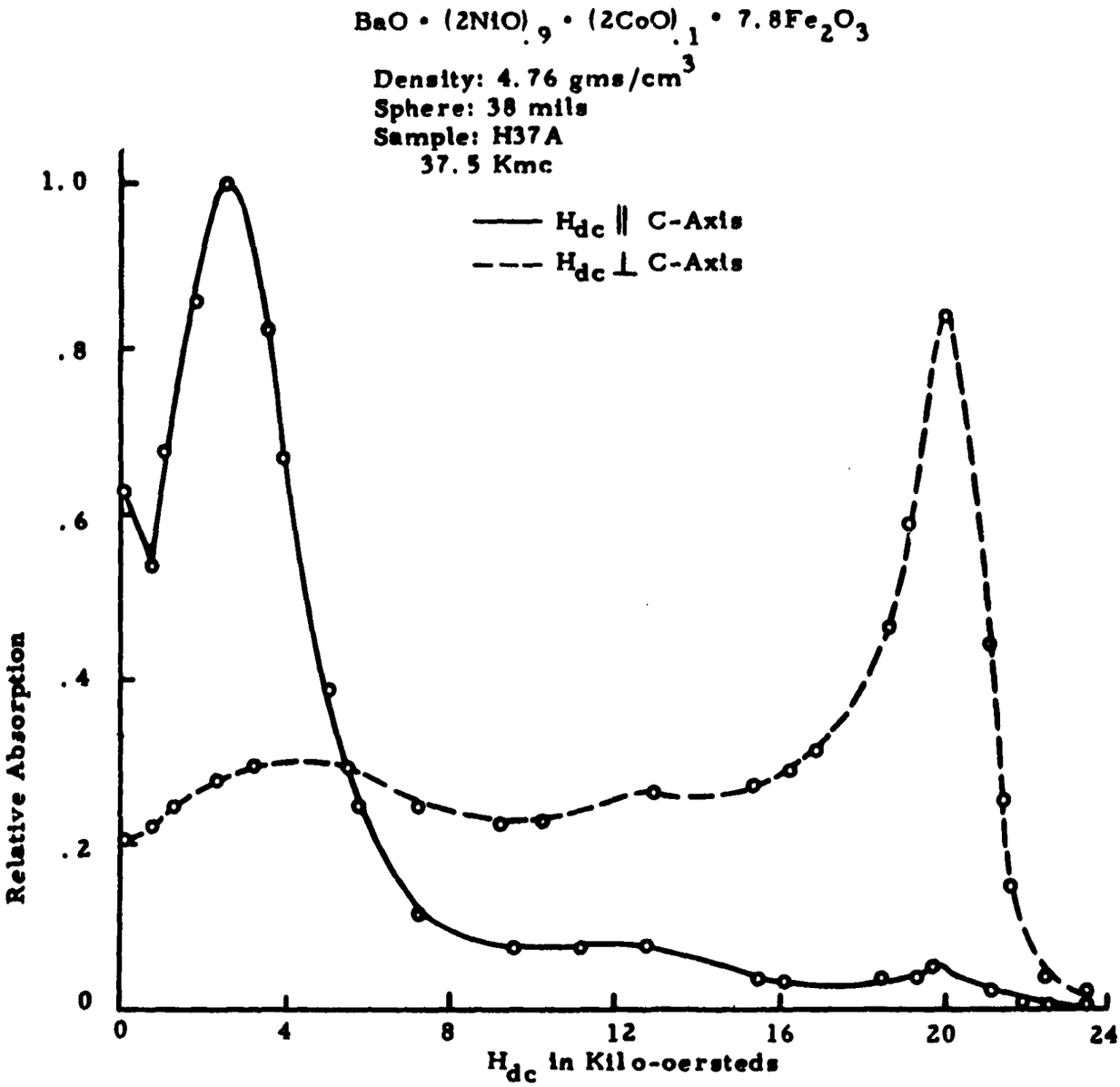

Figure 15. Ferromagnetic resonance in a sphere of $(Ni_{.9}Co_{.1})_2W$ at 37.5 kmc. Material sintered for 2 hours.

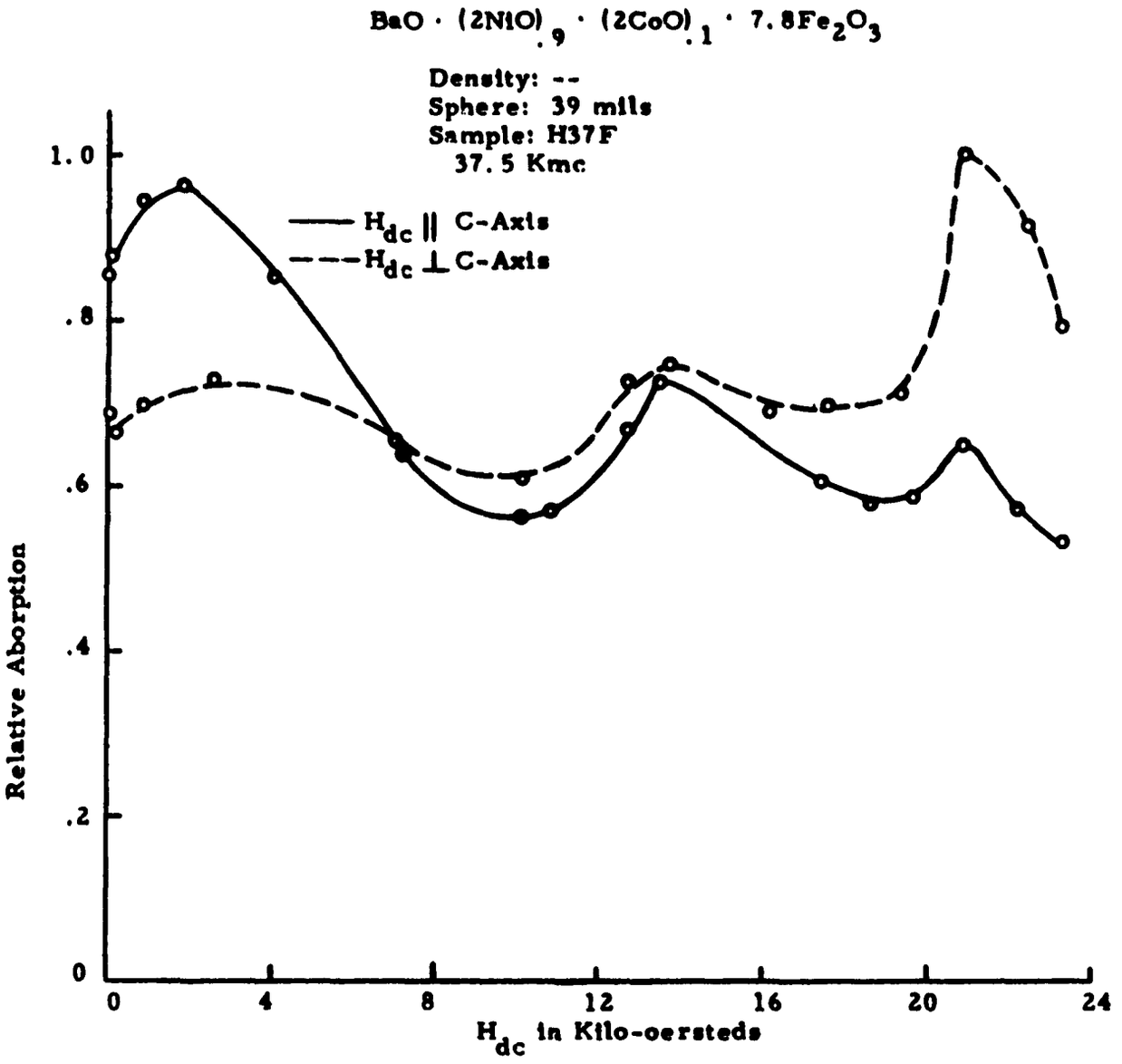

Figure 16. Ferromagnetic resonance in a sphere of $(Ni_{.9}Co_{.1})_2W$ at 37.5 kmc. Material sintered for 10 minutes.

field is decreased the magnetization of a given sized particle will break into a multi-domain configuration and thus further reduce the orienting torque.

This unhappy state can be avoided by using a technique of chemical alignment first proposed by Lotgering.[19] The method was originally proposed for use in preparing oriented planar materials without the use of a rotating magnetic field. Lotgering found that oriented crystals of material could be prepared by the reaction of oriented grains of a highly uniaxial material with non-oriented grains of non-magnetic components. He found, for example, that when a mixture of the highly anisotropic M compound and Fe_3O_4 crystals was pressed in the presence of an orienting field, the c-axes of M crystals were aligned, and the weakly anisotropic Fe_3O_4 remained unaligned. When this mixture was fired, however, the solid state reaction took place forming Fe_2W from the mixture, and the c-axes of this reaction product preserved the orientation of the c-axis of the M crystals. In this technique then the orienting torque is <u>independent</u> of the <u>anisotropy</u> of the <u>final</u> product. It is then feasible to orient materials with vanishingly small anisotropy field.

This technique was applied to the preparation of the $(Ni_{1-x}Co_x)_2W$ series where the anisotropy field approaches zero as x approaches 0.5. In the preparation of the $(Ni_{.6}Co_{.4})_2W$ materials, for example, the Ni_2W compound (H_{an} = 12.7 koe) is first prepared and presintered. To

this presintered material is added sufficient raw non-magnetic material to bring the metallic ion ratio to that of the desired final composition. Upon pressing, the uniaxial crystallites of Ni_2W are oriented with c-axes aligned, and in the final sintering process the solid state reaction

$$0.6\left[BaO\cdot 2NiO\cdot 8Fe_2O_3\right] + 0.4BaCO_3 + 0.4Co_2O_3 + 3.2Fe_2O_3$$
$$\longrightarrow BaO\cdot 2\left[Ni_{.6}Co_{.4}O\right]\cdot 8Fe_2O_3 + 0.4CO_2\uparrow + 0.4\,O_2\uparrow$$

takes place, forming the reaction product $(Ni_{.6}Co_{.4})_2W$ with the liberation of some gases. Final crystallite orientation is undisturbed from that of the Ni_2W crystals.

It was generally found that for the weakly anisotropic materials the Lotgering technique produced significantly better alignment than did the more conventional techniques. The anisotropy fields of fired samples oriented by the different techniques were in good agreement; the Lotgering technique produced samples with slightly higher values of anisotropy field. This is taken as an additional sign of improved alignment. (See discussion of Subsection II. 3. 3.) When this Lotgering technique is employed the material must be sintered long enough for the solid state reaction to transpire. During this time grain growth will also occur (as it must if this reaction is to be carried to completion), and the ultimate particle size will not be as small as that obtainable from the more conventional techniques.

SECTION IV

EVALUATION OF MATERIALS

1. DETERMINATION OF ORIENTATION

As a result of the continuing preparation study discussed in Section III, high quality ceramic materials with densities in excess of 90 per cent of the x-ray density could be reproducibly fabricated. A major problem in the fabrication process was that of orienting individual crystallites within the material. Much effort went into studying and improving the degree of orientation of these materials. The orientation achieved can be judged in several possible ways. A quick estimate of the degree of orientation can be made by noting the asymmetry in shrinkage that occurs on firing. In an oriented polycrystalline sample the shrinkage that occurs during sintering is much greater along the c-axis than in the basal plane. Thus any oriented sample will shrink asymmetrically. If a disc shaped sample is pressed with c-axes oriented in the plane of the disc, upon sintering it will take on an elliptical shape, and the degree of orientation can be estimated from the degree of ellipticity.

A second method of estimating the degree of orientation is by metallographic examination. If one is looking along the c-direction one sees hexagonal shaped plates. At 90^{o} to the c-direction, however, one sees apparently needle shaped grains which are in reality cross sections of the plates. The alignment can be estimated by observation of the departure from the ideal pattern.

Probably the most precise estimate can be obtained from studies of x-ray powder diffraction data taken on the material. If the x-ray beam is reflected from planes parallel to the basal plane, all (hkl) reflections except the (0 · 0 · l) reflections are extinguished. Thus in a completely oriented sample placed in the geometric arrangement shown in Fig. 17 only the (0 · 0 · l) reflections will be observed. In a non-oriented sample (hkl) reflections still occur. Thus the degree of orientation can be judged by comparing the x-ray diffraction pattern of the " unknown" sample with that of a randomly oriented sample of the same crystal structure. As alignment improves the ratio of the sum of the intensities of (00 l) reflections increases with respect to the intensities of (hkl) reflections.

The degree of alignment could most accurately be described by a distribution function that describes the number of crystals with c-axes at various angles to the desired direction as a function of that angle. While this would be the most exact method, it would also be an extremely tedious one. A semi-quantitative approach was instead adapted that yields a single number as an index of the degree of alignment.

This index is calculated as follows. The sum of intensities of all (hkl) and (00l) reflections of a randomly oriented sample is first calculated as is the sum of intensities of (00l) reflections. The ratio of these sums, p_o for a randomly oriented sample is then computed as $p_o = \frac{\sum 00l}{\sum hkl + \sum 00l}$ The same ratio is computed for an oriented

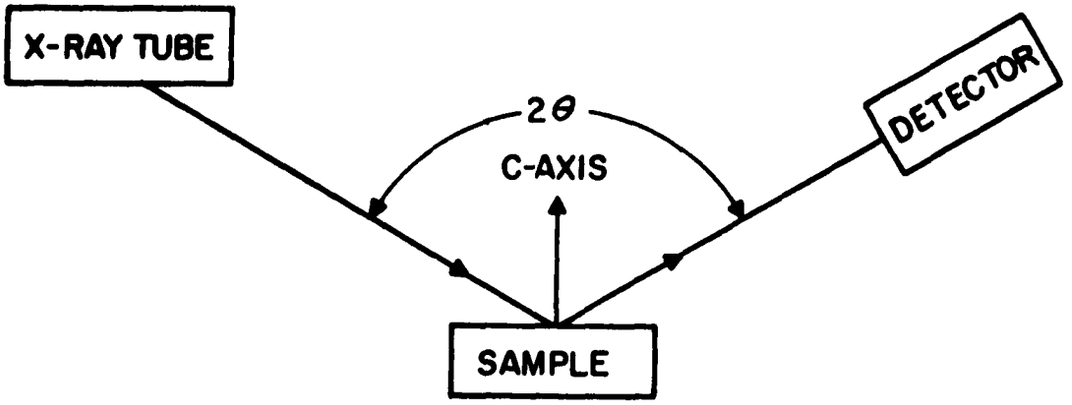

Figure 17. Geometric Arrangement used in X-ray Diffraction Measurements

sample and is denoted by p. As the alignment improves p varies from p_o (for random orientation) to 1.0 (for perfect alignment). As an index of orientation then we can use

$$f = \frac{p - p_o}{1 - p_o} \quad . \tag{4}$$

This quantity increases from 0 for random orientation to 1.0 for perfect alignment and is the same quantity used by Lotgering.[19]

In determining values of p_o it is important that the sample have truly <u>random</u> orientation of crystallites. In preparing this random sample care must be exercised to avoid the accidental occcurance of preferred orientation among the plate shaped grains. Care should also be exercised in taking patterns on oriented material (as well as unoriented) to grind away the surface layer so that the diffraction pattern is characteristic of the true volume of the material. The surface may contain crystallites of extraneous orientations and in some cases extraneous compositions. (The later condition has been occasionally observed and is believed due to the occurance of a minor reaction between the ceramic material being fired and the boat in which it is contained.) In the present effort the surface layers of all materials were removed before diffraction, resonance, or device work was begun.

In the current program x-ray diffraction patterns were recorded on a General Electric XRD-5. Sample patterns indicating orientation indices of 0, 0.74, and 0.95 are shown in Fig. 18. For low

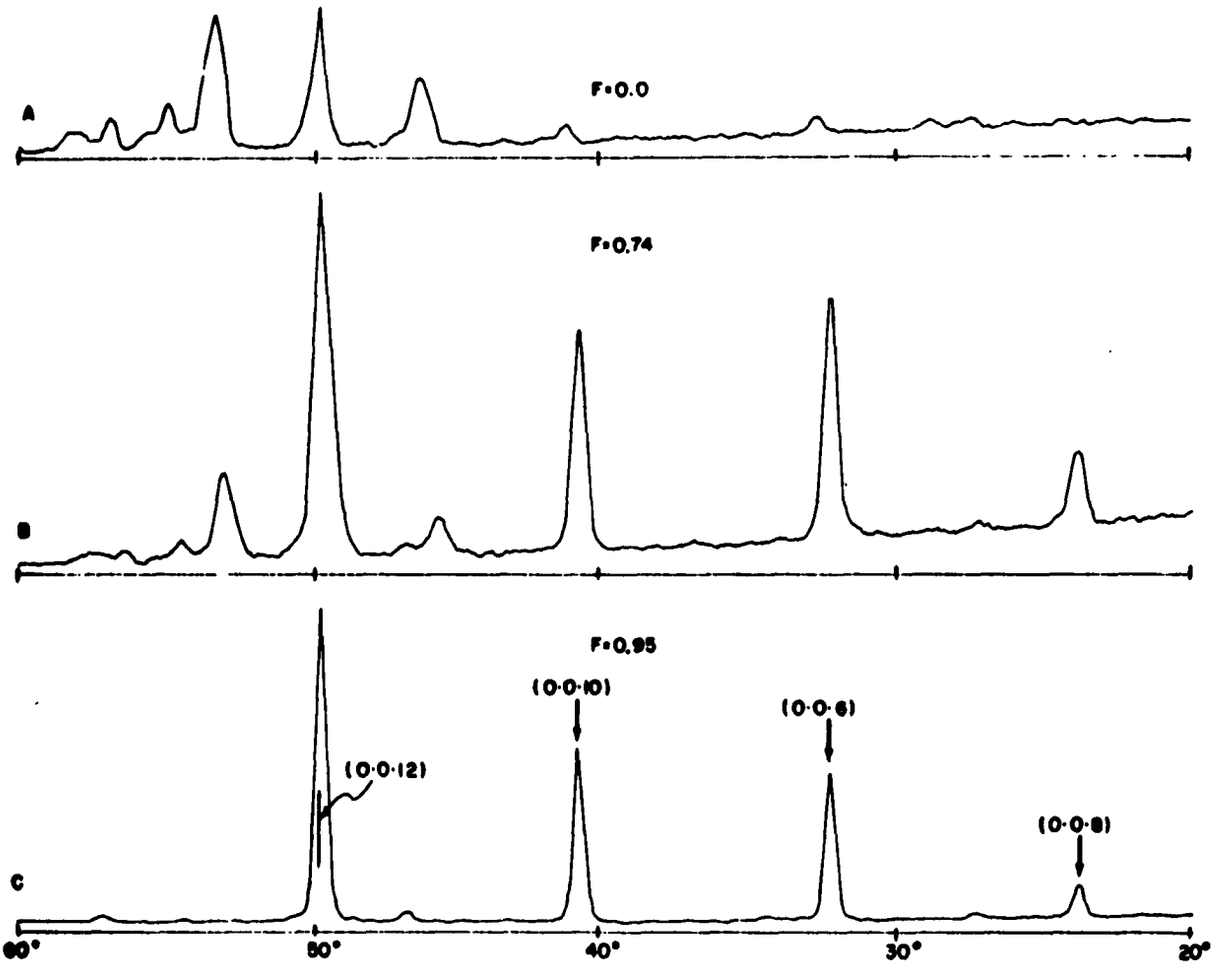

Figure 18. X-Ray Diffraction Pattern on Materials with Orientation Indices of (a) 0.0, (b) 0.74, and (c) 0.95

degrees of alignment some (hkl) reflections overlap (001) reflections and hence contribute some inaccuracy to the lower indices. With regard to Fig. 18 it should be remembered that relative intensity rather than absolute intensity is important here. Note the almost complete absence of (hkl) reflections on the lower trace for $f = 0.95$.

One final method of determining degree of alignment on oriented materials is through examination of the microwave absorption characteristics of the material. The more completely aligned the material, the more narrow its resonance absorption line. Good alignment is also indicated by the presence of only one peak in absorption and by a generally low level of absorption at points away from the main resonance absorption line. This absorption study is only a qualitative test, and not as accurate as the x-ray technique.

During this program no detailed study of the dielectric loss tangents was conducted. The few measurements made indicate loss tangents of the order of 0.03 as measured at 20 mc. If this loss remains at this level up to K and V bands this could account for most of the insertion loss observed in the devices discussed in Section V. As a general rule, however, dielectric loss tangents decrease monatonically with frequency in the microwave range.

2. MEASUREMENT OF SATURATION MAGNETIZATION

Measurements of saturation magnetization were made using a vibrating sample magnetometer [20] shown in Fig. 19 and in the diagram of Fig. 20. The measurement is based on the detection of the ac magnetic field set up by the vibrating magnetic sample. A small sphere of the unknown material is placed in a strong saturating dc magnetic field. The sample is vibrated at a low audio frequency (~ 100 cps) and the oscillating dipole field thus generated is detected by two coils so positioned as to minimize stray pickup. This dipole field is nulled with a signal generated in two similar coils by a permanent magnet attached to the same vibrating rod. The system is calibrated by using a nickel sphere as the "unknown".

The result of magnetization measurements made on spheres of the BaO $2\left[Ni_{1-x}Co_xO\right]\cdot 7.8Fe_2O_3$ series are shown in Figs. 21 through 27 for x = 0.0, 0.05, 0.10, 0.20, 0.25, 0.30, 0.40, and 0.50. The alignment index is shown for each. The magnetization of these materials is almost independent of cobalt content. Measured values do, however, vary with alignment. Some of the poorly aligned materials with high anisotropy fields (see Figs. 21, 24, and 25) exhibit magnetization curves that indicate incomplete saturation of the material. This may account for the lower saturation magnetization of those materials. The incomplete saturation undoubtedly arises from the fact that misaligned crystallites of the highly anisotropic material are not saturated by the

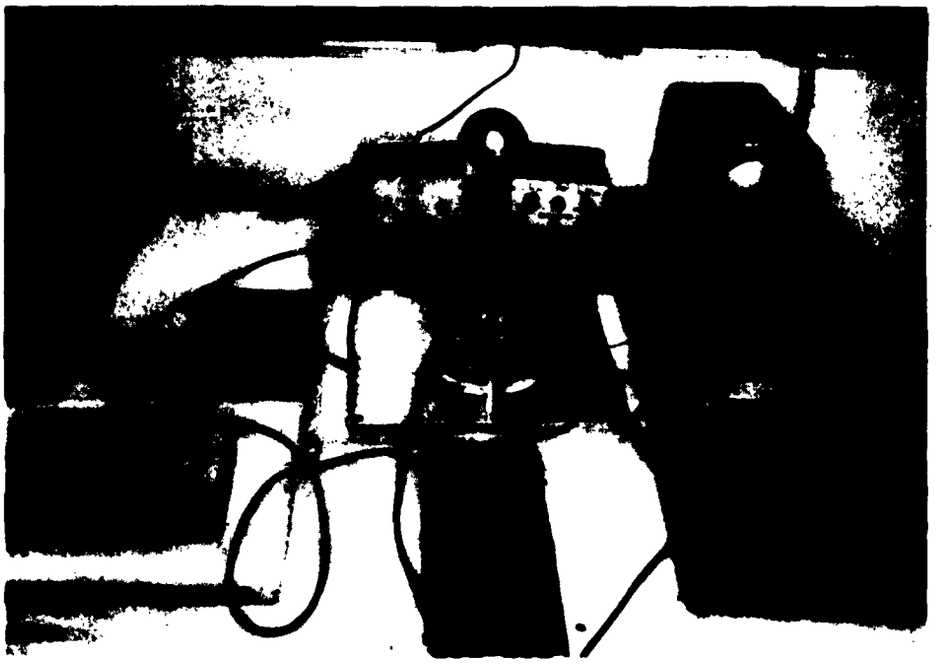

Figure 19. Upper Photo - X-ray Diffractometer
Lower Photo - Vibrating Sample Magnetometer

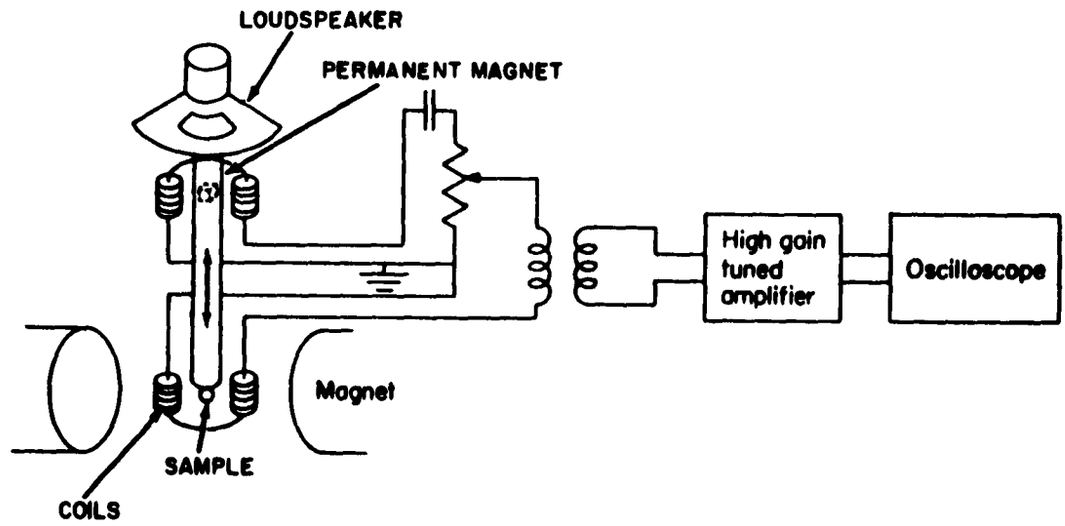

Figure 20. Block Diagram of Vibrating Sample Magnetometer

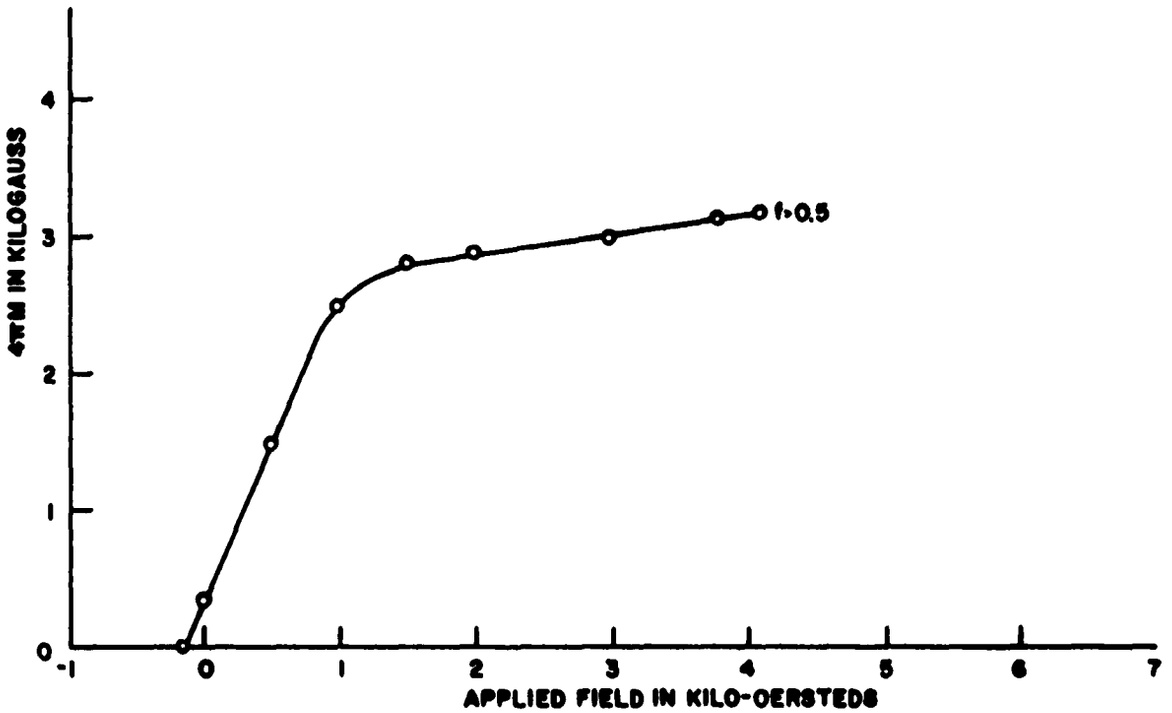

Figure 21. Demagnetization Curve for Ni_2W. Sample No. H35-3AB
Alignment Index Indicated

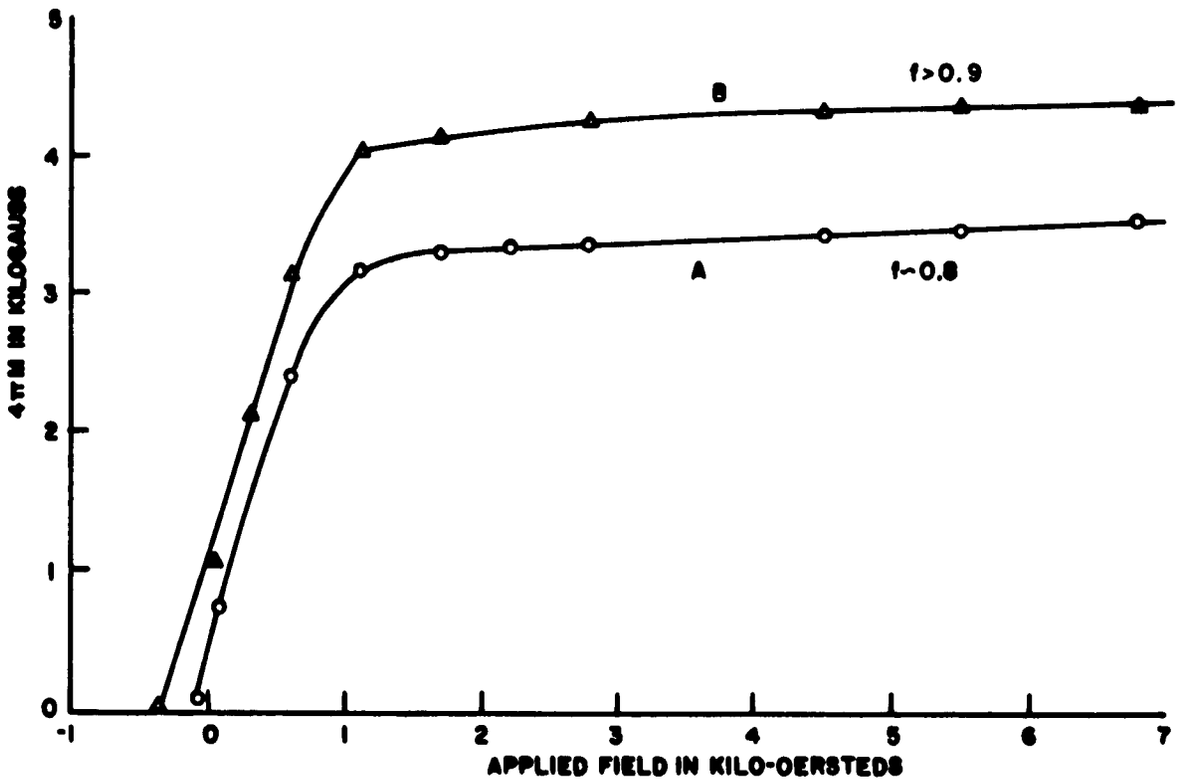

Figure 22. Demagnetization Curves for $(Ni_{.95}\ Co_{.05})_2 W$
Sample Nos. (a) H36A, (b) H36R
Alignment Indices Indicated

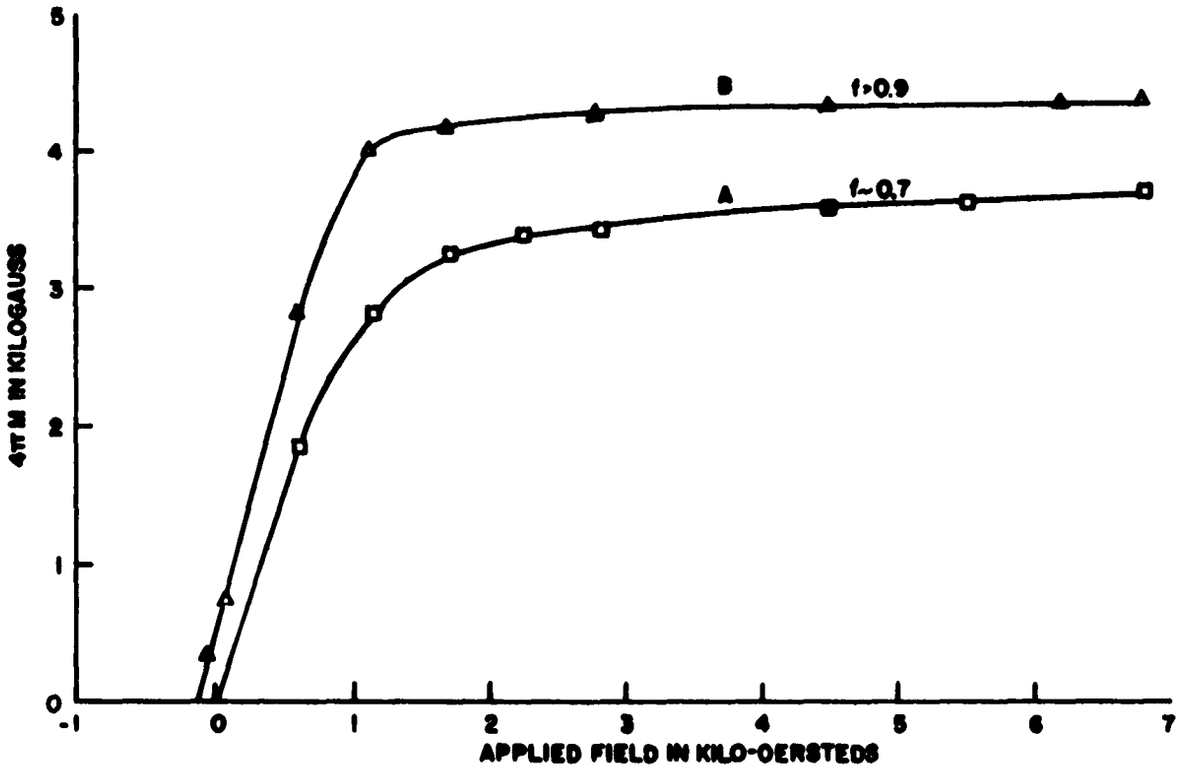

Figure 23. Demagnetization Curves for $(Ni_{.9}Co_{.1})_2W$.
Sample Nos. (a) H37C, (b) H38J
Alignment Indices Indicated

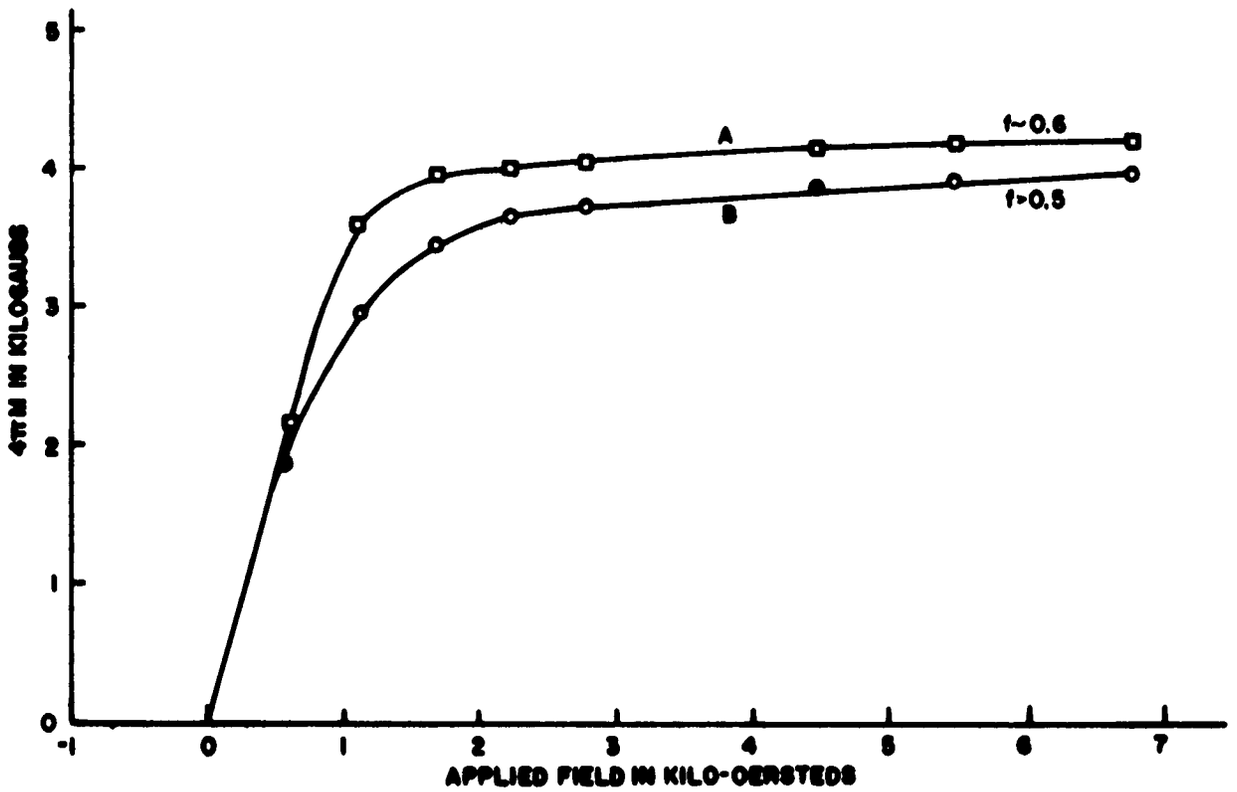

Figure 24. Demagnetization Curves for (a) $(Ni_{.8}Co_{.2})_2W$ Sample No. H39E, (b) $(Ni_{.7}Co_{.3})_2W$, Sample No. H40E Alignment Indices Indicated

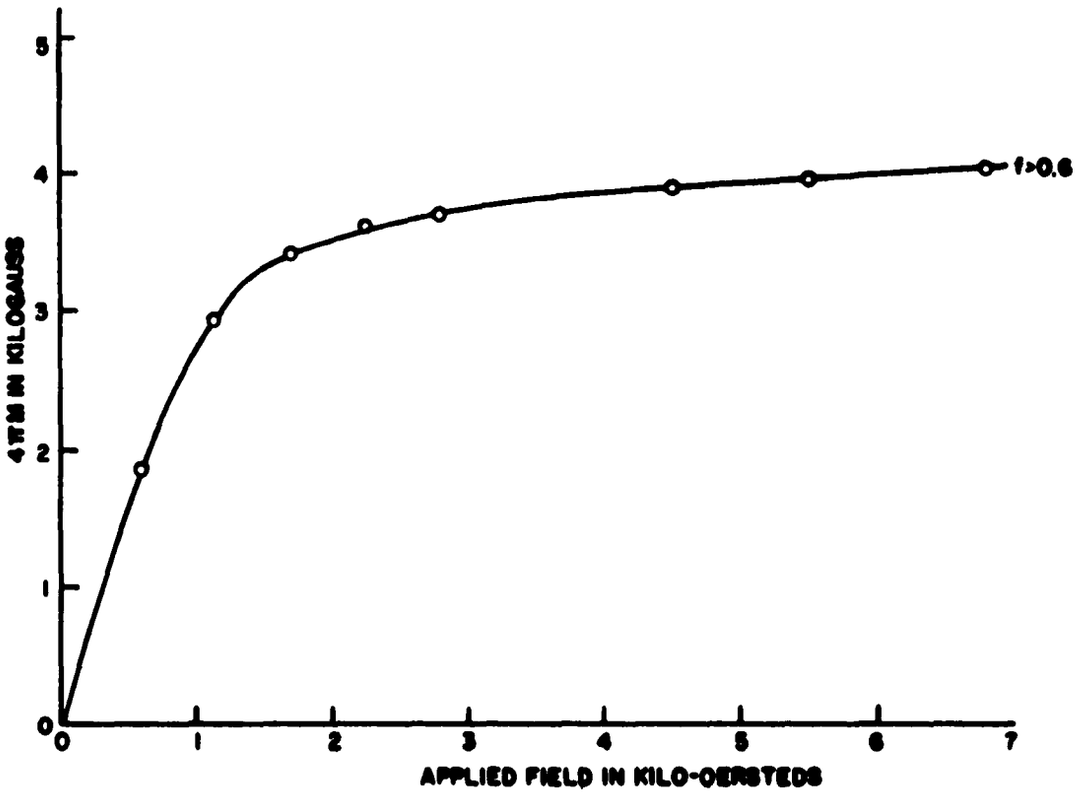

Figure 25. Demagnetization Curve for $(Ni_{.75}\ Co_{.25})_2 W$,
Sample No. H46B
Alignment Index Indicated

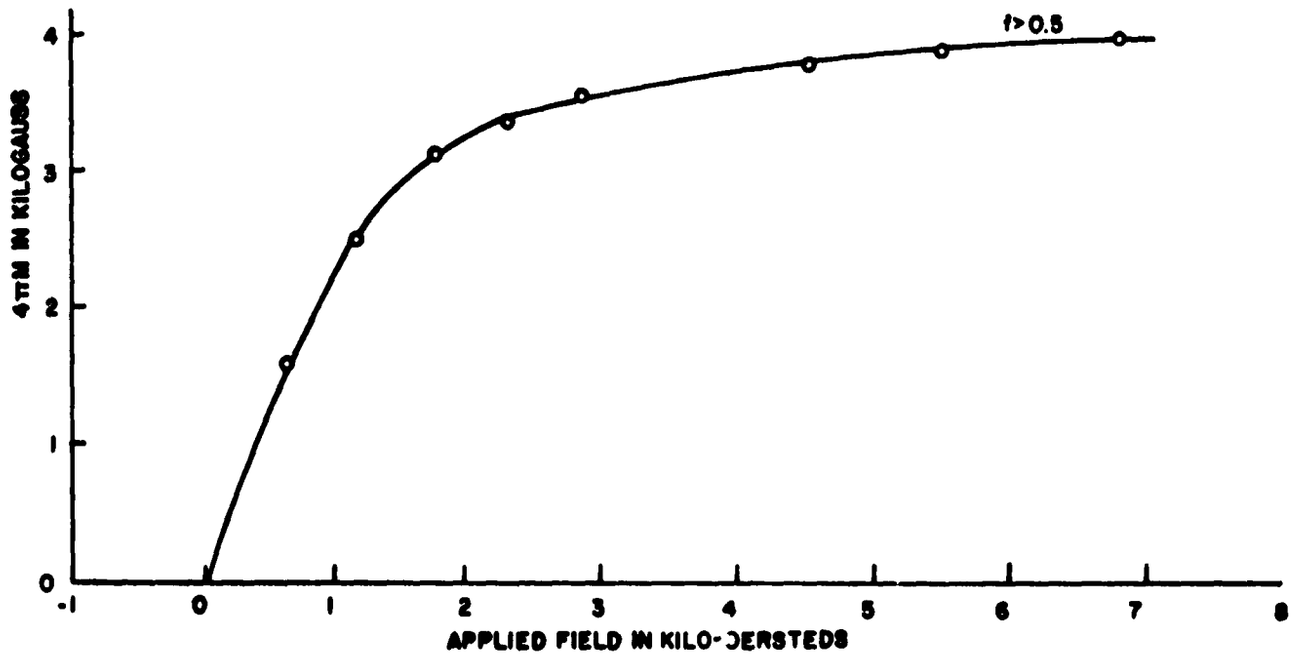

Figure 26. Demagnetization Curve for $(Ni_{.6}Co_{.4})_2W$, Sample No. H43D Alignment Index Indicated

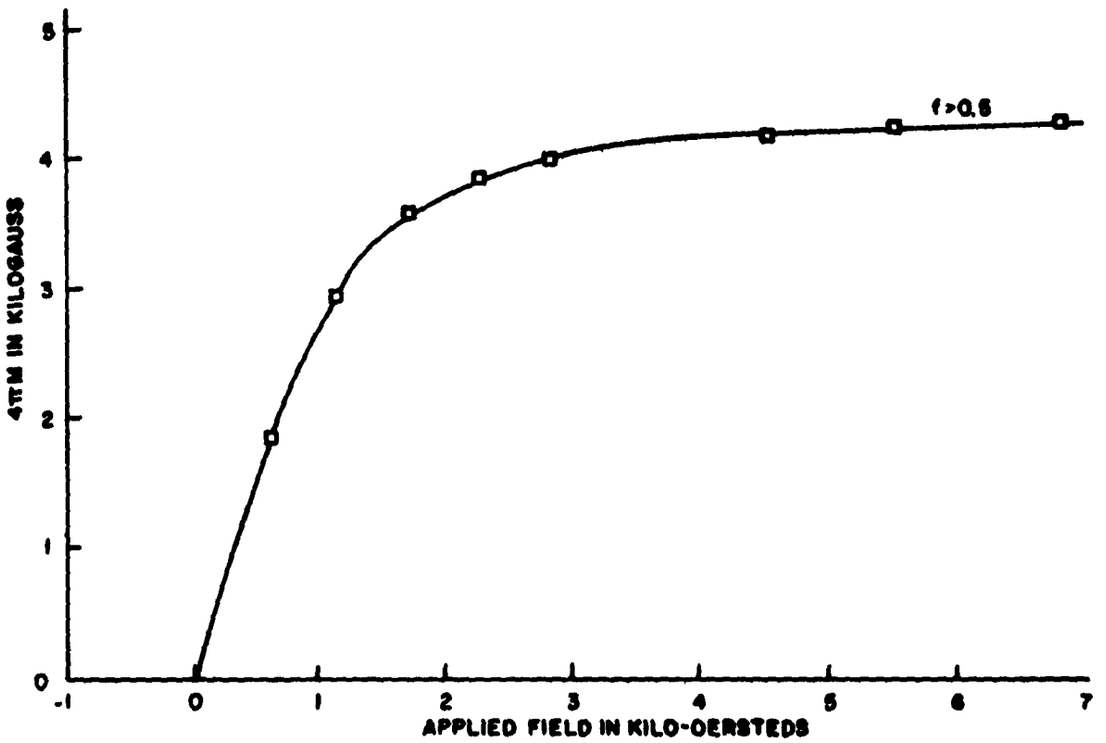

Figure 27. Demagnetization Curve for $(Ni_{.5}Co_{.5})_2W$, Sample No. H45B Alignment Index Indicated

d-c applied field since this field (6800 oe) is not large enough to overcome the anisotropy field of the materials. All data were taken on spherical samples with easy axis parallel to applied field.

The effect of particle size on coercive force and hence permanent magnet properties is seen in Fig. 22. The data of curve A were taken on a sample with average particle size of approximately 7 microns and indicate a coercive force of approximately 100 oe. as measured on a sphere. The data of curve B were obtained on a sample run through the attritor mill whose average particle size was approximately 2 microns. The latter material has a coercive force of approximately 400 oe. as measured on a sphere and better permanent magnet properties.

3. MICROWAVE EVALUATION

3.1 Measurement Techniques

Ferromagnetic resonance studies were conducted on non-oriented samples of Co_2Z, Ni_2Z, Zn_2Z, Mg_2Z, Cu_2Z, Co_2Y, Ni_2Y, Zn_2Y, and Mg_2Y and on oriented samples of the $(Ni_{1-x}Co_x)_2W$ series. These measurements were for the most part carried out at 37.5 kmc with some measurements made at 25 kmc. Data obtained from measurements carried out at 25 kmc were in good agreement with that obtained at 37.5 kmc. The higher frequency facilitates the study of ferromagnetic resonance in materials with a wider range of anisotropy fields.

Data were obtained using a conventional ferromagnetic resonance spectrometer[21] using a reflection cavity. A block diagram of the equipment

is shown in Fig. 28, and this equipment is seen in the photograph of Fig. 29. By sampling the incident and reflected signal the reflection coefficient (and hence VSWR) of the cavity can be obtained. Perturbation calculations show a direct relation between the imaginary part of the diagonal component of the susceptibility tensor $\chi''xx$, and the Q of the cavity. Cavity Q is in turn directly related to the VSWR. Thus by monitoring the reflection coefficent of the cavity as a function of field one may obtain plots of $\chi''xx$ versus H. All such data shown here have been normalized to $\chi''xx/(\chi''xx)_{max}$. From these data the field required for resonance is obtained as well as the linewidth of the material. The latter quantity is defined as the field difference between points where $\chi''xx$ reaches one-half its maximum value. Linewidths measured in this way are independent of sample size so long as the sample is sufficiently small to allow the application of perturbation theory.

Measurements were made of the absorption spectra of oriented materials with the applied magnetic field both parallel and perpendicular to the c-axes (the easy direction). Such data are shown in Figs. 15 and 16. When the applied magnetic field is along the easy direction of magnetization of the material, Kittel's resonance equation becomes (for a spherical geometry)

$$\omega_{res} = \gamma(H_E + H_{an}) , \qquad (5)$$

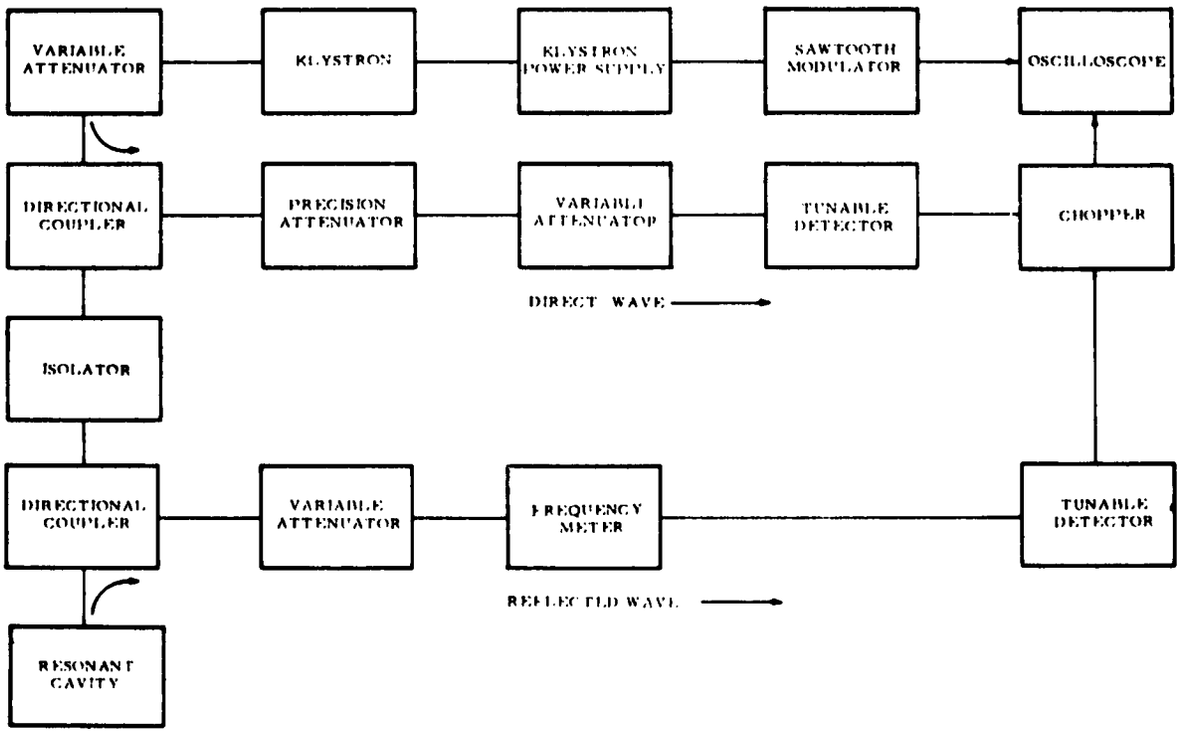

Figure 28. Block Diagram of Ferromagnetic Resonance Spectrometer

Figure 29. Reflection Type Resonance Spectrometers in this Laboratory. Upper Photo Shows V- and K-band Set-ups, and Lower Photo Shows X-band Set-ups.

where H_E is the d-c field required for resonance along an easy direction.

With the applied field perpendicular to the easy direction (along a hard direction) the resonance condition becomes:

$$\omega_{res} = \gamma \sqrt{H_H(H_H - H_{an})} \quad , \tag{6}$$

where H_H is the d-c field required for resonance along the hard direction. These two equations can be solved simultaneously yielding,

$$H_{an} = \frac{-(2H_E + H_a) \mp \sqrt{(2H_E + H_a)^2 + 4(H_H^2 - H_E^2)}}{2} \tag{7}$$

and

$$g_{eff} = \frac{\gamma}{1.40} = \frac{\omega_{res}}{1.40\,(H_E + H_{an})} \tag{8}$$

where g_{eff} is the effective g-factor, and other quantities are as previously defined.

Microwave resonance measurements thus allow the computation of the material anisotropy field, effective g-factor, and linewidths along easy and hard directions as well as providing a further check on orientation.

3.2 Data Taken at Room Temperature

Resonance data recorded on unoriented samples of Co_2Z, Ni_2Z, Zn_2Z, Mg_2Z, Cu_2Z, Co_2Y, Ni_2Y, Zn_2Y, and Mg_2Y are shown in Figs. 30, 31, 32, 33, 34, 35, 36, 37, and 38 respectively. Such absorption spectra on unoriented polycrystalline samples are extremely difficult to

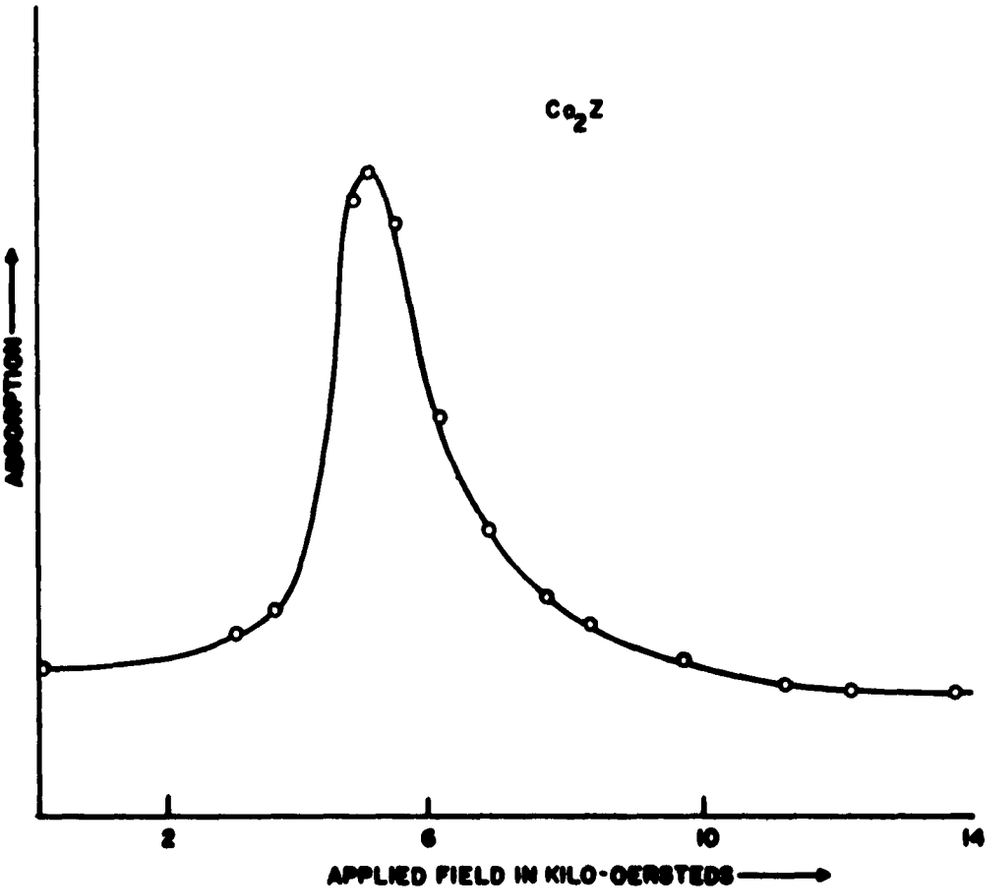

Figure 30. K-band Resonance Absorption Spectrum of Unoriented Co_2Z

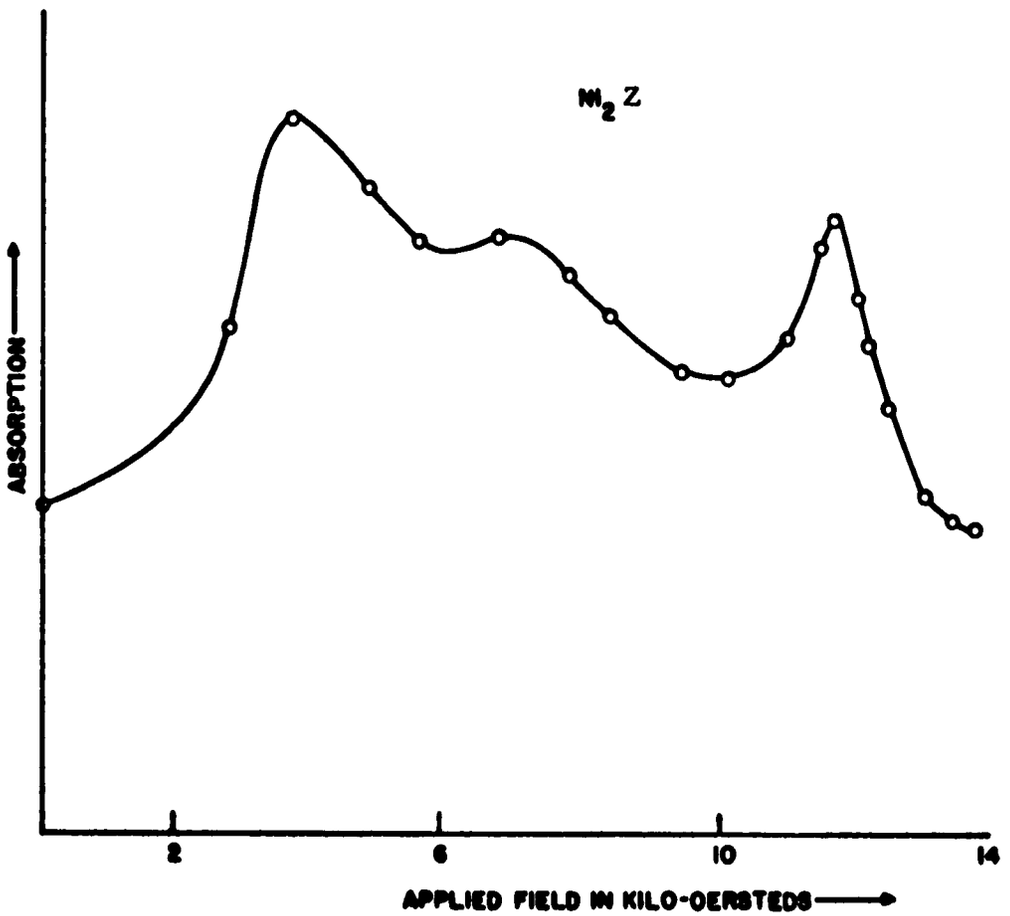

Figure 31. K-band Resonance Absorption Spectrum of Unoriented Ni_2Z

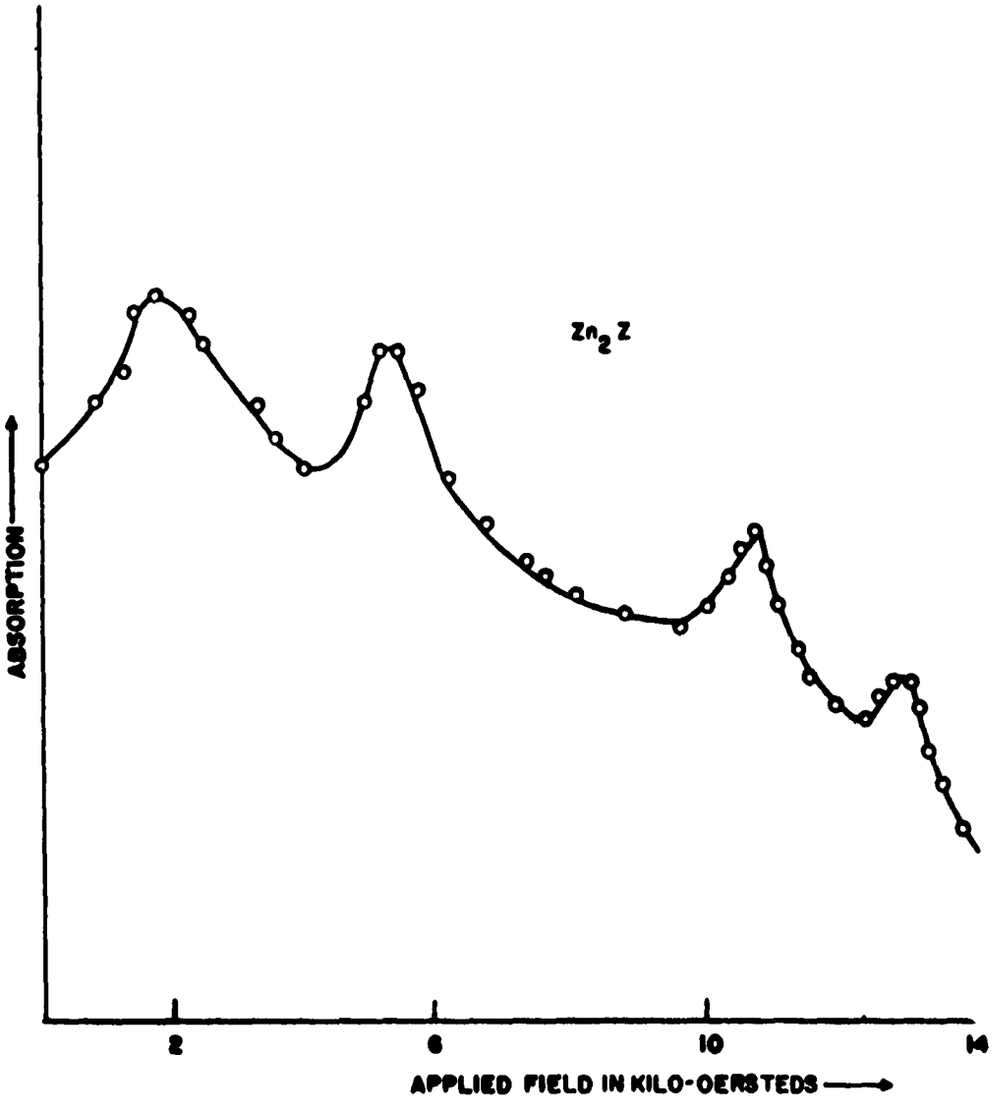

Figure 32. K-band Resonance Absorption Spectrum of Unoriented Zn_2Z

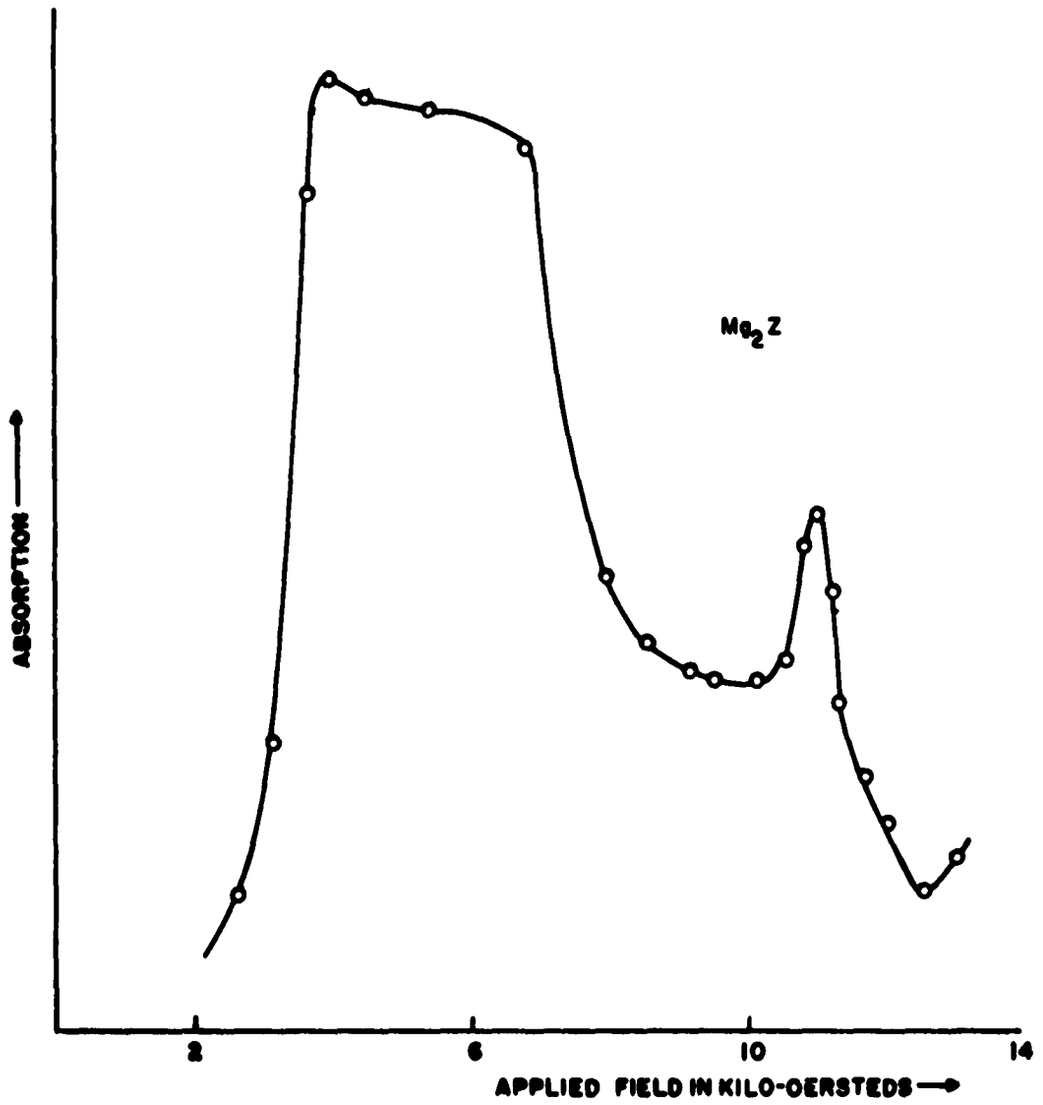

Figure 33. K-band Resonance Absorption Spectrum of Unoriented Mg_2Z

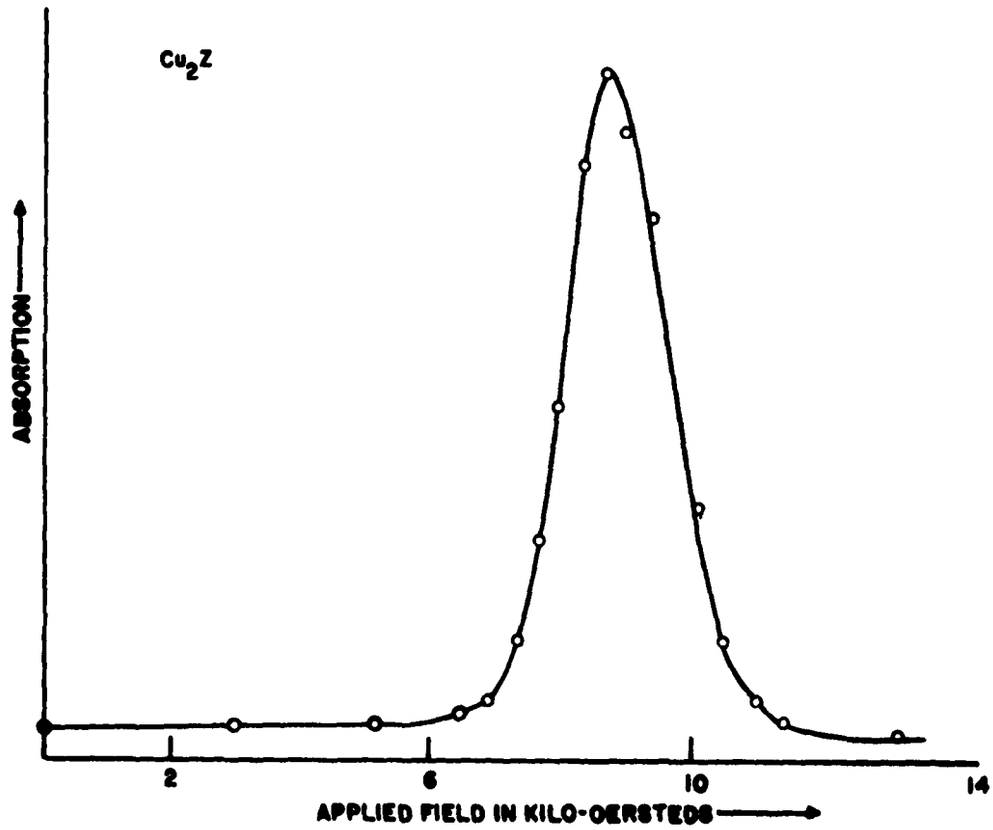

Figure 34. K-band Resonance Absorption Spectrum of Unoriented Cu_2Z

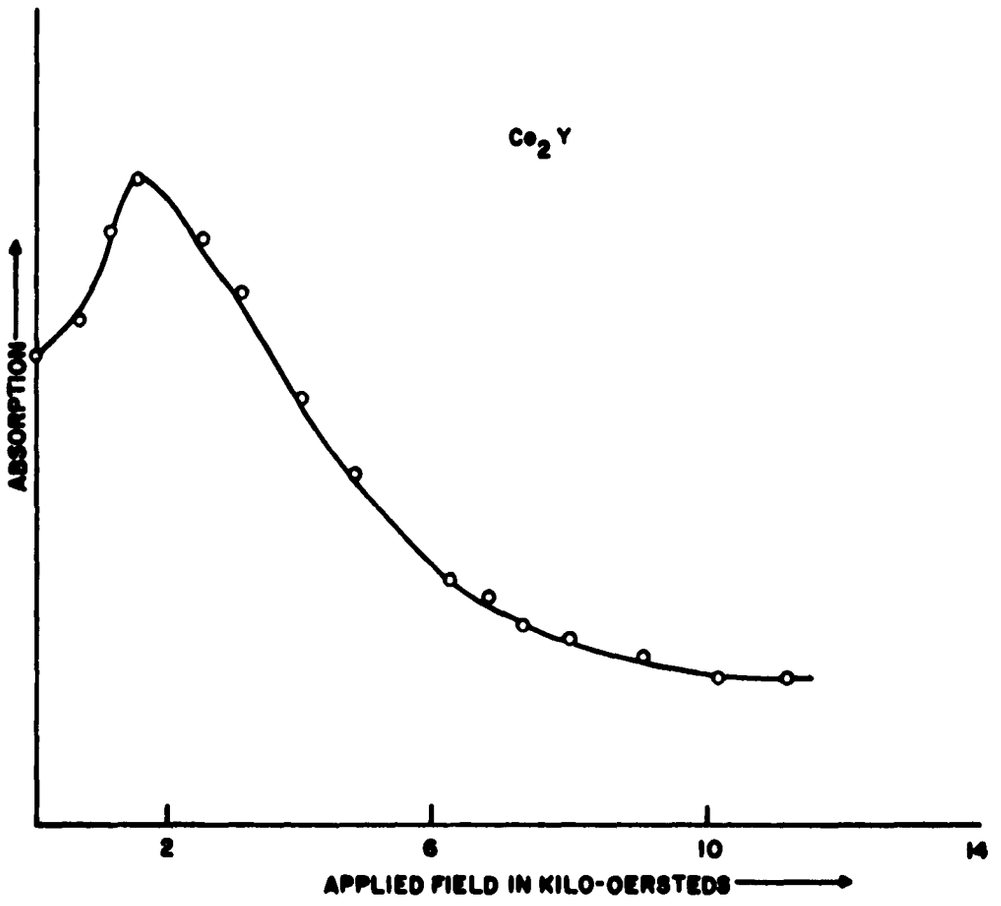

Figure 35. K-band Resonance Absorption Spectrum of Unoriented Co_2Y

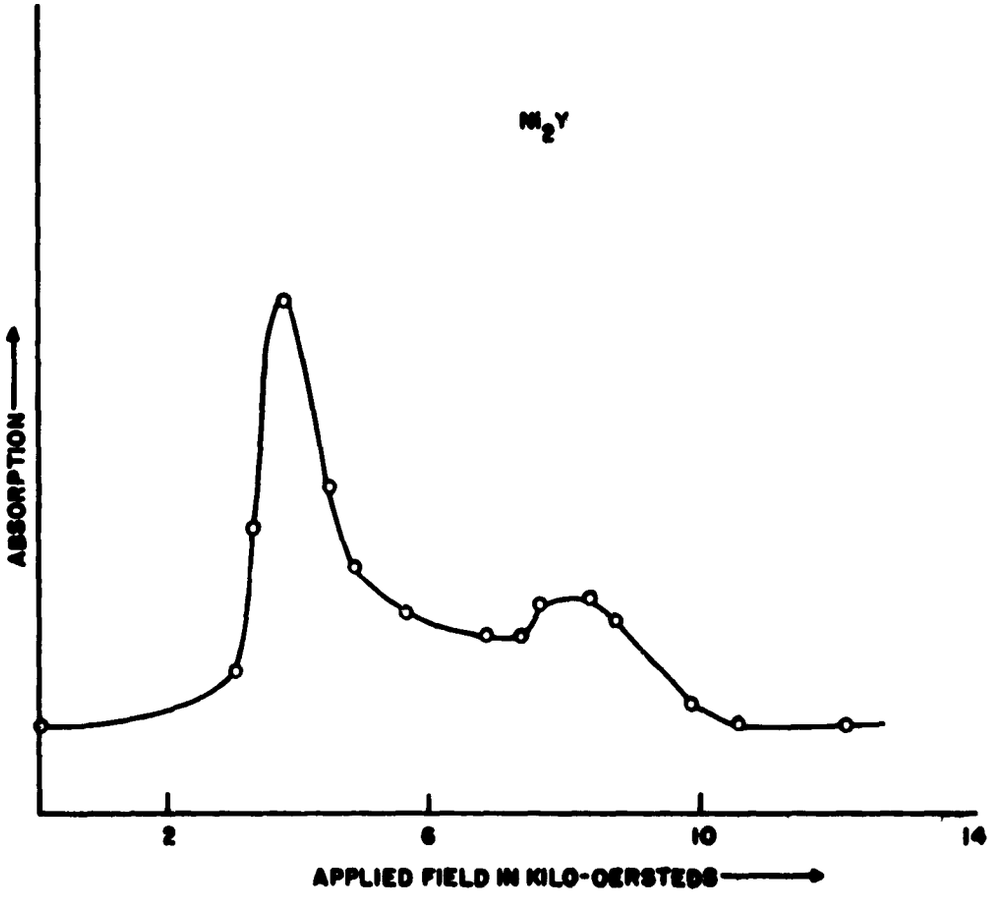

Figure 36. K-band Resonance Absorption Spectrum of Unoriented Ni_2Y

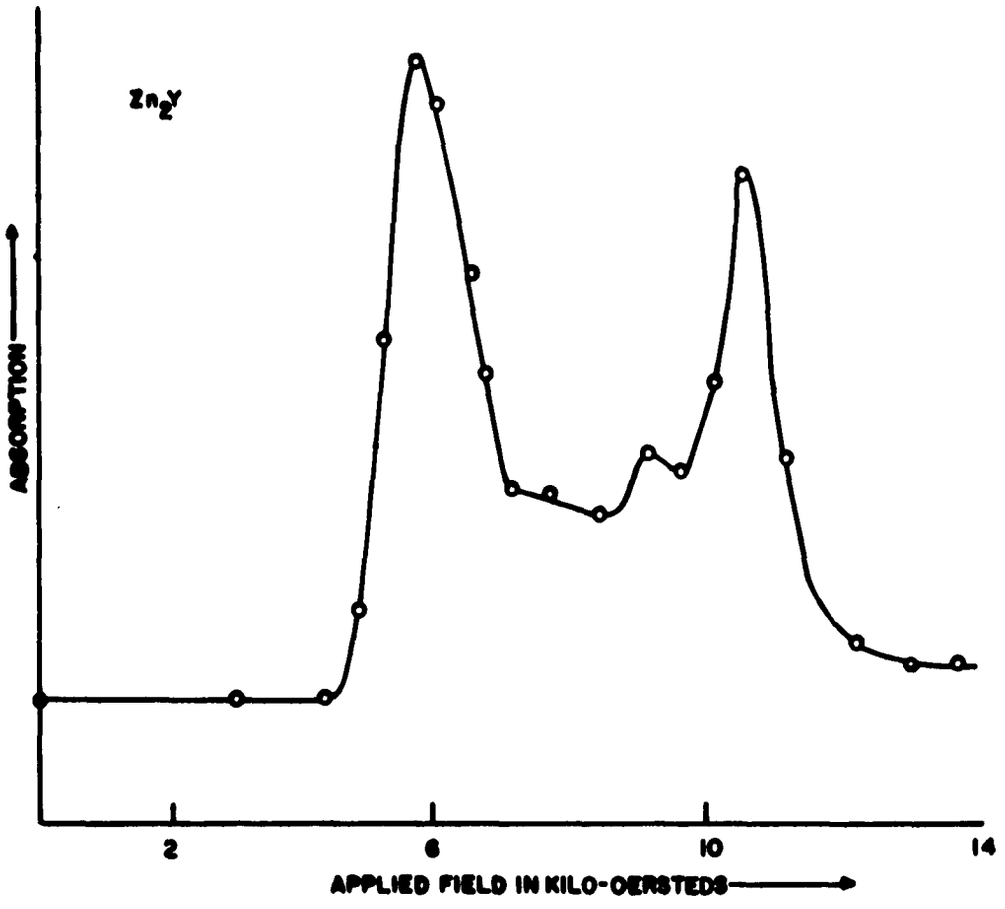

Figure 37. K-band Resonance Absorption Spectrum of Unoriented Zn_2Y

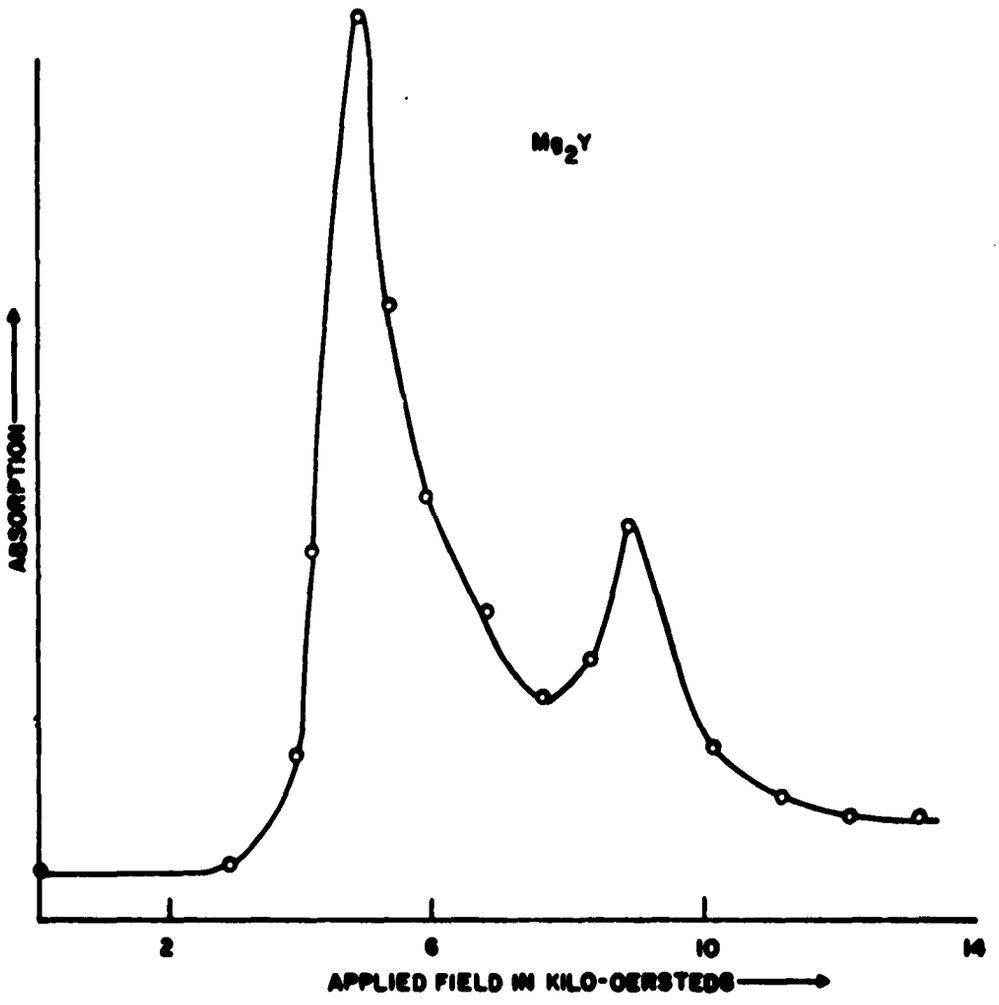

Figure 38. K-band Resonance Absorption Spectrum of Unoriented Mg_2Y

unravel, and only recently have theories[22] appeared that relate such spectra to fundamental parameters. Thus only the most general conclusions can be drawn from such data. While these data were taken at 25 kmc, absorption spectra measured at 37.5 kmc were found to be in in good agreement on all principle features. It appears that the planar materials (all Y materials and Co_2Z) have a less complex absorption spectra with better resolution of the resonance absorption line and perhaps narrower absorption lines in this unoriented state. Narrowest lines were found in the cases of Zn_2Y, Mg_2Y, Ni_2Y and Co_2Z and Cu_2Z.

A thorough resonance study was made of the series of solid solutions of Ni_2W and Co_2W. As previously pointed out it was thought that the substitution of cobalt for nickel in the W structure would make possible the control of the anisotropy field over a useful range of values. In order to determine experimentally the effects of such substitutions a series of W compounds of the formula $BaO \cdot 2\left[(1-x)NiO \cdot xCoO\right] \cdot 7.8Fe_2O_3$ were prepared and investigated with $0 \leq x \leq 0.5$. It was found that this series permits the accurate control of the anisotropy field from 0 to 12.7 kilo oersteds.

This series of materials was prepared and oriented by the techniques described in Section C. Densities of approximately 90 per cent of the x-ray density were obtained on these materials. Resonance absorption spectra taken at 37.5 kmc on samples of $BaO \cdot 2\left[(1-x)NiO \cdot xCoO\right] \cdot 7.8Fe_2O_3$ with x = 0, 0.05, 0.10, 0.20, 0.25, 0.30, 0.40 and 0.50 are

shown in Figs. 39, 40, 41, 42, 43, 44, 45, and 46 respectively. Each figure shows absorption spectra taken with H_{dc} both parallel and perpendicular to the easy direction, i. e., the c-axes of the crystals. From these data and equations (7) and (8) the effective anisotropy field and g-factor can be calculated for each of these materials. These values are tabulated in Table 4 together with measured linewidths of the resonance absorption curves for H_{dc} along both the easy (ΔH_e) and hard (ΔH_h) directions.

The linewidth exhibits no systematic dependence on cobalt content, but depends strongly on degree of orientation. The best aligned materials (alignment index $f > 0.9$) exhibited linewidths of the order of 1500 to 1800 oe. While none of the particular samples listed in the table were that well aligned, such a high degree of alignment has been obtained on the 5, 10, and 30 per cent cobalt substituted nickel W material. Moderate alignment ($0.8 > F > 0.6$) resulted in linewidths of 2000 to 3000 oe., while poor alignment ($f < 0.5$) resulted in arbitrarily large breadth (> 7000 oe.) In the case of well aligned samples where the resonance line was of approximate Lorentzian shape the widths measured along easy and hard directions were approximately equal. For the poorly aligned samples it was frequently difficult to resolve clearly the resonance line along one or the other of these directions.

The variation of anisotropy field with cobalt content is shown in Fig. 47 and the dependence appears to be almost linear. Virtually

TABLE 4

Resonance properties of $BaO \cdot 2(Ni_{1-x} Co_x O) \cdot 7.8Fe_2O_3$ at 37.5 kmc

x	Sample No.	H_{res_e} (oe.)	H_{res_h} (oe.)	H_{an} (oe.)	g_{eff}	ΔH_e (oe.)	ΔH_h (oe.)
0.00	H-35-3A3	200	20,800	12,750	2.09	4,000	2,300
0.05	H-36A	1,400	20,800	12,060	2.00	3,000	2,600
0.10	H-38A	2,800	20,100	10,850	1.97	2,900	2,200
0.20	H-39C	5,100	18,500	8,500	1.97	2,400	3,000
0.25	H-46D	6,350	17,300	7,000	1.98	2,600	4,400
0.30	H-41D	8,200	17,000	5,700	1.93	2,600	3,500
0.40	H-43D	10,900	15,300	2,900	1.94	2,190	5,800
0.50	H-45B	12,500	13,800	850	2.01	2,700	2,800

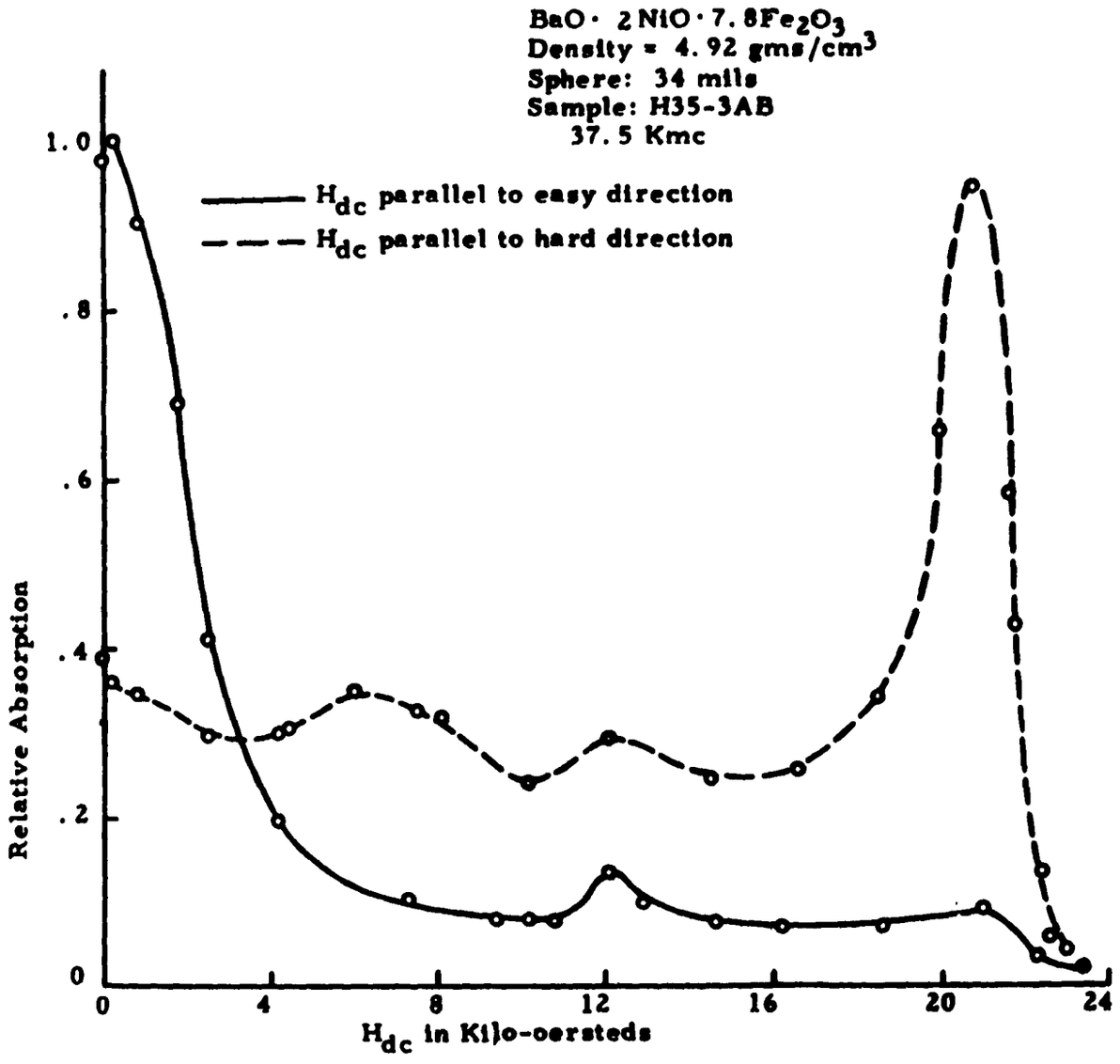

Figure 39. Ferromagnetic Resonance in a Sphere of Ni_2W at 37.5 kmc

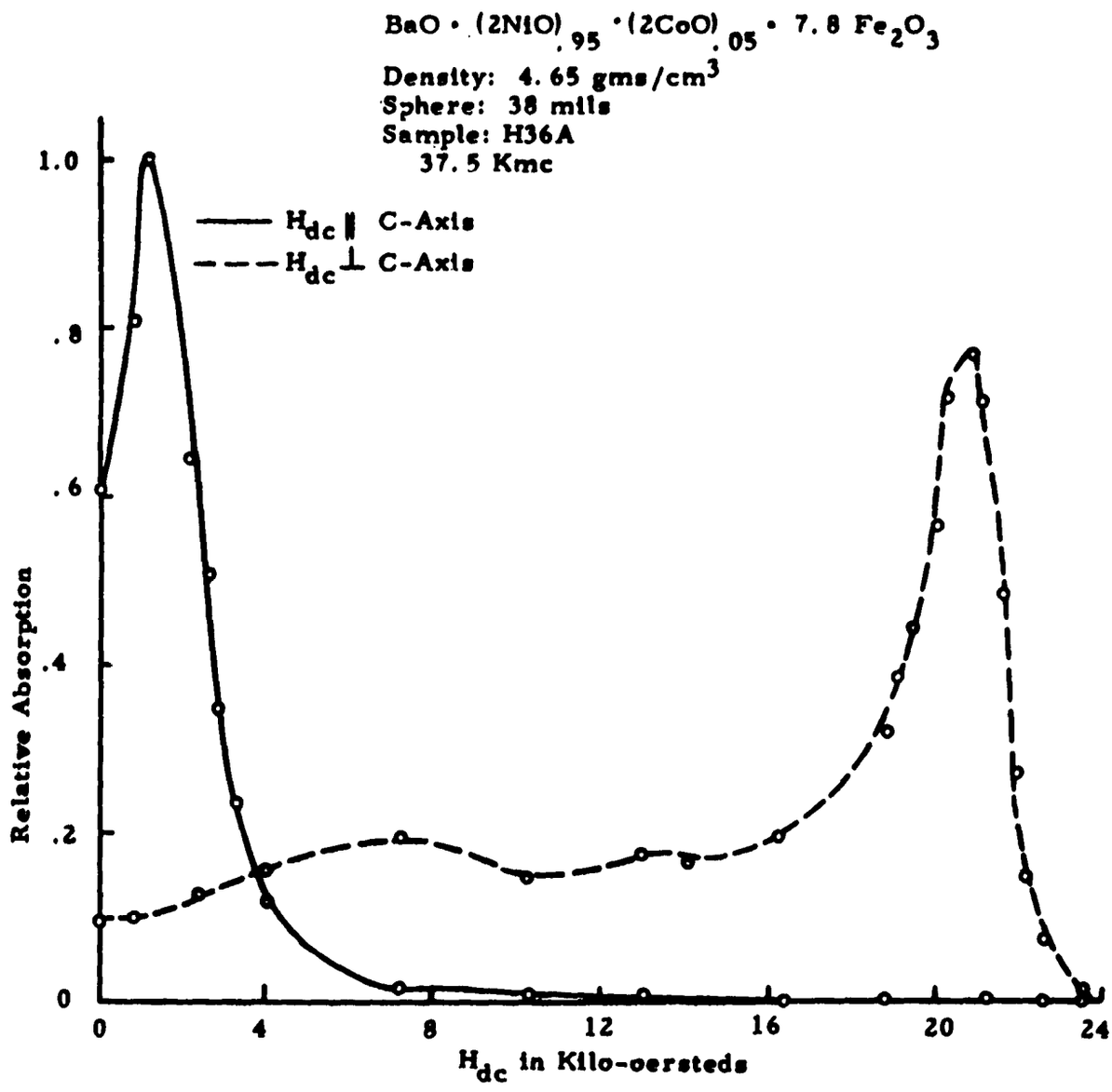

Figure 40. Ferromagnetic resonance in Sphere of $(Ni_{.95}Co_{.05})_2W$ at 37.5 kmc

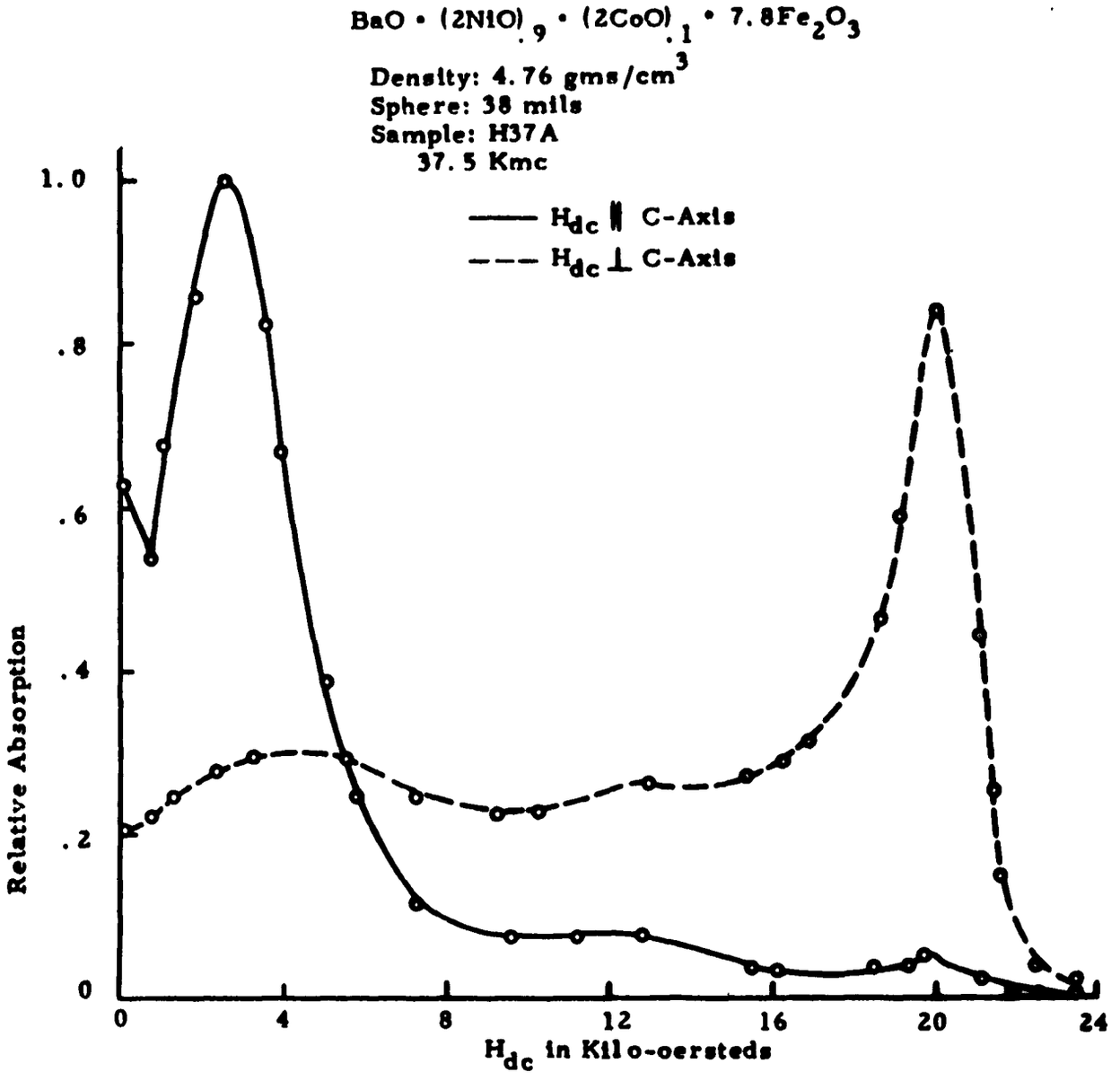

Figure. 41. Ferromagnetic Resonance in a Sphere of $(Ni_{.9}Co_{.1})_2W$ at 37.5 kmc

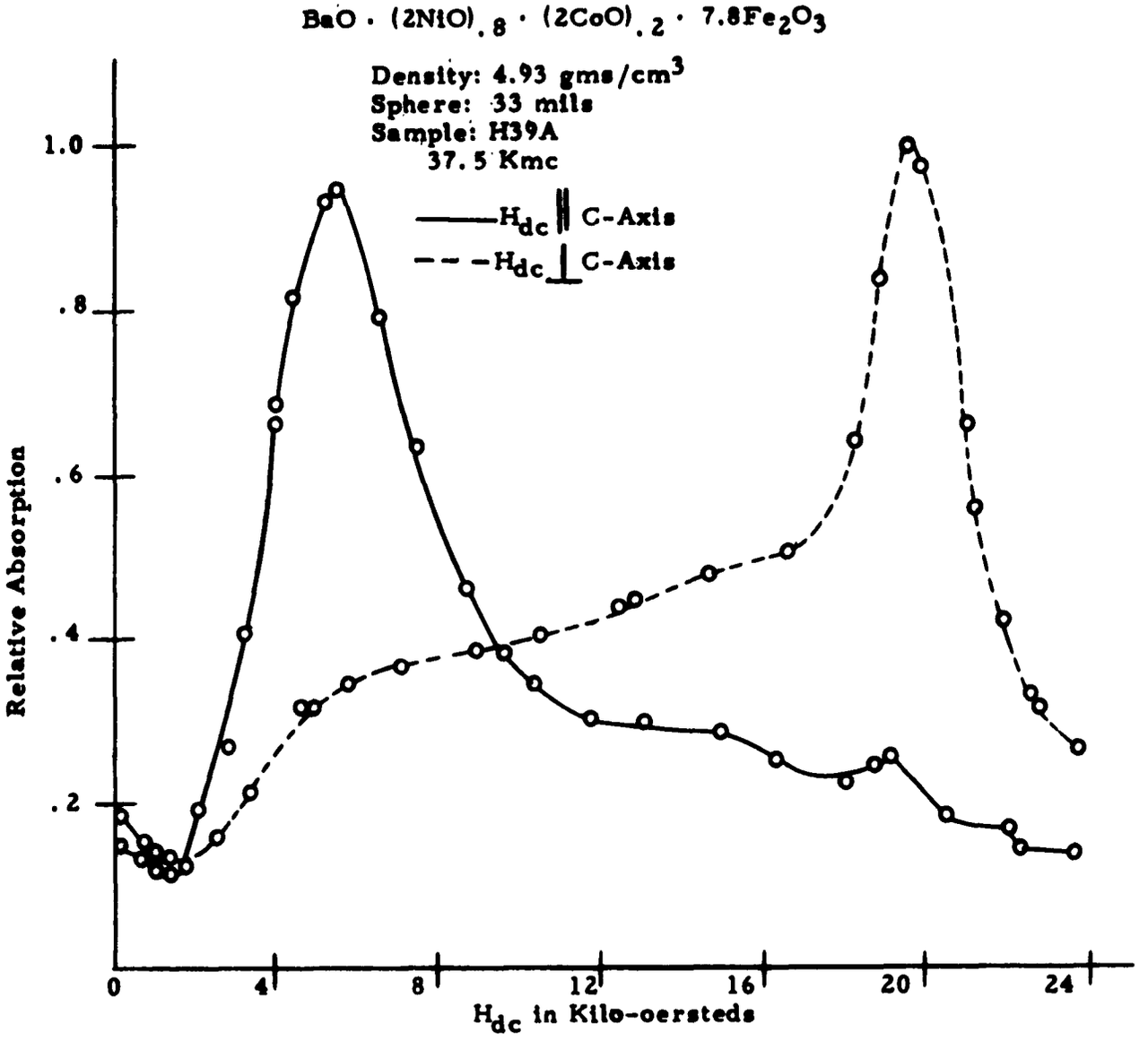

Figure 42. Ferromagnetic Resonance in a Sphere (Ni$_{.8}$Co$_{.2}$)$_2$W at 37.5 Kmc

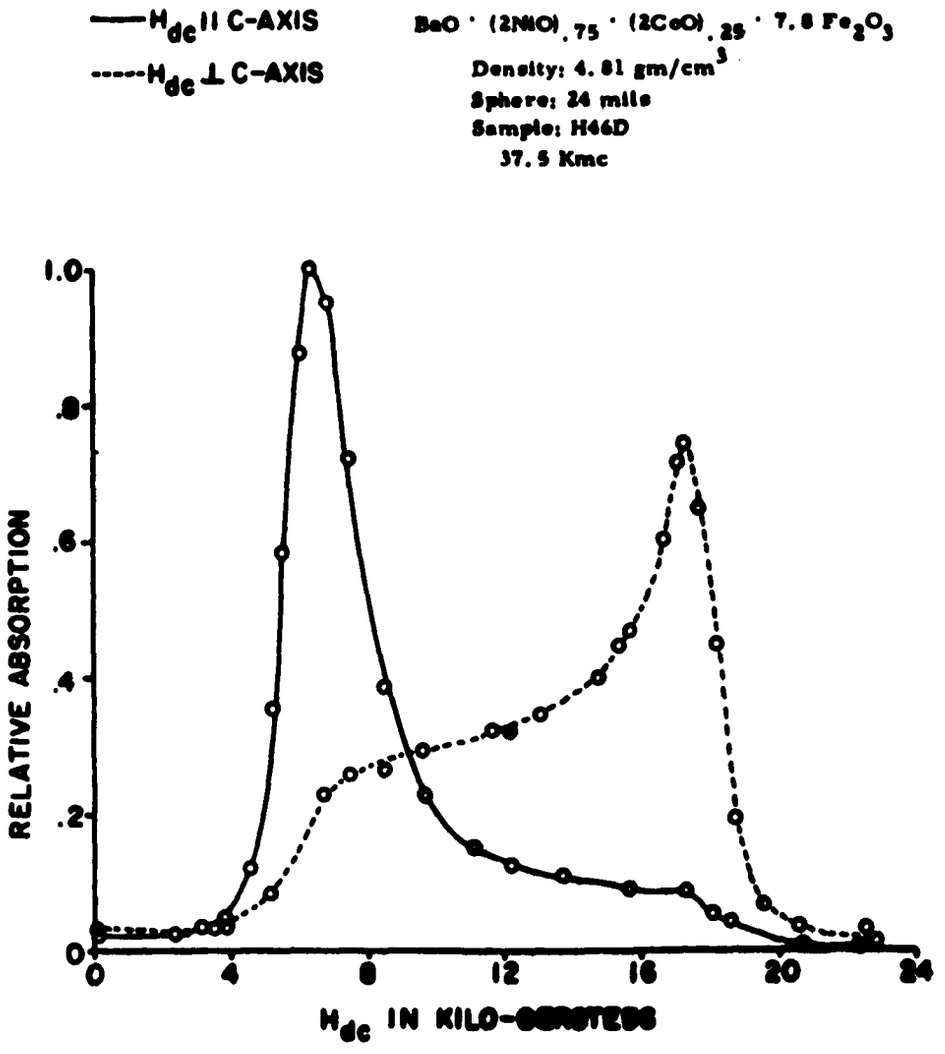

Figure 43. Ferromagnetic Resonance in a Sphere of $(Ni_{.75}Co_{.25})_2W$ at 37.5 kmc

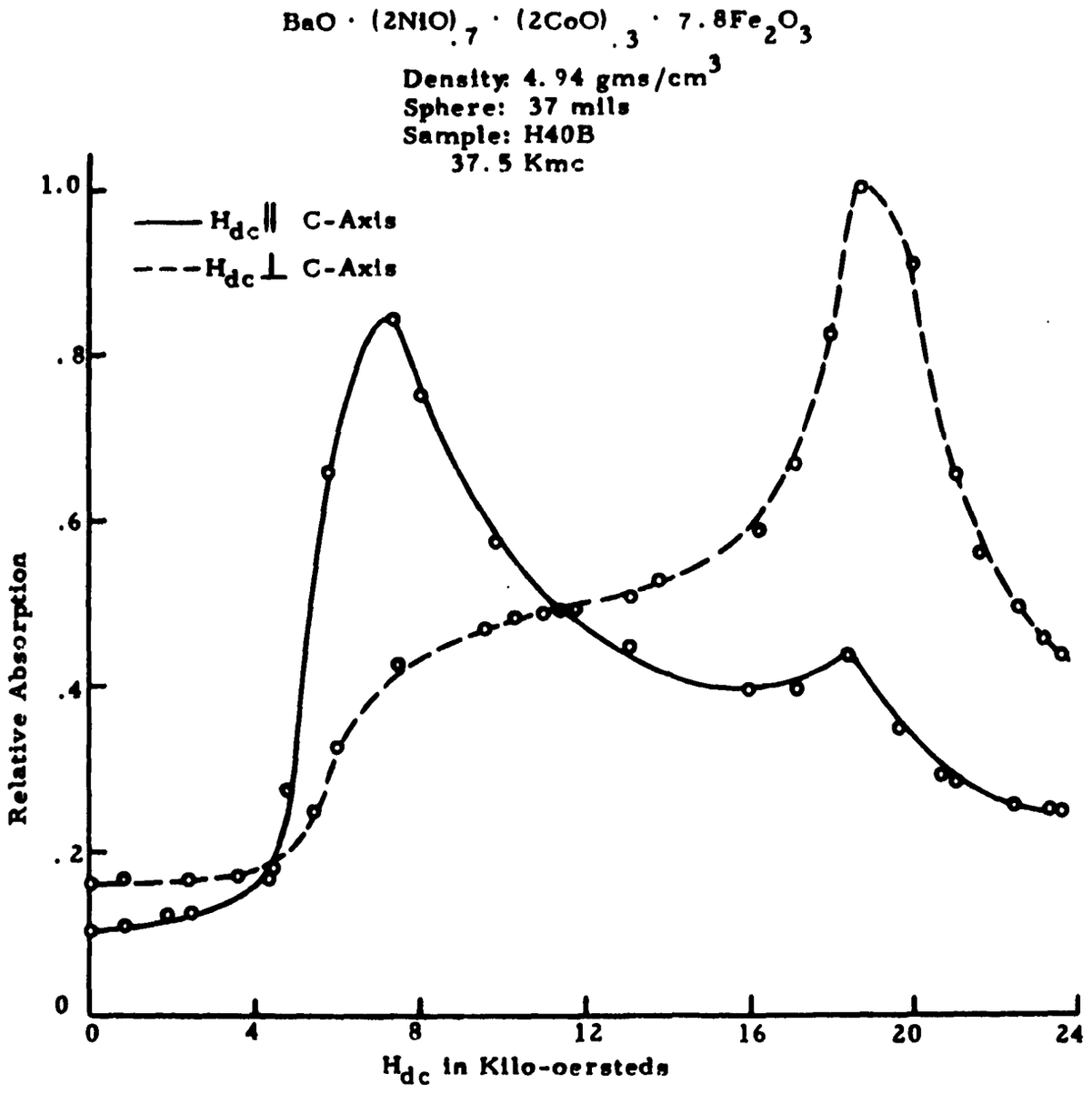

Figure 44. Ferromagnetic Resonance in a Sphere $(Ni_{.7}Co_{.3})_2W$ at 37.5 Kmc.

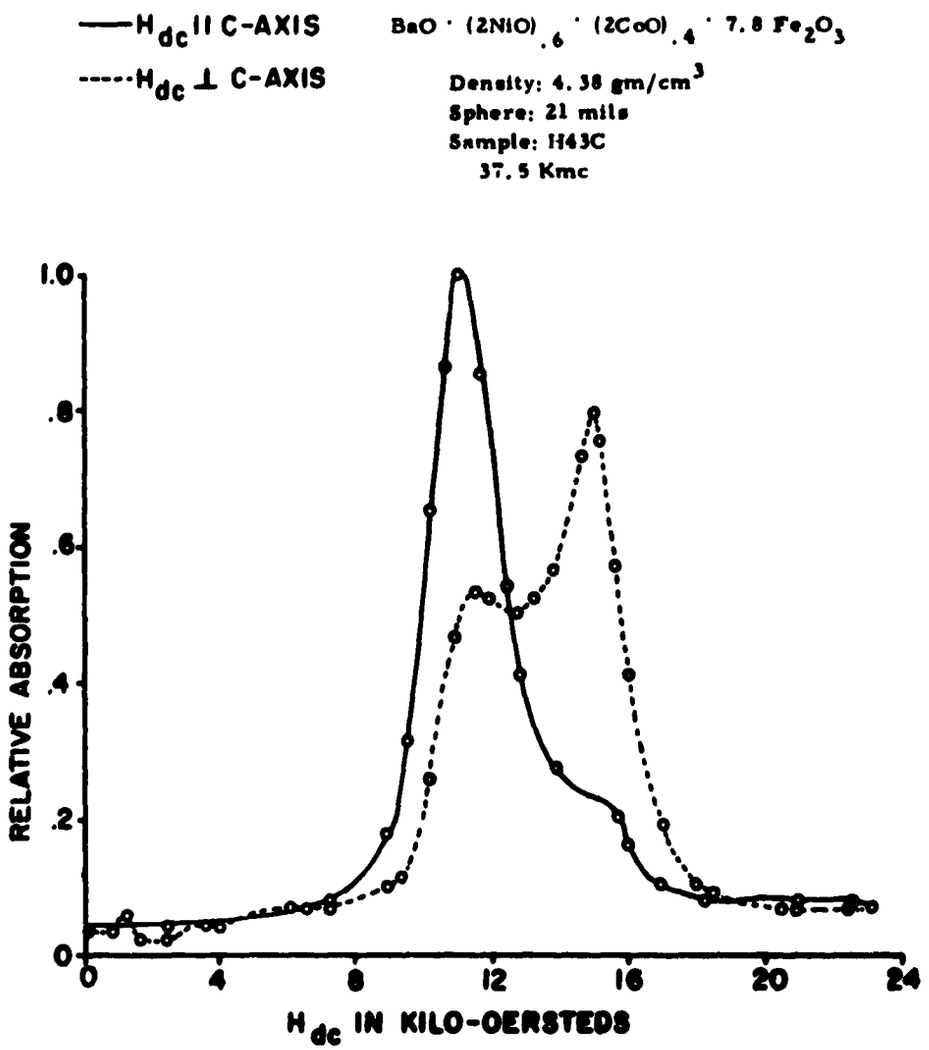

Figure 45. Ferromagnetic Resonance in a Sphere of $(Ni_{.6}Co_{.4})_2W$ at 37.5 kmc

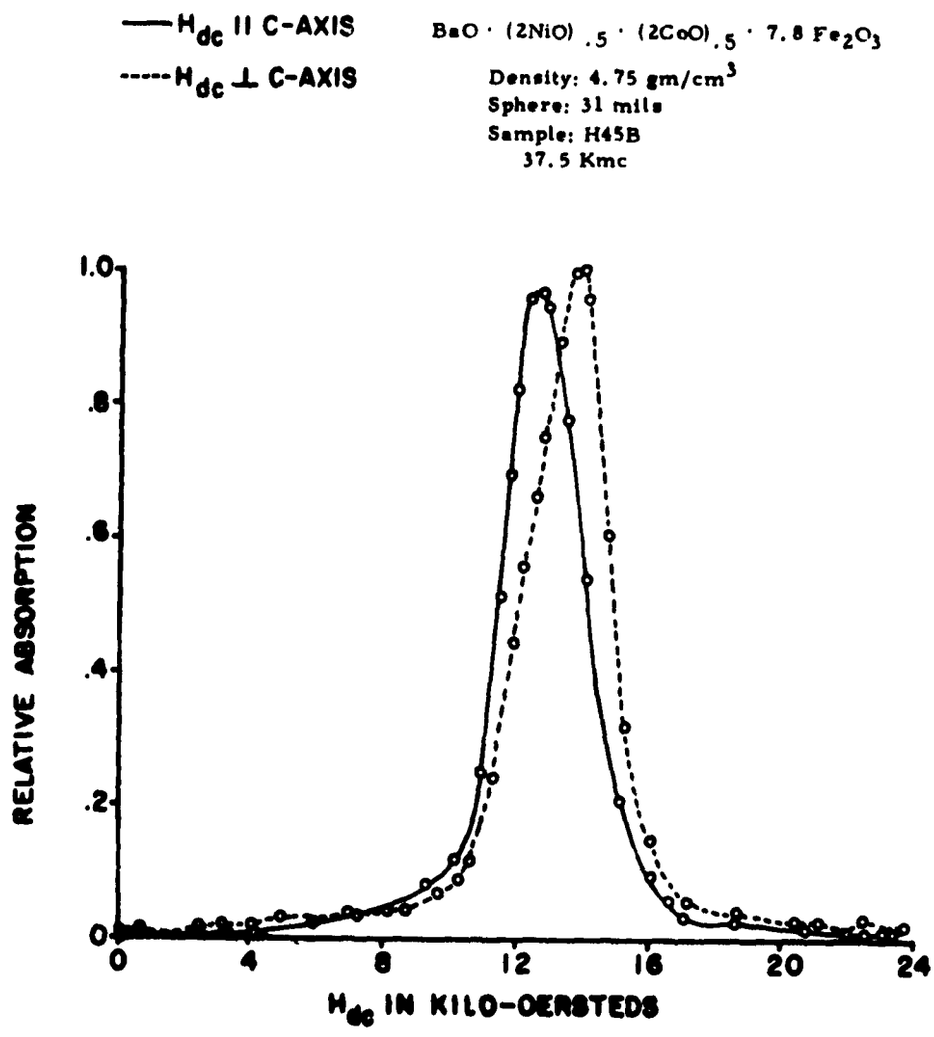

Figure 46. Ferromagnetic Resonance in a Sphere of $(Ni_{.5}\ Co_{.5})_2W$ at 37.5 kmc

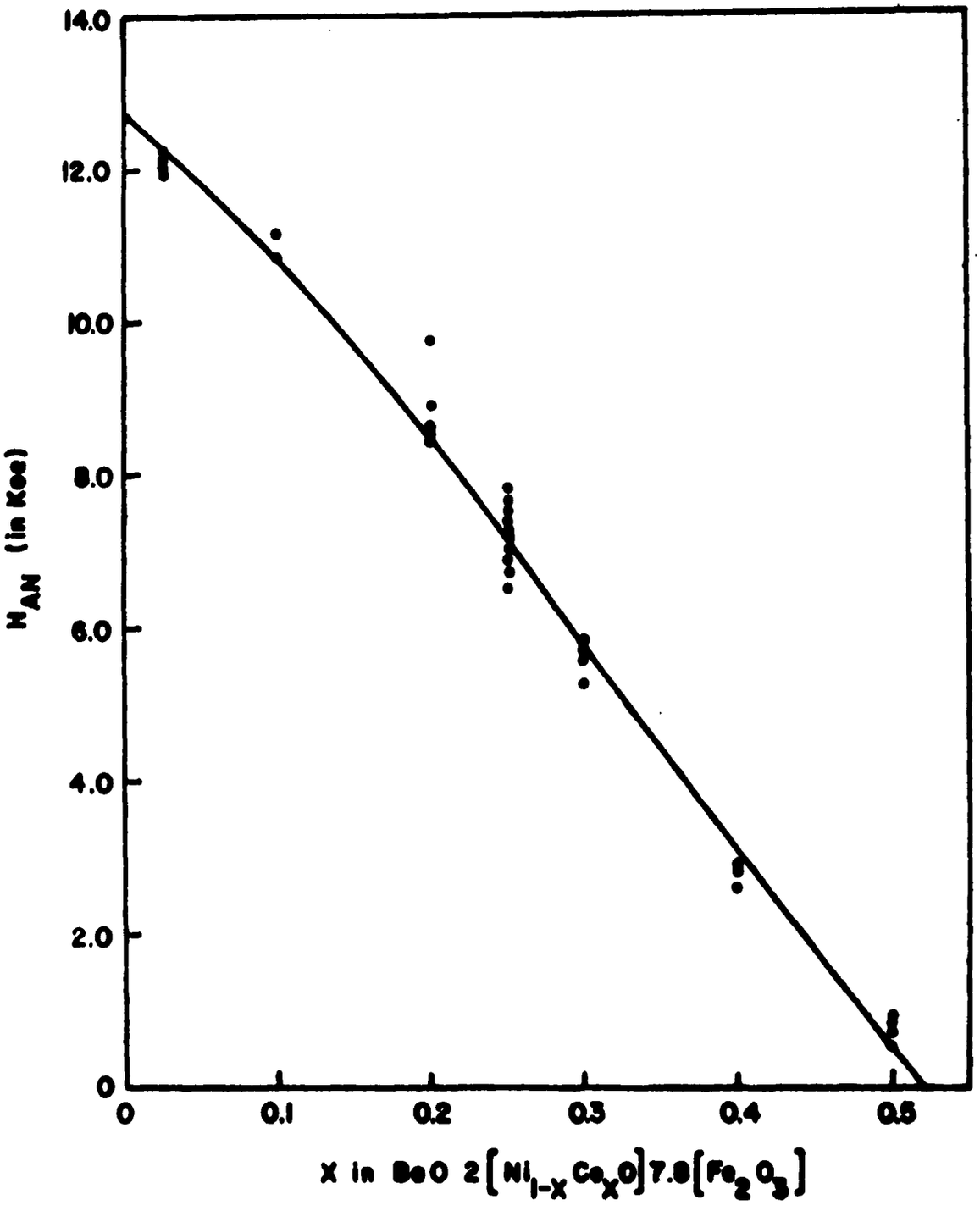

Figure 47. Measured Uniaxial Anisotropy Fields as a Function of Cobalt Content in Nickel-Cobalt W Compounds.

any anisotropy field from 0 to 12,700 oe can be obtained by selecting the proper composition.

The spread in points observed for a given composition may arise from local inhomogenieties within a bar of material. This spread could also arise from improved orientation of some of the samples. It has been found that the greater the alignment the larger the measured anisotropy field. The cause of increase in anisotropy field with orientation can be deduced from the following considerations. With the applied field along the easy direction those crystals in precise alignment are biased to resonance by a certain value of H_{ap}; improperly aligned crystallites require a slightly higher field for resonance. The result is that the apparent absorption curve is broadened on the high field side of resonance, and the peak of the curve shifted somewhat toward that direction. A similar argument can be applied when the external field is along a hard direction; in this case the shift is toward the low field side. The net result is that any improperly aligned crystallites cause a broadening of the resonance absorption line and an apparent reduction in computed anisotropy field.

Values of effective g-factor computed from resonance absorption spectra and equation (8) for each material are shown in Fig. 48 as a function of observed anisotropy field. While a large spread is observed, the general trend is for the effective g-factor to decrease to a minimum of approximately 1.8 before rising again to about 2.0. The observed

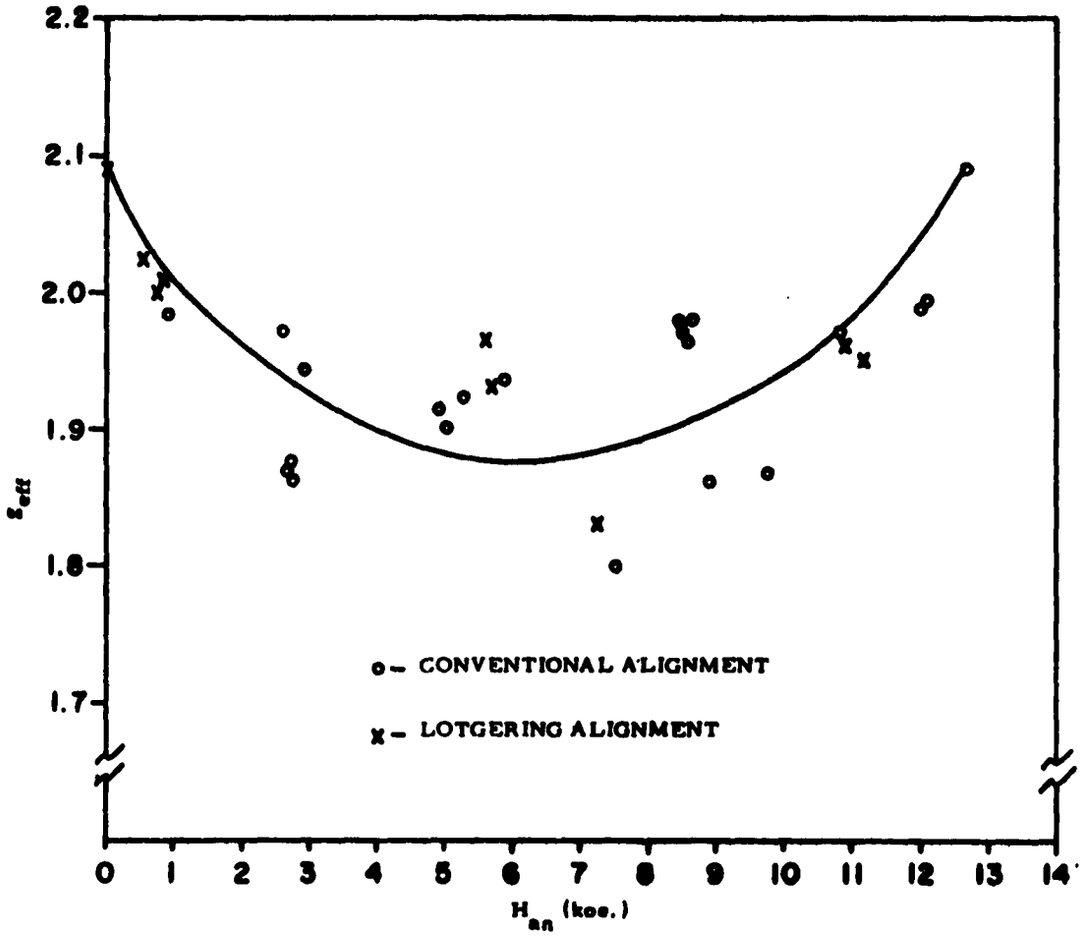

Figure 48. Observed Values of Effective g-Factor as a Function of Anisotropy Field.

increase in g-factor as the anisotropy field approaches zero may result from higher order anisotropy constants taking on increasing importance as K_1 decreases. Higher order terms have not been included in these calculations as anisotropy in the plane is not observable on polycrystalline samples whose c-axes are the only uniquely oriented crystallographic direction.

3.3 Data Taken as a Function of Temperature

Resonance measurements were conducted as a function of temperature from room temperature to 125 °C. The observed dependence of anisotropy field on temperature for three different compositions is shown in Fig. 49. The anisotropy field of these compounds is found to increase almost linearly with temperature, and the positive slope of the lines is larger for the higher cobalt content materials. The positive slope and the increase in slope with increasing cobalt content both indicate that the anisotropy constant of cobalt W is a stronger function of temperature than is that of nickel W. This behavior is similar to that of the spinel ferrites where the anisotropy of cobalt ferrite[23] falls off more rapidly with temperature than does that of nickel ferrite.[24]

The anisotropy field of the five per cent cobalt substituted nickel W material is seen to be almost independent of temperature, increasing only slightly over this temperature range. In the other materials the temperature dependence is more marked. It is felt that the breadth of the resonance lines should render devices fabricated from these materials

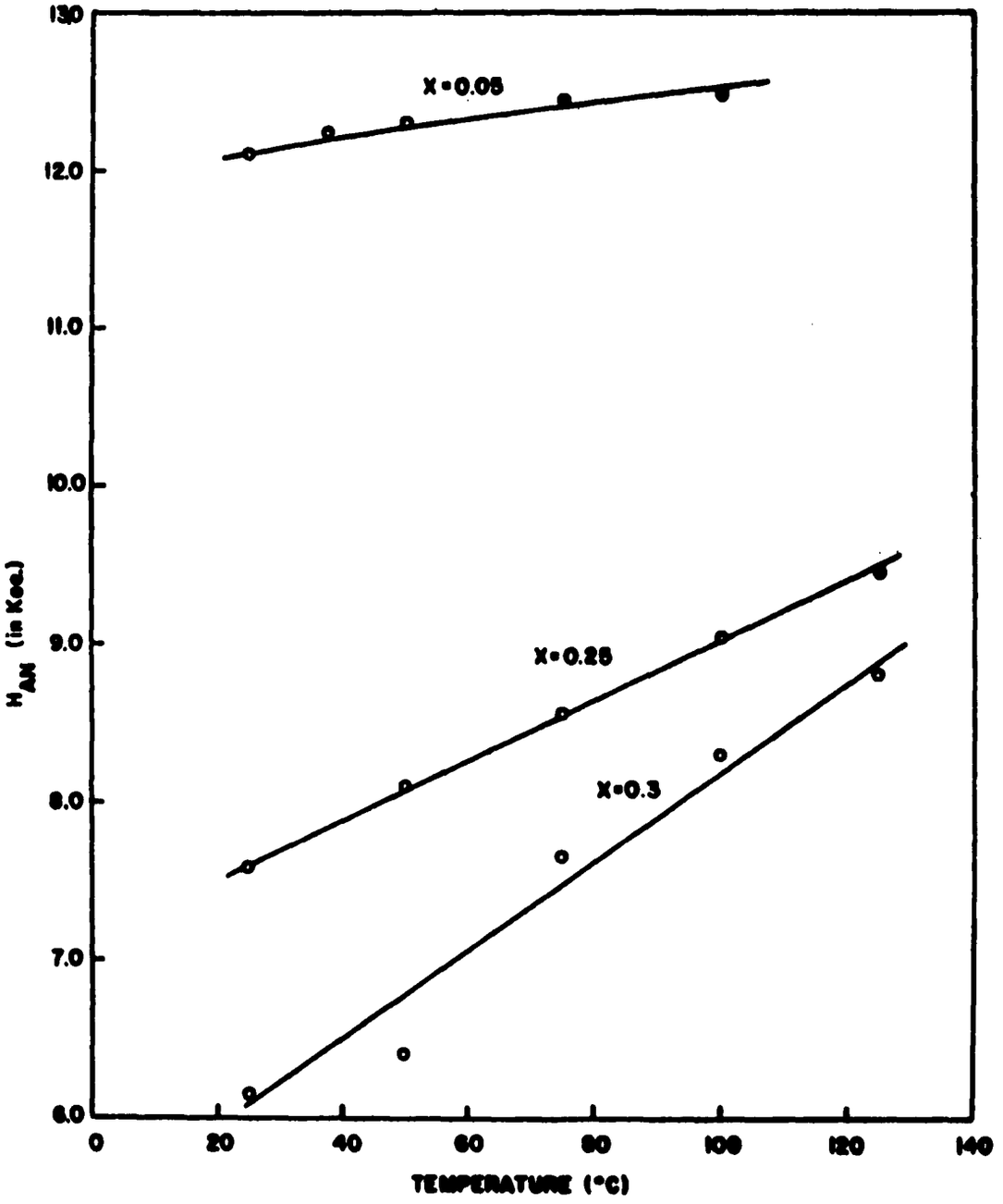

Figure 49. Variation of Anisotropy Field with Temperature in Three Compositions of Nickel Cobalt W. The Parameter is x in $BaO \cdot 2(Ni_{1-x}Co_xO) \cdot 7.8(Fe_2O_3)$.

relatively insensitive to temperature variations. Furthermore, since the field produced by a permanent magnet will decrease with increasing temperature, by proper choice of permanent magnet material the two temperature effects can be made to compensate for one another in applications where the anisotropy field is used to augment an external field.

Linewidths measured on these materials as a function of temperature were found to be essentially constant over the range studied, and computed values of effective g-factor show it increasing with temperature in all cases approaching 2.0 near 125 ^{o}C.

SECTION V

DEVICE FEASIBILITY STUDIES

Evaluation of these materials in practical applications was carried out as an integral part of this program. Measurements aimed at determining the applicability of these uniaxial compounds in resonance isolators were carried out at V-, K-, and X-bands. Information gained in this and the resonance study was used to improve the quality of the material through more careful preparation.

1. V-BAND RESONANCE ISOLATORS

At V-band four different configurations were used. These are shown in Figs. 50 a, 50 b, 50 c and 51. The vertical slabs shown in Figs. 50 a and 51 require the least applied field since demagnetizing effects are minimized, and the material can be saturated with a small externally applied field. The configuration shown in 50 b has a demagnetizing factor nearly equal to 1.0 in the direction of the applied field and hence requires a field roughly equal to the saturation magnetization ($4\pi M_s$) greater than that necessary to resonate the vertical slab. In general, larger isolation ratios and greater bandwidths are possible with this arrangement than with that of 50 a. The configuration shown in 50 c requires a field intermediate between those required for 50 a and 50 b, and this dielectric loaded isolator had improved isolation ratios. It should perhaps be pointed out that the prime goal was an evaluation of the material rather than the perfection of an isolator.

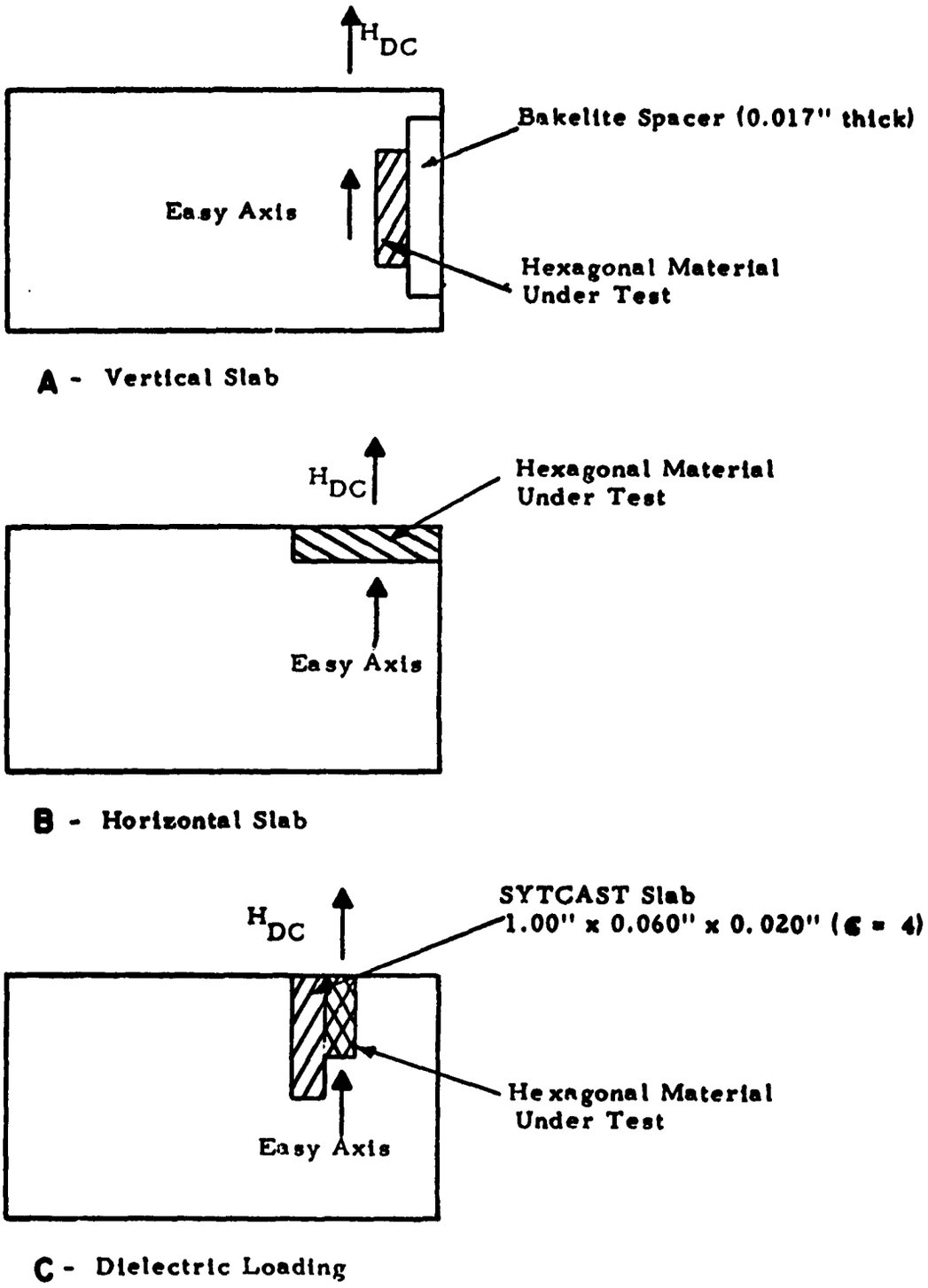

Figure 50. Three Configurations used in Fabricating V-Band Isolators. (Drawing not to scale.)

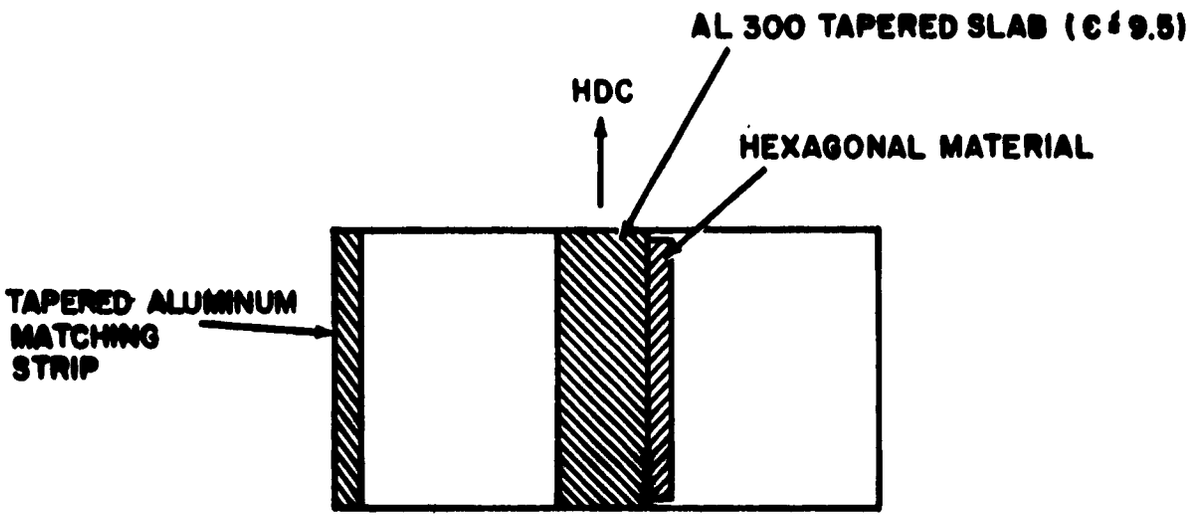

Figure 51. Full Height Dielectric Loaded Isolator Configuration. Taper is in E-plane

Table 5 summarizes results obtained on five different materials in terms of field required for resonance, isolation ratio at maximum resonance absorption, and material parameters for the vertical slab (Fig 50a) configuration at a frequency of 36 kmc. The invariance of the sum of field required for resonance and the anisotropy field shown in column 6 of this table illustrates that this anisotropy does indeed act like an internal applied field.

TABLE 5

Summary of results obtained with different materials in vertical slab configuration of V-band isolator at 36 kmc.

Material No.	H_{an} (oe.)	ΔH_{easy} (oe.)	$\left(\frac{\text{Isolation loss}}{\text{Isolation loss at res.}}\right)$	H_{res} (oe.)	$H_{res} + H_{an}$ (oe.)
H-36A	12,060	3,000	14.7	480	12,540
H-38B	10,800	3,000	14.0	1,250	12,050
H-39C	8,500	2,400	12.0	4,000	12,500
H-39E	8,650	2,800	11.5	4,200	12,850
H-41C	5,600	2,450	11.3	7,250	12,850

In Fig. 52 are plotted the isolation and insertion losses of a vertical slab of H-36A at 35.68 kmc as a function of applied magnetic field. A maximum isolation ratio of 14.5 to 1 was obtained at a field of approximately 300 oe. The frequency response of an isolator using a vertical slab with an aspect ratio of 10:1 is shown in Fig. 53. The applied field of approximately 1000 oe is supplied by ceramic bar magnets. This V-band isolator has a maximum isolation ratio of 18:1. The characteristics of this vertical slab isolator can be greatly improved

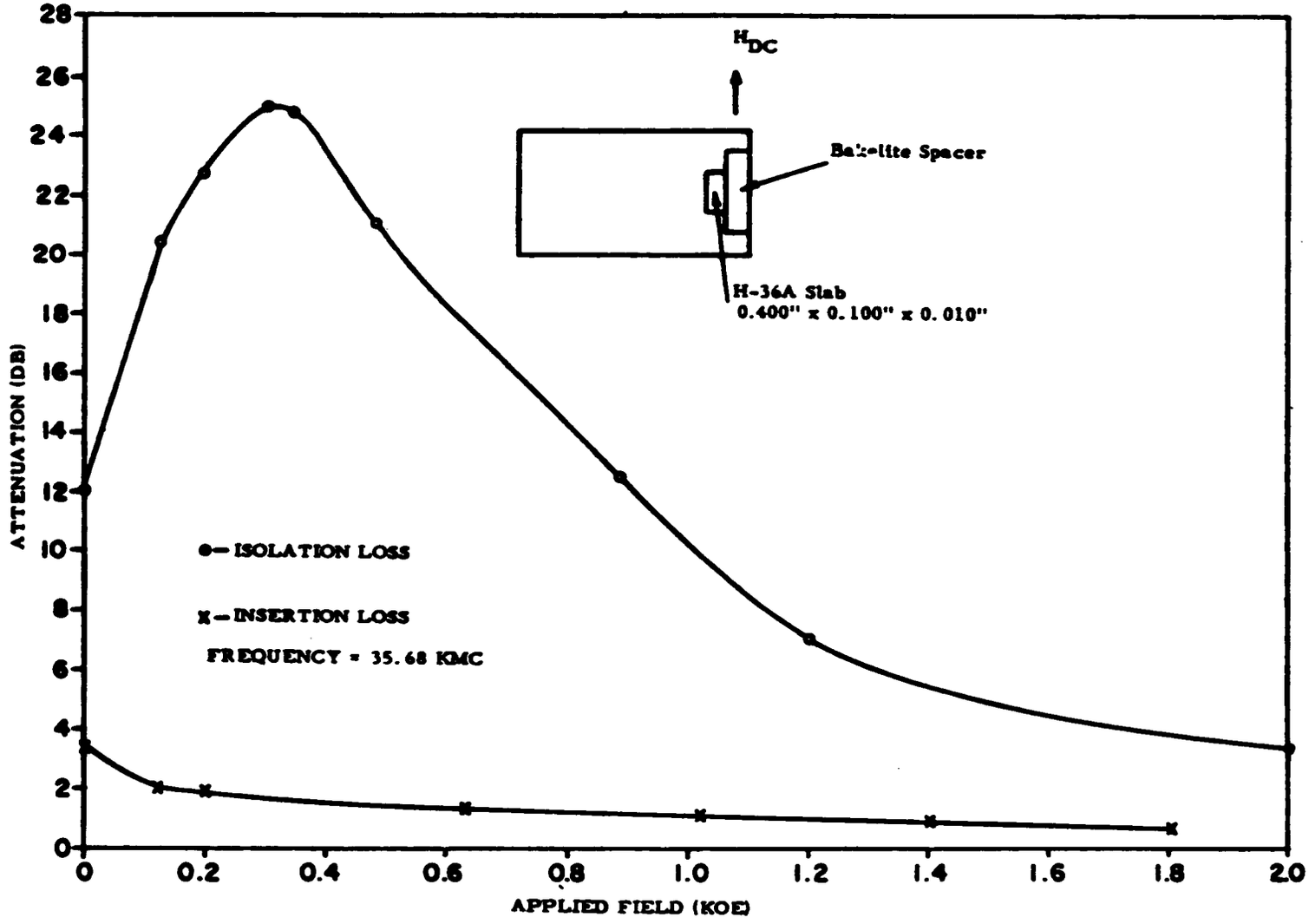

Figure 52. Isolation and Insertion Losses versus Applied Field for Vertical Slab of $(Ni_{0.95}Co_{0.05})_2W$

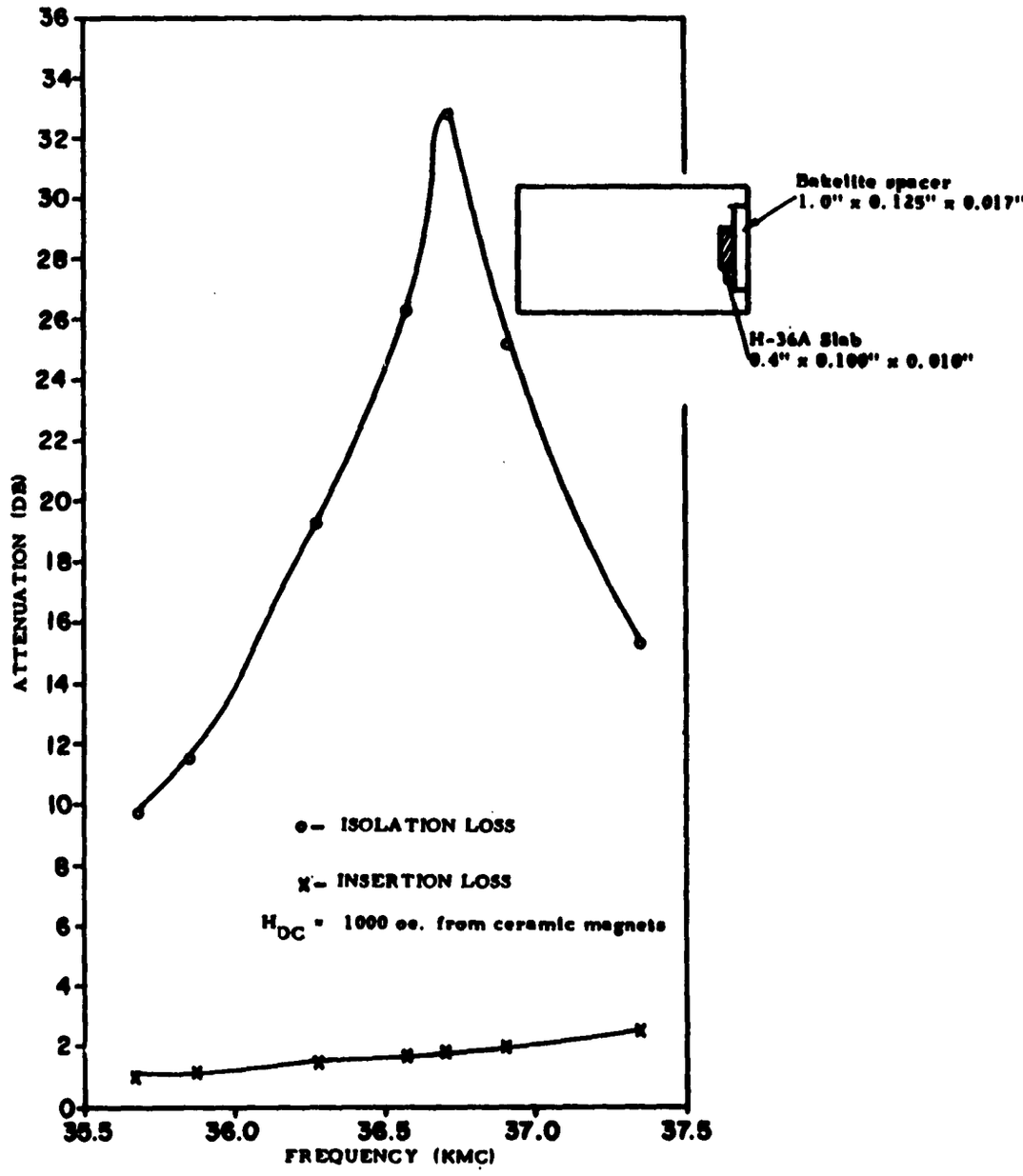

Figure 53. Frequency Response of V-band Isolator using Vertical Slab of $(Ni_{0.95}Co_{0.05})_2W$

through dielectric loading as in the configuration of Fig. 51. (See below.)

The horizontal slab geometry (Fig. 50b) generally yields broader bandwidths and higher isolation ratios than does the vertical slab. Measurements were taken with the slab placed in the corner of the V-band waveguide test piece as indicated in Fig. 50b. Again dielectric loading and/or positioning the slab closer to the plane of circular polarization would improve results. The corner positioning was selected solely because of its ease and reproducibility. The response of a slab of H-38B at 35.07 kmc to a varying magnetic field is shown in Fig. 54. A maximum isolation ratio of 14.5 to 1 is obtained, and the response is noticeably broader than that of Fig. 52. Fig. 55 shows results obtained for an isolator of this configuration using a slab of H-38B and a biasing field of 5700 oe. The insertion loss remained below 1.0 db and the isolation greater than 10 db from 34.75 to 36.75 kmc with a maximum ratio of 16:1.

Results obtained on the configuration of Fig. 50c are shown in Fig. 56, and a maximum isolation ratio of 37 to 1 is observed. The frequency response obtained with this isolator and a biasing field of 3200 oe. applied to a slab of H-36A is shown in Fig. 57. Here the insertion loss was less than 1 db and the isolation greater than 10 db from 35.0 kmc to 36.6 kmc with a maximum isolation ratio of 37:1. This device could be easily broadbanded by using a second slab of material having a slightly different aspect ratio in tandem with the first.

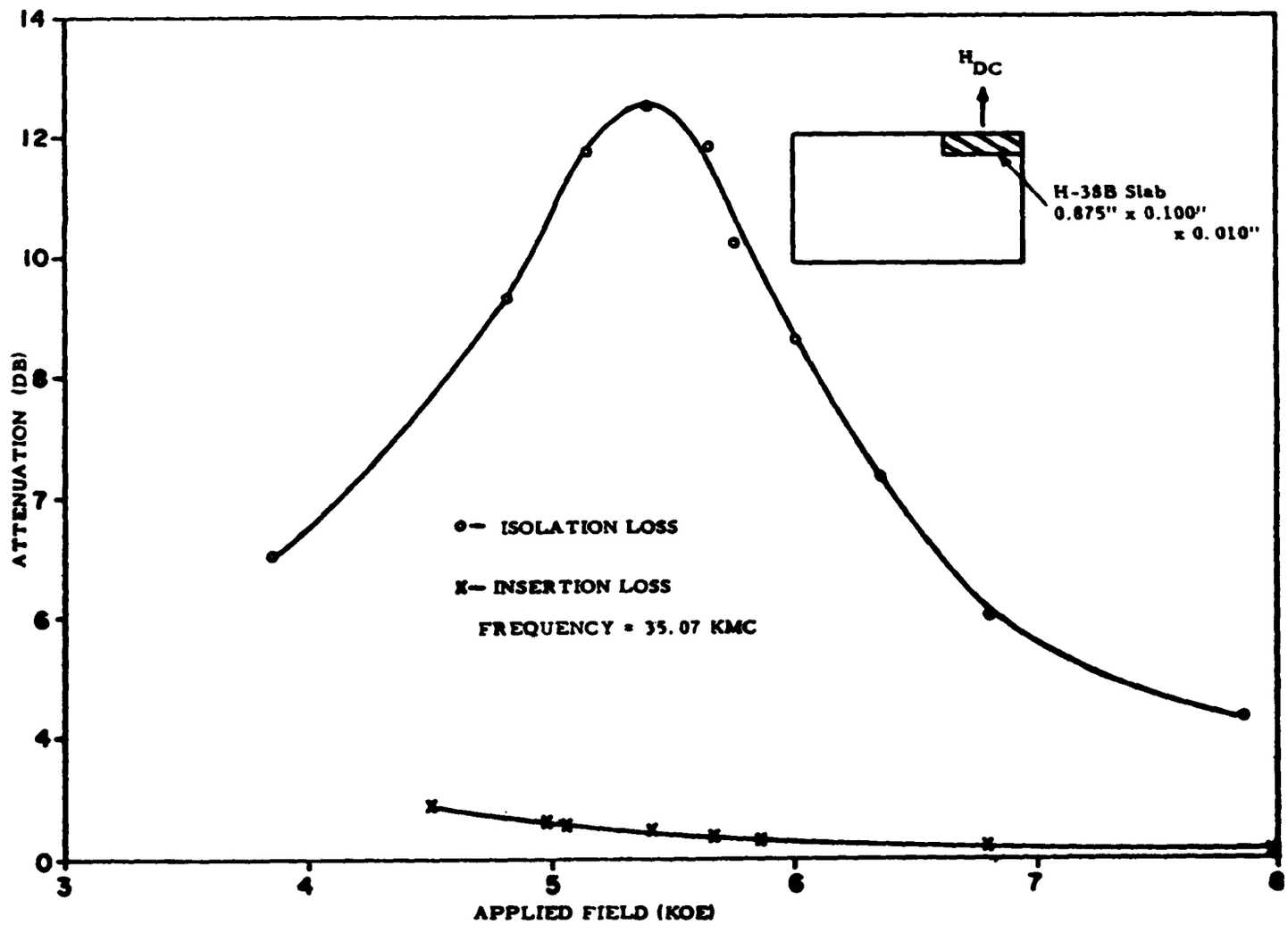

Figure 54. Isolation and Insertion Losses versus Applied Field for a Horizontal Slab of $(Ni_{0.9}Co_{0.1})_2W$.

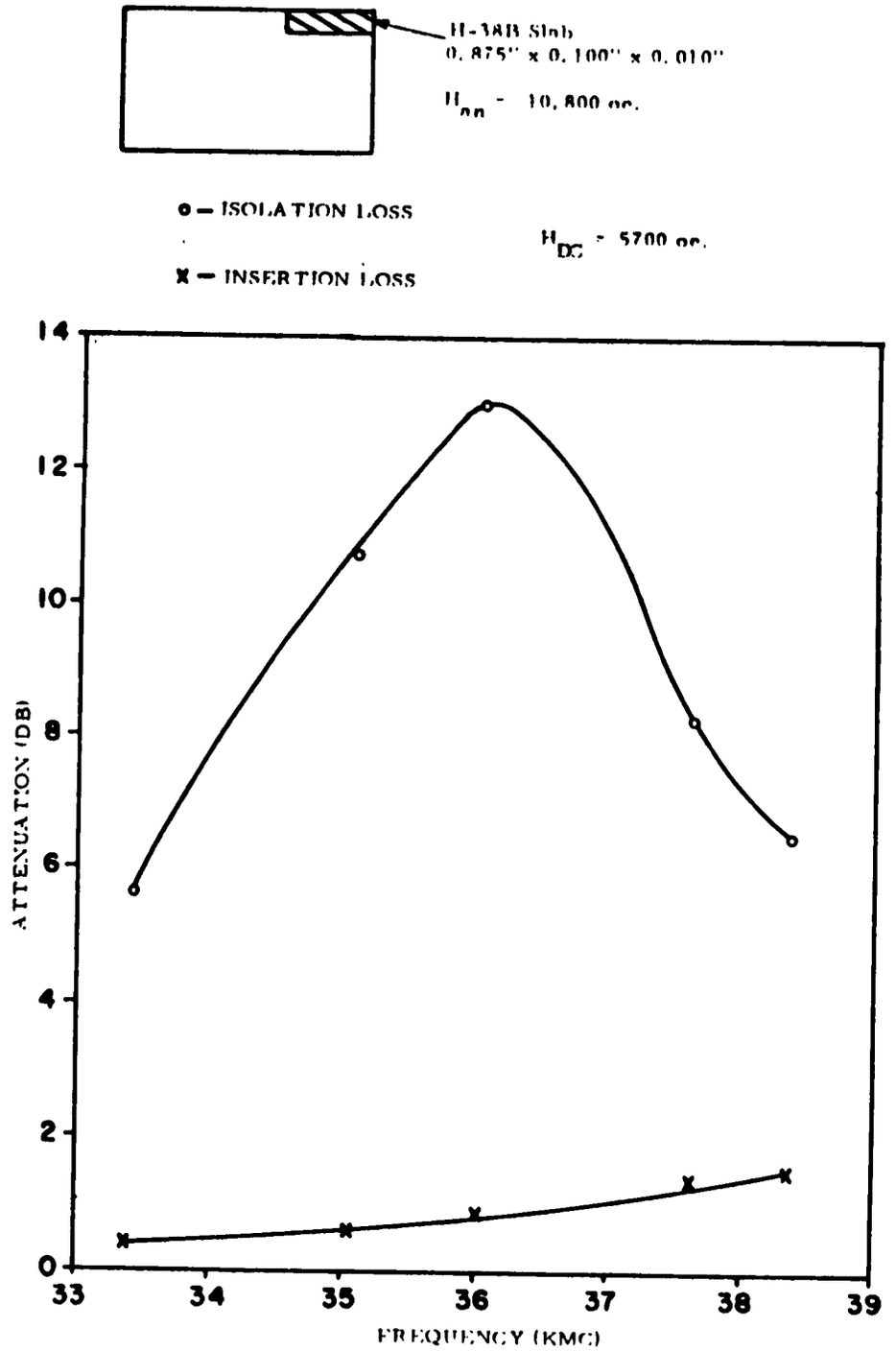

Figure 55. Frequency Response of V-Band Isolator Using Horizontal Slab of $(Ni_{0.9}Co_{0.1})_2W$.

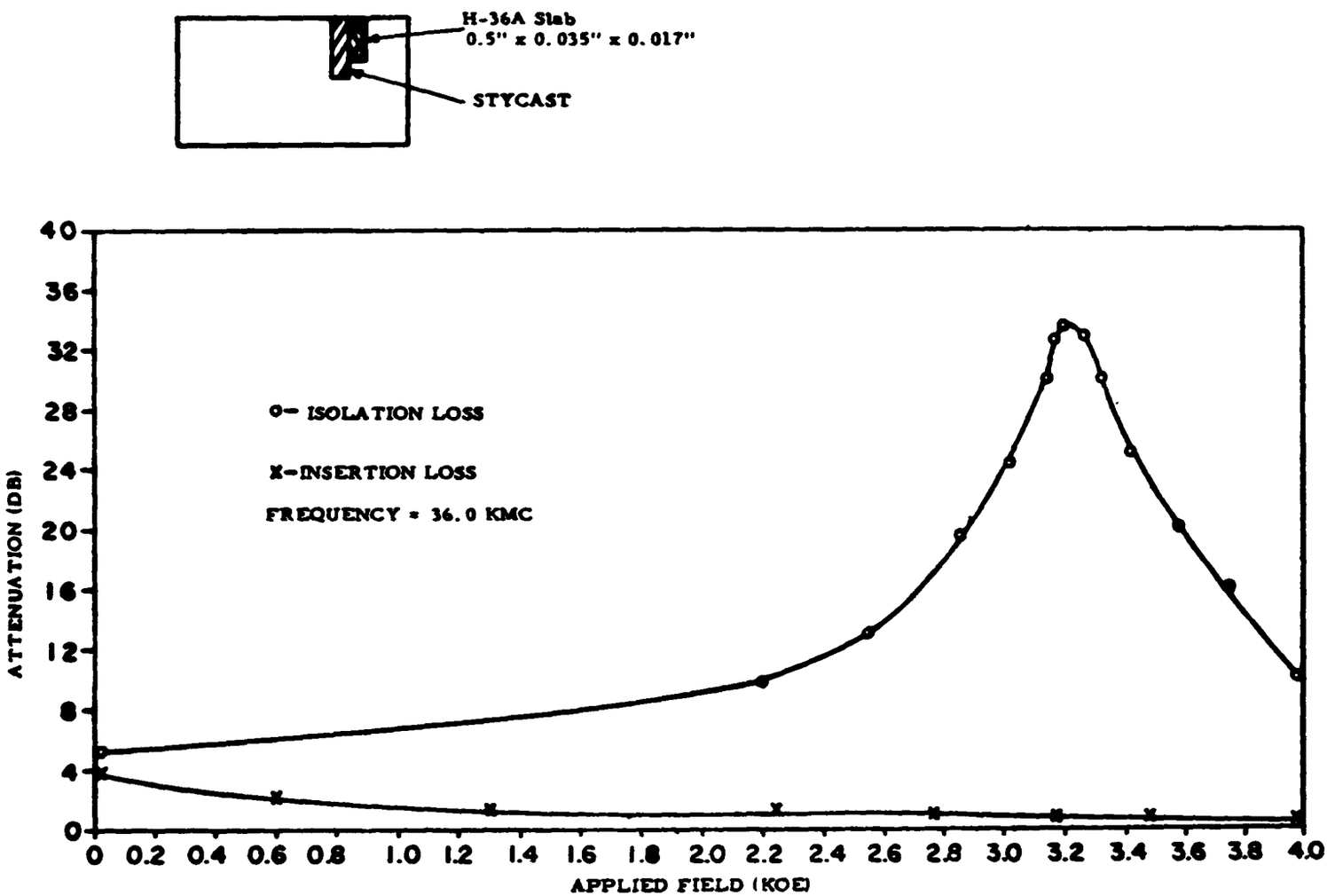

Figure 56. Isolation and Insertion Losses versus Applied Field in Dielectric Loaded Isolator at 36.0 kmc using $(Ni_{0.95}Co_{0.05})_2W$.

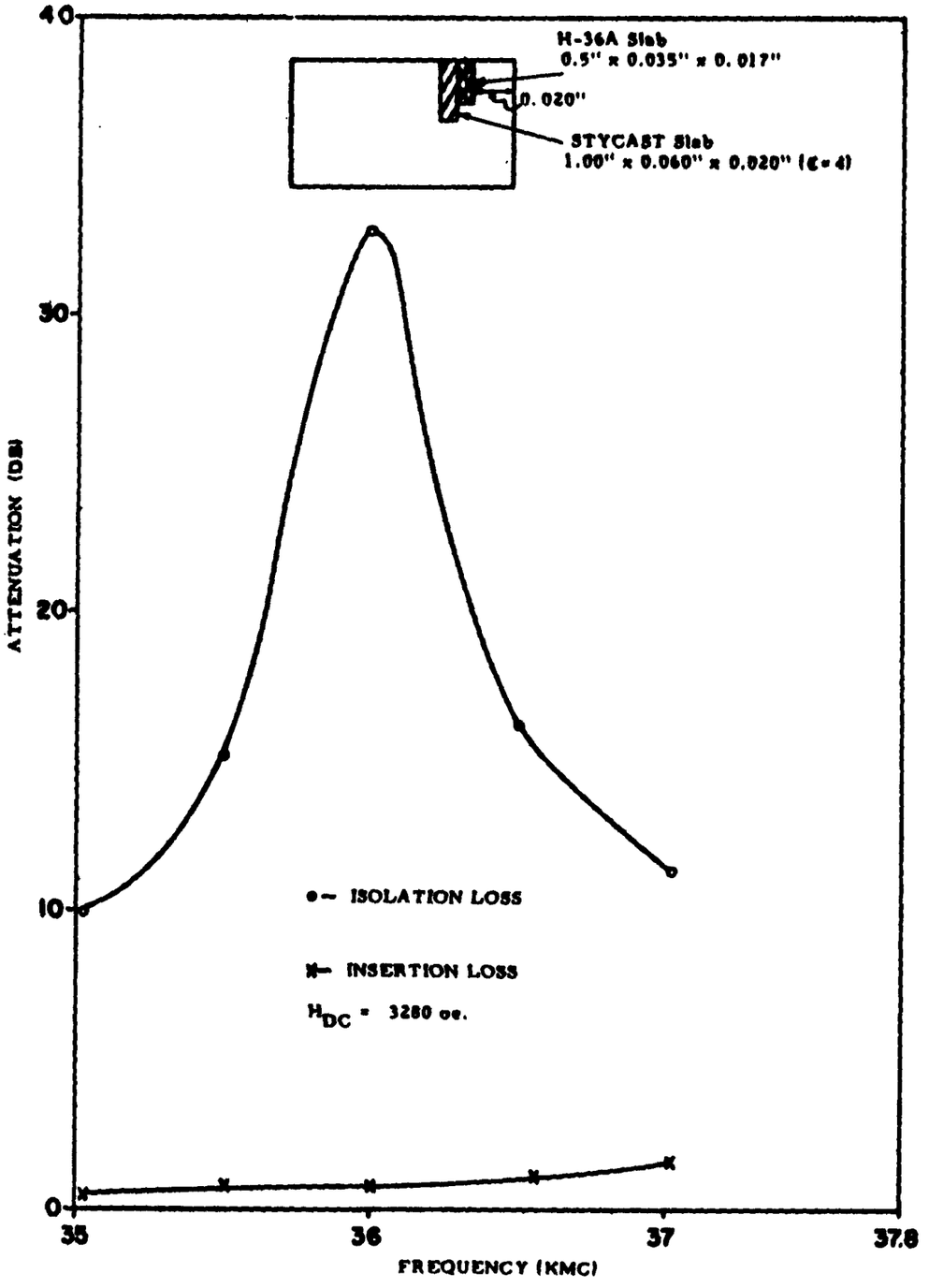

Figure 57. Frequency Response of Dielectric Loaded V-Band Isolator using $(Ni_{0.95}Co_{0.05})_2W$.

Best results at V-band were obtained with the dielectric loaded configuration shown in Fig. 51; the frequency response of the device is plotted in Fig. 58. A photograph of the unit indicating its small size is shown in Fig. 59. The permanent ceramic magnets used supply approximately 1000 oe. which place the center of the operating band at 38.2 kmc. The insertion loss of this unit remains below 1.0 db and the isolation greater than 10 db from 36.2 kmc to 39.5 kmc. Maximum isolation ratios of 18:1 were obtained at the center frequency.

Using a highly aligned sample of ten per cent cobalt substituted nickel W material that had been prepared with small particle size it was possible to obtain isolator operation with no externally applied magnetic field. This class 2 device again had the configuration of Fig. 51. A maximum isolation ratio of 30/1.5 was obtained with a 10 to 1 bandwidth of 2.2 kmc. The response of this device is plotted in Fig. 60.

These results show clearly that these materials can be used quite successfully in V-band resonance isolators requiring little or no externally applied d-c magnetic fields. A V-band resonance isolator using conventional ferrite would require a biasing field of about 12,000 oe.

2. K-BAND RESONANCE ISOLATORS

At K-band two configurations were tried - both dielectric loaded. The first used an H-plane tapered dielectric as shown in Fig. 61. The second was a scaled version of Fig. 51. A summary of results obtained with the configuration of Fig. 61 on several different materials is given

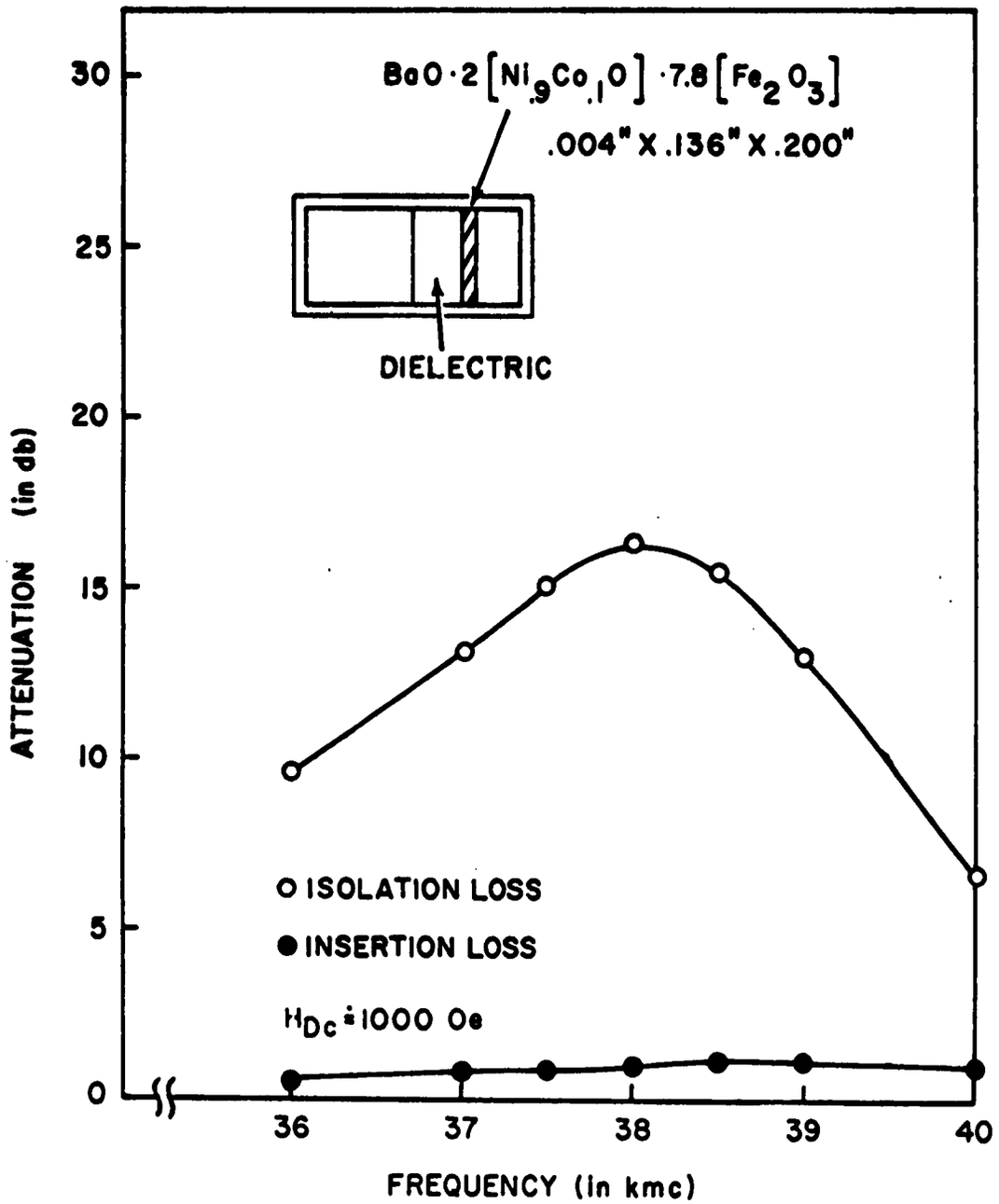

Figure 58. Frequency Response of Dielectric Loaded V-band Isolator Using Configuration of Figure 51. Material Used is $(Ni_{.9}Co_{.1})_2W$

Figure 59. Photograph of V-band Resonance Isolator. Bias Field Supplied by Ceramic Magnets Shown

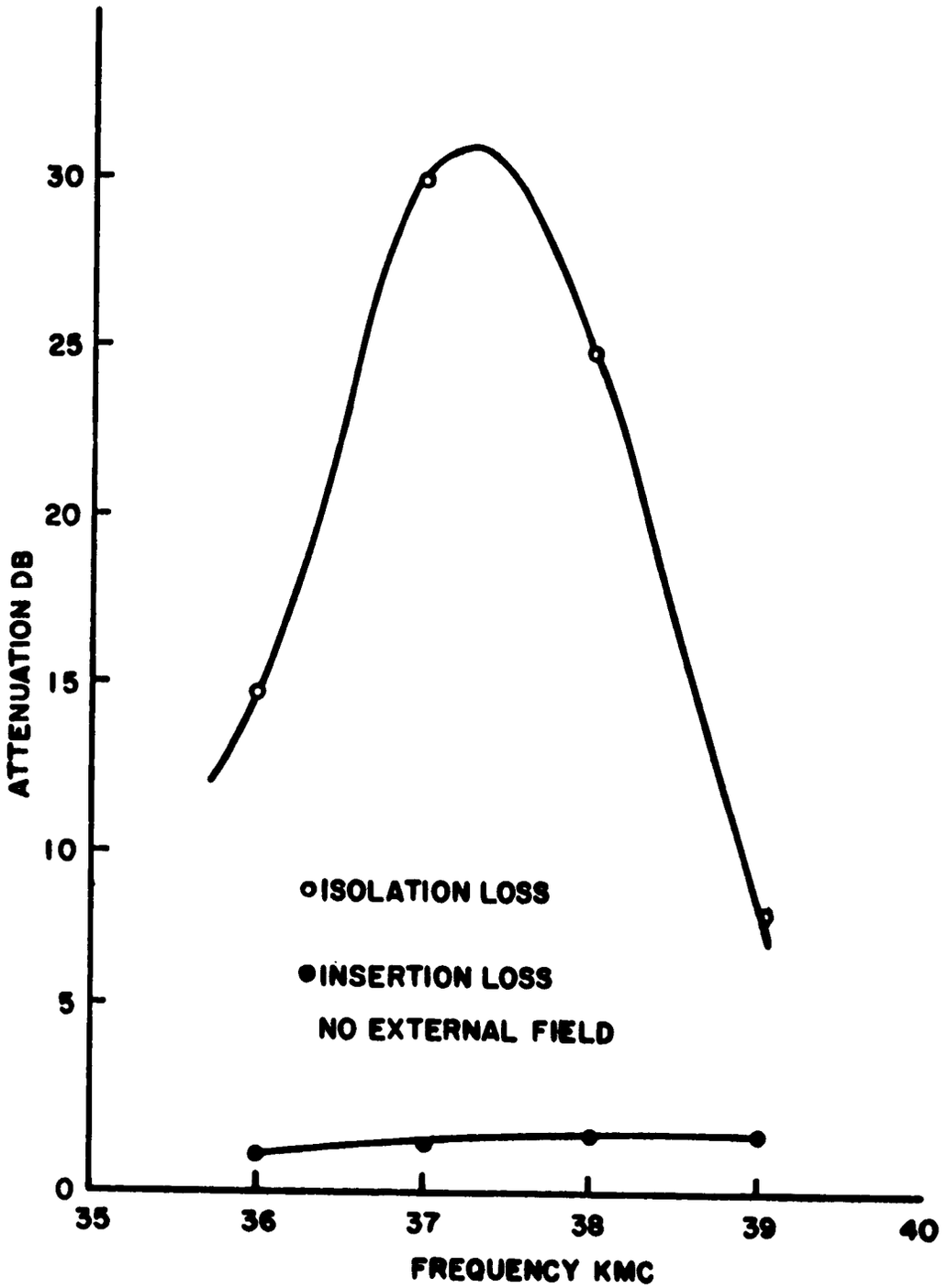

Figure 60. Frequency Response of V-band Resonance Isolator Using Configuration of Figure 51. Material is $(Ni_{.9}\ Co_{.1})_2W$ with No Field Applied

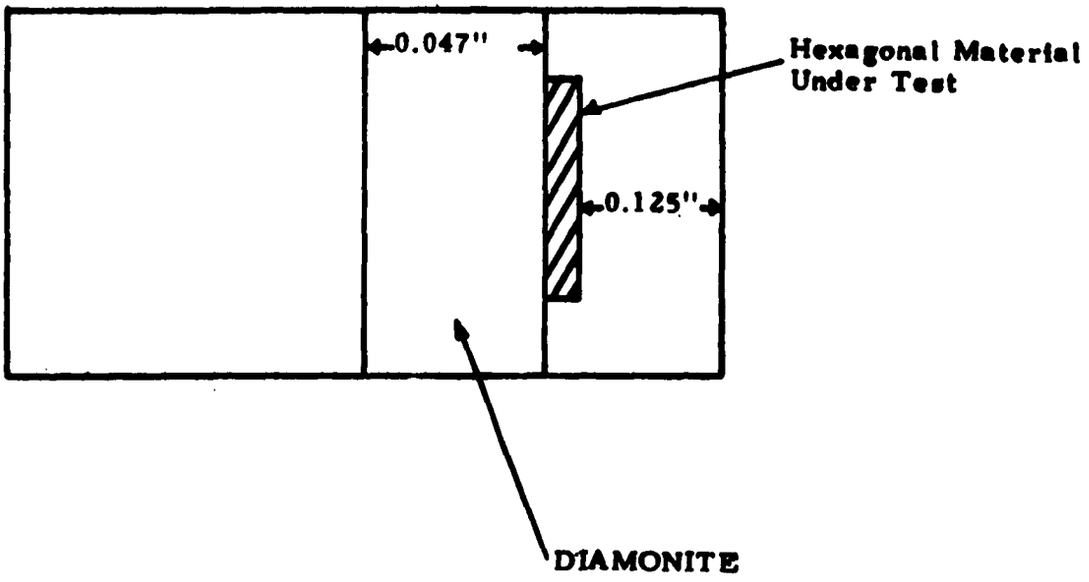

Figure 61. Dielectric Loaded Configuration Used for K-band Isolator Study. (Diamonite Bar is Full Waveguide Height in Center and Tapered in H-plane at ends. Drawing not to scale.)

in Table 6. Fig. 62 shows isolation and insertion losses as a function of applied field for a slab of H-41D at 25.24 kmc. Maximum isolation ratio is 17.5 to 1 and the isolation loss remains greater than 20 db from 1500 to 4150 oe. The frequency response obtained on this isolator using a slab of H-41D with dimensions 0.010" x 0.100" x 1.00" is shown in Fig. 63. The response is seen to be quite flat as a function of frequency, and the applied field is only 2000 oe. The use of material with a higher anisotropy field would permit this isolator to be operated with negligibly small biasing fields.

TABLE 6

Summary of results obtained with different materials in a dielectric loaded K-band isolator at 25.2 kmc.

Material No.	H_{an} (oe.)	ΔH_{easy} (oe.)	$\left(\frac{\text{Isolation loss}}{\text{Insertion loss}}\right)$ at res	H_{res} (oe.)	$H_{res} + H_{an}$ (oe.)
H-39E	8,650	2,800	self resonant at higher frequency	-	<8,650
H-41D	5,700	2,600	17.5	2,500	8,200
H-43C	2,600	2,700	23.6	5,800	8,400
H-45B	850	2,700	25.3	7,100	7,950

The K-band modification of the configuration shown in Fig. 51 was used with the thirty per cent cobalt substituted nickel W compound that has an anisotropy field of approximately 7000 oe. This device produced a maximum isolation ratio of 35 to 1 at a frequency of 23 kmc. The applied field was approximately 1000 oe. and was supplied by small

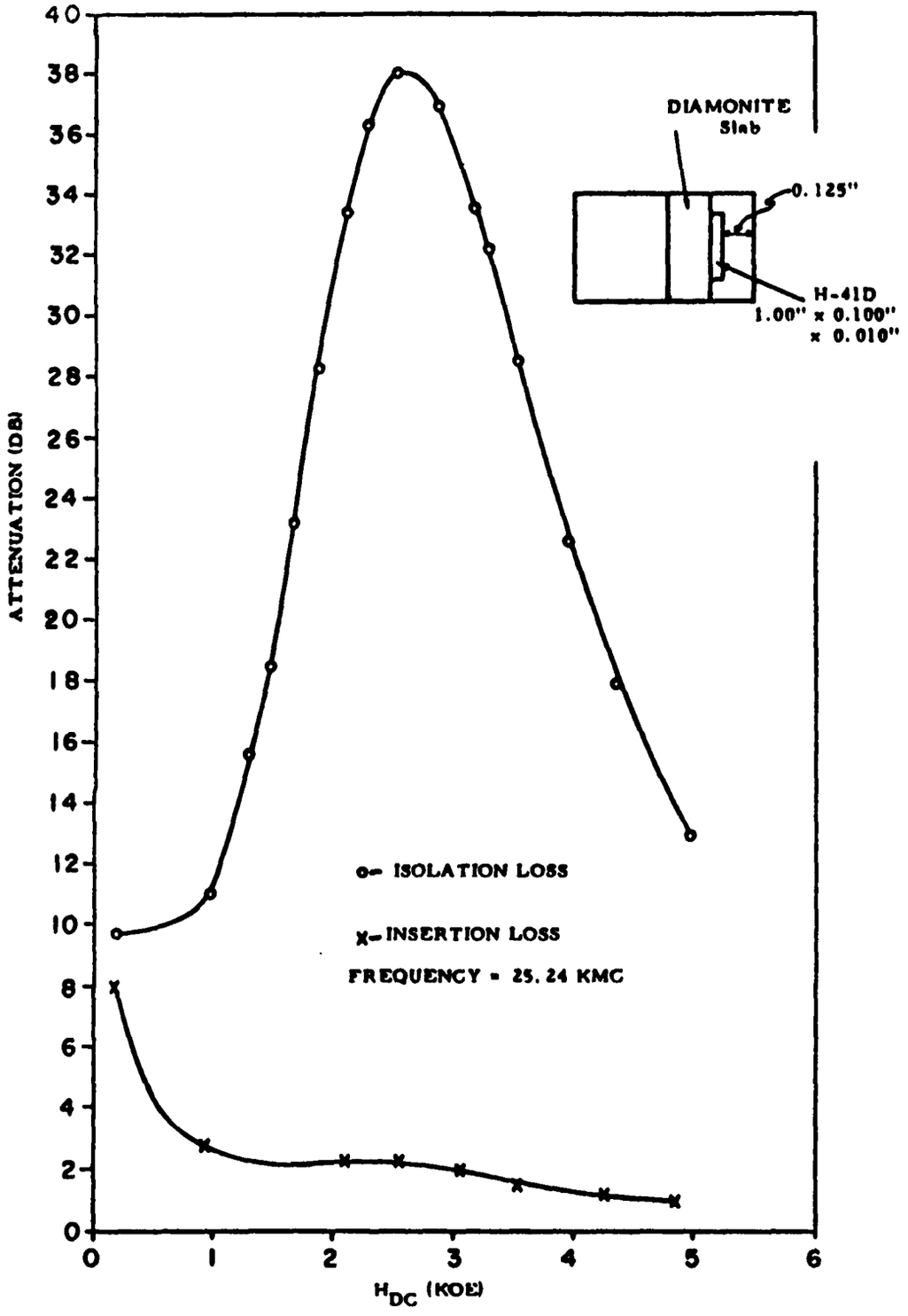

Figure 62. Isolation and Insertion Losses versus Applied Field for K-band Isolator Using $(Ni_{0.7}\ Co_{0.3})_2 W$

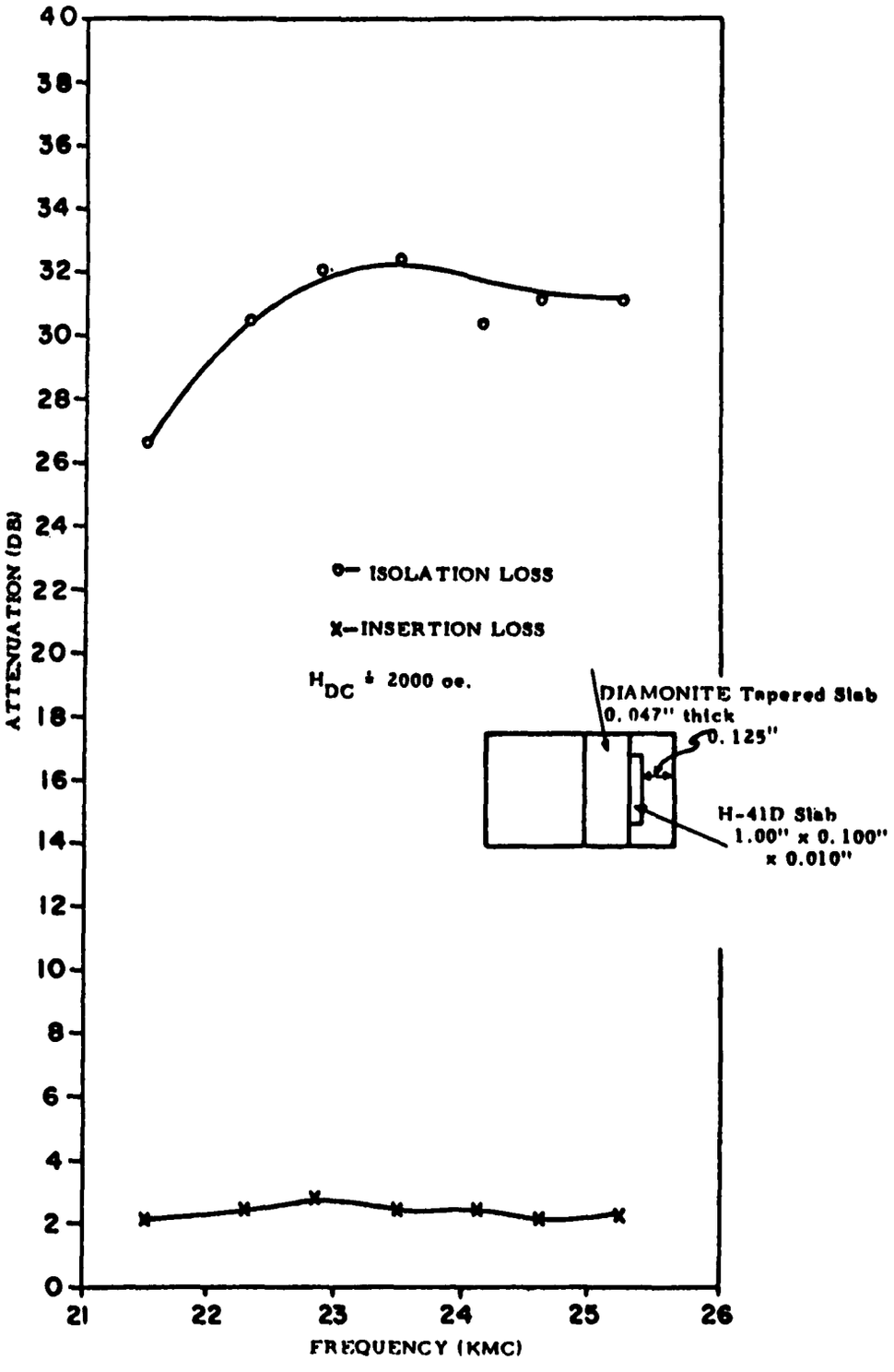

Figure 63. Frequency Response of K-band Dielectric Loaded Isolator Using $(Ni_{0.7}Co_{0.3})_2W$

ceramic magnets. The frequency response is shown in Fig. 64 where it is seen that the ten to one bandwidth is greater than 6 kmc or about 25 per cent bandwidth. This compact device is shown in Fig. 65.

An isotropic ferrite requires a field of approximately 8000 oe to bias it to resonance at K-band.

3. OTHER DEVICE DATA

The forty percent cobalt substituted nickel W material ($H_{an} \sim$ 2800 oe.) was evaluated at X-band, but isolation ratios of no better than 8 to 1 were obtained. This material had a linewidth of 2700 oe. and it is expected that improved orientation would so reduce the linewidth as to make considerably higher isolation ratios feasible.

Measurements of differential phase shift were also made at V-band in rectangular waveguide. These measurements were carried out on the normally magnetized slab configuration of Fig. 50b. Typical of the data obtained are that shown in Fig. 66. These data do not appear to be those of a material in a region of pure circular polarization. These results indicate that when the reverse wave experiences no phase shift the positive wave is shifted by 80 degrees and both waves are attenuated by approximately 1 db. Greater differential phase shift should occur if pure circular polarization were present, and improved alignment should lower the loss. The zero permeability region of the negative wave occurs when the applied field is approximately 4000 oe. Nearly 12,000 oe are required to bias isotropic ferrites to this operating point.

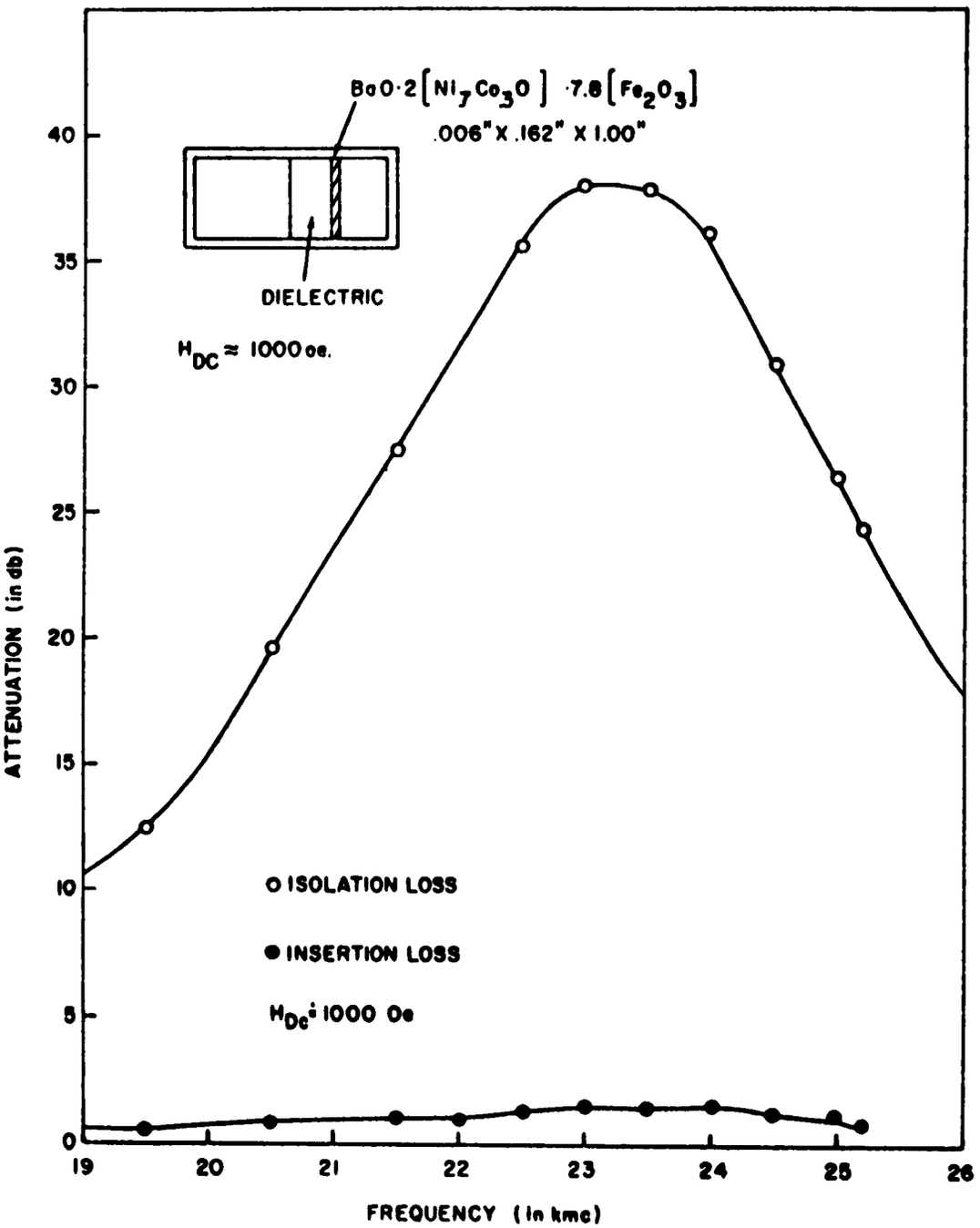

Figure 64. Frequency Response of K-band Resonance Isolator Using Configuration of Figure 51. Material is $(Ni_{.70}Co_{.30})_2W$

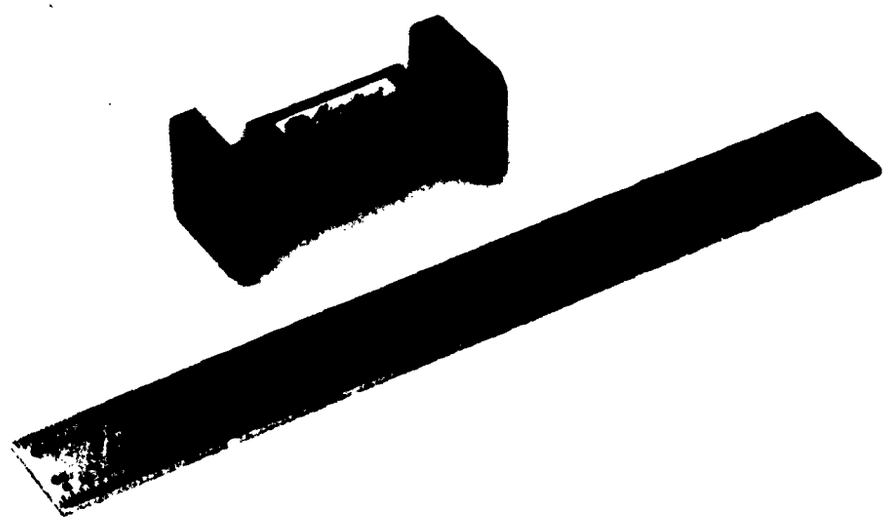

Figure 65. K-band Resonance Isolator Bias Field Supplied by Ceramic Magnets Shown

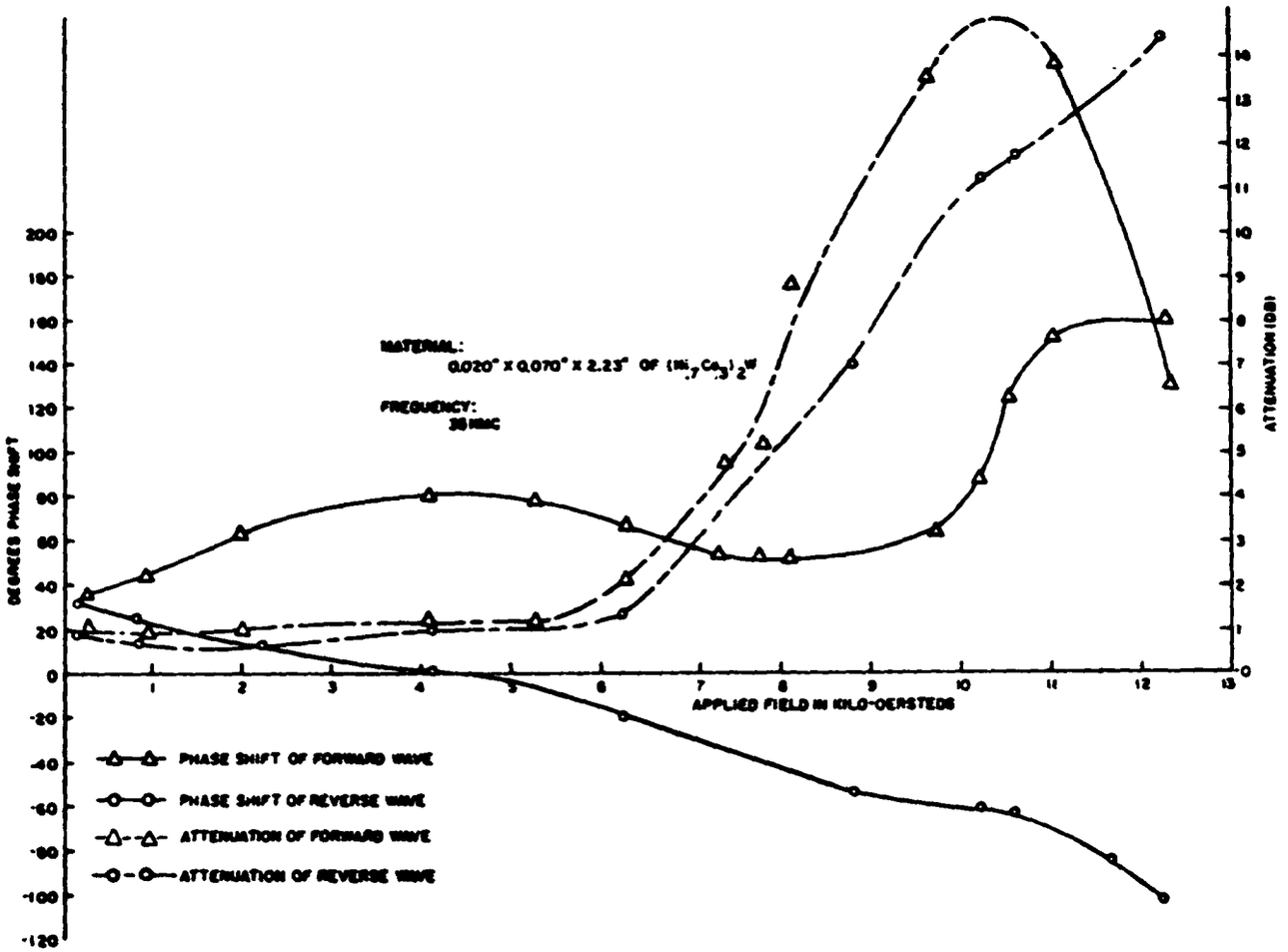

Figure 66. V-band Phase Shift and Attenuation Data Measured on Slab of $(Ni_{.7}Co_{.3})_2W$ at 37 kmc

SECTION VI

CONCLUSIONS

1. GENERAL CONCLUSIONS

This program has resulted in the synthesis of a new series of oriented hexagonal materials in which the effective internal anisotropy field can be controlled and varied over a range from 0 to 12,700 oersteds. This control is achieved through the ionic substitution of divalent cobalt for divalent nickel in the W structure.

Insight has been gained into the problem of preparing oriented polycrystalline material with good microwave properties. The results of this study indicate that a high degree of alignment can best be achieved by reducing particle size to a minimum at the pressing stage and allowing considerable grain growth during the sintering process. Desirable particle size decreases with decreasing anisotropy field.

It can be concluded from the data collected that the anisotropy field of Co_2W is a stronger function of temperature than that of Ni_2W. As a result the anisotropy fields of solid solutions of these compounds display an increasingly strong temperature dependence as the cobalt content is increased.

Measured ferromagnetic resonance linewidths of these materials are almost independent of both cobalt content and temperature over the range studied. The breadth of the resonance line does, however, depend strongly on the degree of orientation.

The ability to fabricate uniaxial materials with an internal anisotropy field of any desired value within a specified range, in principle, permits the construction of devices requiring minimum external fields over a broad frequency range. With data like those shown in Fig. 47 a device engineer can determine a composition that will provide him with an internal field suited to a particular application in any one of a wide range of frequency bands. This is a case of true tailoring of the material to the particular function and frequency of the desired device.

The ability to employ these materials in useful devices was demonstrated in an overlapping phase of this program. Different materials with appropriate values of internal anisotropy field were selected for evaluation in V- and K-band resonance isolators. Experimental data obtained on the various isolator configurations at V- and K-bands clearly demonstrate the usefulness of these materials.

The fact that resonance isolators were successfully fabricated at 25.0 and 37.5 kmc by applying the same field (supplied by small ceramic magnets) to different materials is worthy of note. It illustrates the possibility of using different materials with the same applied field to simplify the design of harmonic suppressors and other more sophisticated components.

SECTION VII

RECOMMENDATIONS

1. RECOMMENDED IMPROVEMENTS IN MATERIAL

Further improvement in the degree of orientation of the crystallites within these materials might result in still narrower resonance absorption lines and generally improved magnetic properties. The problem of alignment is essentially one in ceramics having to do with the type and consistency of slurry used and the particle size of material used. Firing time and temperature also play a part in determining alignment. The technique of pressing fine, dispersed particles and allowing for considerable grain growth in firing might be further extended.

A second area of possible improvements in materials is that of dielectric loss properties. A careful study should be made to determine if, in fact, the dielectric loss tangent is excessively high at microwave frequencies and what steps might be necessary to control it. Control of the dielectric loss tangent has in the past been achieved through small additions of ions, non-stoichiometric starting compositions, and control of firing temperature.

2. RECOMMENDED AREAS OF APPLICATION

With the improved alignment of materials even now obtainable it should be possible to attain resonance isolator operation at Ku- and

X-band frequencies. Better alignment should also make possible the application of these materials to phase shift devices. The use of different members of the nickel-cobalt W series in harmonic suppressors with simplified magnet requirements is also suggested by the present results.

REFERENCES

1. J. J. Went, G. W. Rathenau, E. W. Gorter, and G. W. Van Oosterhout, Philips Technical Review 13, 194 (1952). Also Phys. Rev. 86, 424 (1952).

2. D. J. DeBittetto, F. K. du Pré, and F. G. Brockman, Proceedings of the Symposium on Millimeter Waves, p 95, Polytechnic Institute of Brooklyn (1959).

3. J. Smit and H. P. J. Wijn, Ferrites (John Wiley and Sons, New York, 1959) p. 208.

4. D. J. De Bittetto, F. K. du Pré, F. G. Brockman, and W. G. Steneck, Jr., Report Nos. 1 and 2, Contract No. DA36-039 SC-85279, Philips Laboratories, Irvington-on-Hudson (1960).

5. G. H. Jonker, H. P. J. Wijn, and P. B. Braun, Proceedings of the Second Conference on Magnetism and Magnetic Materials, Boston (1956) p. 478. Also Philips Technical Review 18, 145 (1956).

6. H. G. Beljers, Philips Tech. Rev. 22, 11 (1960).

7. J. Smit and H. P. J. Wijn, op. cit., p 177ff.

8. I. Bady, "Ferrites with Planar Anisotropy at Microwave Frequencies," paper presented at 1960 PGMTT Symposium, San Diego, California.

9. R. L. Jepsen, Scientific Rep. No. 15 Contract No. AF 19(604)-1084, Gordon McKay Lab., Harvard Univ. (1958).

10. H. P. J. Wijn, Nature 170, 707 (1952).

11. P. B. Braun, Nature 170, 708 (1952).

12. A. J. Stuijts and H. P. J. Wijn, Philips Technical Review 19, 209 (1958).

13. K. Yosida and M. Tachiki, Progr. Theoret. Phys. (Kyoto) 17, 331 (1958).

14. G. P. Rodrigue, H. Meyer, and R. V. Jones, J. Appl. Phys. 31, 376S (1960).

REFERENCES (Cont'd)

15. P. E. Tannenwald and M. H. Seavey, Proc. IRE 44, 1343 (1956).

16. J. E. Pippin and C. L. Hogan, IRE Trans MTT-6, 77 (1958).

17. K. J. Sixtus, K. J. Kronenberg, and R. K. Tenzer, J. Appl. Phys. 27, 1051 (1956).

18. A. L. Stuijts, Trans. Brit. Ceramic Soc. 55, 57 (1956).

19. F. K. Lotgering, J. Inorg, Nucl. Chem. 9, 113 (1959).

20. S. Foner, Rev. Sci. Instr. 30, 548 (1959).

21. J. O. Artman and P. E. Tannenwald, J. Appl. Phys. 26 1124 (1955).

22. E. Schlömann and R. V. Jones, J. Appl. Phys. 30, 117S (1959).

23. H. Shenker, Navord Report 3858, U. S. Naval Ordnance Laboratory (1955).

24. D. W. Healy, Jr., Phys. Rev. 86, 1009 (1952)

PARTIAL BIBLIOGRAPHY ON HEXAGONAL MATERIALS

1. Ayres, Wesley P., "Millimeter Wave Generation Experiment Utilizing Ferrites," IRE Transactions on Microwave Theory and Techniques, Vol. MTT-7, No. 1, 1959.

2. Bady, I., and Schlömann, E., "Spin Wave Excitation in Planar Ferrites," 7th Conference on Magnetism and Magnetic Materials, Phoenix, Arizona, (November, 1961). To be published.

3. Beljers, H. G., "Faraday Effect in Magnetic Materials with Traveling and Standing Waves," Philips Research Report, 9, 131, 1954.

4. Belson, H. S., and Kriessman, C. J., "Microwave Resonance in Hexagonal Ferrimagnetic Single Crystals," J. Appl. Phys. 30, No. 4, 175S - 176S, (April, 1959).

5. Bertaut, E. F., Deschamps, A., Pauthenet, R., "The Substitution of Fe by Al, Ga., and Cr in Barium HexaFerrite Ba O $6Fe_2O_3$", C. R. Academy of Science (Paris), Vol. 246, No. 18, 2594-7, May 5, 1958 (In French).

6. Bertaut, E. F., Deschamps, A., Pauthenet, R., and Pickart, S., "Substitution in Hexaferrites of the Fe^{3+} Ion by Al^{3+}, Ga^{3+}, Cr^{3+}," J. Phys. Radium, 20, No. 2-3, 404-8, (February - March, 1959). (In French).

7. Bickford, L. R., Jr., "Intrinsic and Anneal-Induced Anisotropy in Cobalt Substituted W-Type Hexagonal Oxides," J. Appl. Phys., 31, No. 5, 259S - 260S, (May, 1960).

8. Bickford, L. R., Jr., "Trigonal Magnetocrystalline Anisotropy in Hexagonal Oxides," Phys. Rev. 119, No. 3, 1000-9,(August 1, 1960).

9. Borovik, E. S., and Mamalui, Yu. A., "Dependence of the Magnetic Susceptibility of Ba Ferrite on Temperature," Fiz. Metallov i Metallovedenie, 9, No. 1, 36 - 40, (January, 1960), (In Russian).

10. Braun, P. B., "The Crystal Structures of a New Group of Ferromagnetic Compounds," Philips Research Report, Vol. 12, 491 - 548, (December, 1957).

11. Braun, P. B., "Crystal Structure of Ba $Fe_{18}O_{27}$," Nature (London), 170, 708, (1952).

12. Brockman, F. G., "A New Permanent Magnet Material of Non-Strategic Material," Elect. Engineering (New York), 71, 644-7, (July, 1952).

13. Bruijning, H. G., and Rademakers, A., "Pre-Magnetization of the Core of a Pulse Transformer by Means of Ferroxdure," Philips Technical Review, 19, No. 1, 28 - 37, (1957-1958).

14. Buffler, C. R., "Resonance Properties of Single Crystal Hexagonal Ferrites," 7th Conference on Magnetism and Magnetic Materials, Phoenix, Arizona (November, 1961). To be published.

15. Campbell, G., "Some New Electrical and Magnetic Ceramics," Jour. Sci. Instruments, 34, No. 9, 337,(September, 1957).

16. Casimir, H. B. G., Smit, J., Enz, U., Fast, J. F., Wijn, H.P.J., Gorter, E. W., Duyvesteyn, A. J. W., Fast, J. D., and de Jong, J.J., "Report of Some Research in the Field of Magnetism at the Philips Laboratories," J. Phys. Radium, 20, No. 2-3, 360 - 373 (February, March, 1959) (In French).

17. Craik, D. J., and Griffiths, P. M., "Domain Configurations on Ferrites, " Proc. Phys. Soc. 73, Pt. 1, 1 - 13, (January, 1959).

18. Dixon, S., Jr., "High-Power Characteristics of Single-Crystal Ferrites with Planar Anisotropy," 7th Conference on Magnetism and Magnetic Materials, Phoenix, Arizona, (November, 1961). To be published.

19. du Pré, F. K., de Bitetto, D. J., and Brockman, F. G., "Magnetic Materials for Use at High Microwave Frequencies," J. Appl. Phys., Vol. 29, No. 7, 1127 - 1128, (July, 1958).

20. Fahlenbach, H., "Commercial Permanent Magnets, Particularly for Measuring Instruments I-II, " Arch. Tech. Messen., Issue No. 249, 237 - 240, (October) and Issue No. 250, 263 - 264, (November, 1956) (In German).

21. Fox, A. G., "Notes on Microwave Ferromagnetics Research," Proc. Instr. Elect. Engrs. B, Supplement No. 6, 371 - 378, 395 - 398, (October, 1956).

22. Fox, M., and Tebble, R. S., "The Demagnetizing Energy and Domain Structure of a Uniaxial Single Crystal," Proc. Phys. Soc., Vol. 72, Pt. 5, 765 - 770, (November, 1958).

23. Frei, E. H., Schieber, M., and Shtrikman, S., "Hexagonal Ferrimagnetic Compound Containing Fluorine," Phys. Rev. 118, No. 3, 657 (May 1, 1960).

24. Frei, E. H., Shtrikman, S., and Treves, D., "Method of Measuring the Distribution of the Easy Axes of Uniaxial Ferromagnets," J. Appl. Phys. 30, No. 3, 443 (March, 1959).

25. Geach, G. A., "The Theory of Sintering," Progress in Metal Physics, Vol. 4, 174 - 204 (Edited by B. Chalmers, London, Pergamon Press, 1953).

26. Giron, V. S., and Pauthenet, R., "The Field Dependence of the Magnetization of Uniaxial Substances; Application to $BaO \cdot 6Fe_2O_3$," Comp. rend. 248, No. 7, 943 - 946, (February 16, 1959).

27. Goodenough, J. B., "A Theory of Domain Creation and Coercive Force in Polycrystalline Ferromagnetics," Phys. Rev. 95, 917 - 932, (August 15, 1954).

28. Gordon, I., "Preparation and Properties of Ceramic Permanent Magnets," Am. Cer. Soc. - Bull., Vol. 35, No. 5, 173, (May, 1956).

29. Gorter, E. W., "Saturation Magnetization of Some Ferrimagnetic Oxides with Hexagonal Crystal Structures," Proc. Instr. Elect. Engrs., Vol. 104, Pt. B, Suppl. 5, 255 - 260 and 265 - 266, (1957).

30. Guillard, C., and Villers, G., "Effect of Al^{3+} Ions Substituted for Fe^{3+} Ions on the Magnetic Properties of the Compounds $6Fe_2O_3 \cdot BaO$, $6Fe_2O_3 \cdot SrO$, and $6Fe_2O_3 \cdot PbO$," C. R. Academy of Science (Paris), Vol. 242, No. 24, 2817 - 2820, (June 11, 1956) (In French).

31. Heimke, G., "Anomalous Magnetic Properties of Barium Ferrite as a Function of Sintering Temperature," Naturwissenschaften, Vol. 45, No. 11, 260 - 261, (1958) (In German).

32. Heimke, G., "Investigating the Temperature Dependence of the Magnetization of Magnetically Hard Ferrites," Ferromagnetism Working Party, Berlin (1959) p 213 - 221 (In German).

33. Heister, W., "Characteristic Properties of Magnetically Soft and Hard Ferrites and their Comparison with Known Metallic Magnetic Materials," VDE - Fachber 18, No. 5, V/6 - V/16, (1954) (In German).

34. Heister, W., and Fahlenbrach, H., "Oxydische Dauermagnete aus Bariumoxy und Eisen (III) - oxyl., "Archiv. fuer das Eisenhuettenwesen, Vol. 24, No. 11-12, 523 - 528, (November, December, 1953) (In German).

35. Hennig, G. R., "Applying Ceramic Permanent Magnets to Motor Design," Elec. Mfg., Vol. 60, No. 1, 100 - 105, (July, 1957).

36. Henry, W. E., "Magnetization Studies and Possible Magnetic Structure of Barium Ferrate III, " Phys. Rev. 112, No. 2, 326 - 327, (October 15, 1958).

37. Hrabak, J., "Some Properties of a Hard Ferrite Material," Slaboproudy Obzor, Vol. 17, No. 12, 711, (1956) (In Czech).

38. Iida, S., "Layer Structures of Magnetic Oxides," Jour. Phys. Soc. Japan, Vol. 12, No. 3, 222 - 233, (March, 1957).

39. Jonker, G. H., Wijn, H. P. J., and Braun, P. B., "Ferroxplana, Hexagonal Ferromagnetic Iron Oxide Compounds for Very High Frequencies," Philips Tech. Rev. 18, No. 6, 145 - 154, (1956-1957).

40. Jonker, G. H., Wijn, H. P. J., and Braun, P. B., "A New Class of Oxidic Ferromagnetic Materials with Hexagonal Crystal Structures," Proc. Instn. of Elect. Engrs., Vol. 104B, Suppl. 5, 249 - 254 and 265 - 266, (1957).

41. Jonker, G. H., "Ferrimagnetic Iron Oxide Compounds with Hexagonal Crystal Structure," Paper Presented in June, 1957 to 16th Congrès Intern. Chimie Pure et Appl., Paris.

42. Kojima, H., "Effects of Some Additionals for the Magnetic Properties of Ba and Sr Oxide Magnets," Sci. Rep. Res. Insts. Tohoku Univ. A, 10, No. 2, 175 - 182, (April, 1958).

43. Kostyanitsyn, Yu. B., "Magnetostriction of the Hexagonal System Ferromagnetics," Fiz. Metallov i Metallovedenie, 4, No. 2, 375 - 376 (1957) (In Russian).

44. Kozlowski, L., Kozlowski, Z., and Raxumowski, B., "Production of Barium Ferrite, Structure and Magnetic Properties," Przeglad electrotech, Vol. 31, No. 10 - 11, 610, (1955) (In Polish).

45. Kronenberg, K. J., and Bohlmann, M. A., "Long-Term Magnetic Stability of Alnico and Barium Ferrite Magnets," J. Appl. Phys. 31, No. 5, 82S - 84S, (May, 1960).

46. Kubota, B., and Okazaki, C., "Multipolarization in the Hexagonal Barium Iron Oxide Magnets," Note in Jour. Phys. Soc. Japan, 10, No. 8, 723, (August, 1955).

47. Lappa, R., "Powder Patterns on Monocyrstals of Ba $Fe_{12}O_{19}$," Prace Inst. Tele-i Radiotech, 3, 101 - 106, (1959) (In Polish).

48. Lilley, B. A., "Energies and Widths of Domain Boundaries in Ferromagnetics," Phil. Mag., 41, 792 - 813,(August, 1950).

49. Lotgering, F. K., "Topotactically Crystal-Oriented Ferromagnetics," Philips Tech. Rev. 20, No. 12, 354 - 356, (1958-1959).

50. Mason, W. P., "Derivation of Magnetostriction and Anisotropic Energies for Hexagonal, Tetragonal, and Orthorhombic Crystals," Phys. Rev. 96, No. 2, 302 - 310, (October 15, 1954).

51. McClure, J. W., "Axial Ratios in Hexagonal Crystals," Phys. Rev. 98, No. 2, 449 - 461, (April 15, 1955).

52. Mones, A. H., and Banks, E., "Cation Substitution in Ba $Fe_{12}O_{19}$," J. Phys. Chem. Solids, 4, No. 3, 217 - 222, (1958).

53. Morrish, A. H., and Watt, L. A. K., "Effect of the Interaction Between Magnetic Particles on the Critical Single Domain Size," Phys. Rev. 105, No. 5, 1476 - 1478, (March 1, 1957).

54. Morrison, C. A., and Karayianis, N., "Ferromagnetic Resonance in Uniaxial Polycrystalline Materials," J. Appl. Phys. 29, No.3, 339 - 340, (March, 1958).

55. Montague, B. W., "The Application of Ferroxdure to Television Focusing Magnets," Mullard Tech. Commun. 1, 39 - 43, (October, 1952).

56. Muller, H. G., "On the Theory of the Coercive Force of the Barium Ferrite Permanent Magnet Material Maniperm," Deutsch Elektrotech 9, No. 8, 286 - 290, (August, 1955) (In German).

57. Nagakura, M., and Yamaguchi, T., "Magnetic Domain Patterns on Barium Ferrites," Res. Rep. Fac. Engng Meiji Univ. (Japan), No. 13, 22- 26, (1959).

58. Néel, L., Pauthenet, R., Rimet, G., and Giron, V. S., "On the Laws of Magnetization of Ferromagnetic Single Crystals and Polycrystals Application to Uniaxial Compounds," J. Appl. Phys. 31, No. 5, 27S - 29S, (May, 1960).

59. Néel, L., "Crystal Structures and Magnetic Properties," Bull. Soc. Franc. Mineral. Crist. 77, 257 - 274, (January, March, 1954) (In French).

60. Paulus, M., "Elementary Domains on the (100) Faces of Nickel Ferrite Crystals and on the (0001) Face of Barium Ferrite Crystals," C. R. Academy of Science, Paris, Vol. 245, No. 25, 2227 - 2230, (December 16, 1957) (In French).

61. Pawlek, F., and Reichel, K., "Progress in Magnetic Materials and their Applications," A.E.G. Mitt., Vol. 46, No. 11 - 12, 339, (November, December, 1956) (In German).

62. Pearson, R. F., "Domain Patterns on Ferrite Single Crystals," Proc. Phys. Soc. B, Vol. 70, Part 4, 441, (April, 1957).

63. Rathenau, G. W., Smit, J., and Stuijts, A. L., "Ferromagnetic Properties of Hexagonal Iron Oxide Compounds with and without Preferred Orientations," Z. Phys., 133, 250, (1952).

64. Rathenau, G. W., "Saturation and Magnetization of Hexagonal Iron Oxide Compounds," Rev. Mod. Phys., 25, 297 - 301, (1953).

65. Rodrigue, G. P., Pippin, J. E., and Wallace, M. E., "Hexagonal Ferrites for Use at X- to V-Band Frequencies," 7th Conference on Magnetism and Magnetic Materials, Phoenix, Arizona, (November, 1961). To be published.

66. Rupprecht, J., and Heck, C., "Anisotropy of the Dielectric Properties of Oriented Barium Ferrite," Naturwissenschaften, 45, No. 21, 511, (1958).

67. Salpeter, J. L., "Developments in Sintered Magnetic Materials," Proc. IRE, Vol. 42, No. 3, 514, (March, 1954).

68. Schilpin, G., "Ferroxcube and Ferroxdure," Schweizer Archiv., Vol. 20, No. 2, 51 - 56, (February, 1954).

69. Schlömann, E., and Jones, R. V., "Ferromagnetic Resonance in Polycrystalline Ferrites with Hexagonal Crystal Structure," J. Appl. Phys., 30, No. 4, 177S - 178S, (April, 1959).

70. Schwabe, E., "The Temperature Dependence of the Magnetic Properties of Barium Ferrite," Z. Angew. Phys., Vol. 9, No. 4, 183 - 187, (April, 1957) (In German).

71. Sixtus, K. J., Kronenberg, K. J., and Tenzor, R. K., "Investigations on Barium Ferrite Magnets," Jour. Appl. Phys., 27, No. 9, 1051 - 1057, (September, 1956).

72. Smit, J. and Beljers, H. G., "Ferromagnetic Resonance Absorption in $BaFe_{12}O_{19}$, Highly Anisotropic Crystal," Philips Res. Rep., Vol. 10, No. 2, 113 - 130, (April, 1955).

73. Smit, J., Lotgering, F. K., and Enz, U., "Anisotropy Properties of Hexagonal Ferrimagnetic Oxides," J. Appl. Phys. 31, No. 5, 137S - 141S, (May, 1960).

74. Standly, K. J., "Ferromagnetic Resonance Phenomena at Microwave Frequencies," Sci. Progress, 38, 231 - 245, (April, 1950).

75. Stuijts, A. L. and Wijn, H. P. J., "Crystal-Oriented Ferroxplana," Philips Tech. Rev., Vol. 19, No. 7-8, 209 - 217, (1957-1958).

76. Stuijts, A. L., Rathenau, G. W., and Weber, G. H., "Ferroxdure II and III, Anisotropic Permanent Magnet Materials," Philips Tech. Rev., 16, No. 5-6, 141 - 147, (November, December, 1954).

77. Stuijts, A. L. and Haanstra, H. B., "Grain Growth in Ceramic Material Studied by Means of Electron Microscopy," Philips Gloeilampenfabrieken-Separaati, No. 2501, 671 - 699, (1957).

78. Stuijts, A. L., and Wijn, H. P. J., "Preparation and Properties of Crystal Oriented Ferroxplana Samples," J. Appl. Phys., Vol.29, No. 3, 468 - 469, (March, 1958).

79. Stuijts, A. L., "Sintering of Ceramic Permanent Magnet Material," Trans. of Brit. Cer. Soc., 55, 57, (January, 1956).

80. Stuijts, A. L., Rathenau, G. W., and Gorter, E. W., "Preferred Crystal Orientation in Ferromagnetic Ceramics," Letter in J. Appl. Phys., 23, 1282, (November, 1952).

81. Sucksmith, W., "Magnets and Magnetism - Recent Developments," Brit. Jour. Appl. Phys., Vol. 4, No. 9, 257 - 262, (September,1953).

82. Summergrad, R. N., and Banks, E., "New Hexagonal Ferrimagnetic Oxides," Phys. & Chem. of Solids, Vol. 2, No. 4, 312 - 317, (1957).

83. Tauber, A., Savage, R. O., Gambino, R., and Whinfrey, C., "Growth of Single-Crystal Hexagonal Ferrites Containing Zn," 7th Conference on Magnetism and Magnetic Materials, Phoenix, Arizona, (November, 1961). To be published.

84. Turner, E. H., "A Fast Ferrite Switch for use at 70 Kmc," IRE Trans. Mt & T, Vol. MTT-6, No. 3, 300, (July, 1958).

85. Tyahlikov, S. V., "The Quantum Theory of Magnetic Anisotropy," Jour. Exp. Theor. Phys. USSR, 20, 661 - 668, (July, 1950) (In Russian).

86. Van Uitert, L. G., "Magnetic Saturation and Coercive Force Data on Members of the Series $BaAl_xFe_{12-x}O_{19}$ and Related Oxides," J. Appl. Phys., Vol. 28, No. 3, 317, (March, 1957).

87. Van Uitert, L. G., Read, M. H., and Schnettler, F. J., "New Permanent Magnet Oxides," J. Appl. Phys. Vol. 28, No. 2, 280 - 281, (February, 1957).

88. Van Uitert, L. G., and Swanekamp, F. W., "Permanent Magnet Oxides Containing Divalent Metal Ions - II," J. Appl. Phys., Vol. 28, No. 4, 482, (April, 1957).

89. Verhoef, J. A., "The Focusing of Television Picture Tubes with Ferroxdure Magnets," Philips Tech. Rev., 15, 214 - 220, (January, 1954).

90. Verweel, J., "Fyische Eigenschappen van Ferromagnetische Oxydes," Ingenieur, Vol. 70, No. 2, 7 - 11, (January 10, 1958).

91. Weiss, M. T., and Dunn, F. A., "A 5 mm Resonance Isolator," IRE Trans. MT & T, Vol. MTT-6, No. 3, 331, (July, 1958).

92. Weiss, M. T., and Anderson, P. W., "Ferromagnetic Resonance in Ferroxdure," Phys. Rev., 98, No. 4, 925 - 926, (May 15, 1955).

93. Weiss, M. T., "The Behavior of Ferroxdure at Microwave Frequencies," IRE National Convention Record, Part 8, 95, (1955).

94. Went, J. J., Rathenau, G. W., Gorter, E. W., and Van Oosterhaut,G.W., "Ferroxdure, A Class of New Permanent Magnet Materials, " Philips Tech. Rev., 13, 194 - 208, (January, 1952).

95. Went, J. J., Rathenau, G. W., Gorter, E. W., and Van Oosterhaut,G.W., "Hexagonal Iron Oxide Powders as Permanent Magnet Materials," Letter in Phys. Rev., 86, 424, (May, 1952).

96. Wijn, H. P. J., "A New Method of Melting Ferromagnetic Crystal with High Crystal Anisotropy," Nature, (London), 170, 707, (1952).

97. Wijn, H. P. J., "Ferromagnetic Domain Walls in Ferroxdure," Physica, 19, 555 - 564, (July, 1953).

98. Wohlfarth, E. P., and Tonge, D. G., "Remanent Magnetization of Single Domain Ferromagnetic Particles," Phil. Mag., Vol. 2 (8th series), No. 23, 1333 - 1344, (November, 1957).

99. Yakovlev, E. N., "Calculation of the Magnetization of a Uniaxial Ferrite at Low Temperatures," Dokl. Akad. Nauk. USSR, Vol. 115, No. 4, 699 - 701, (1957) (In Russian).

100. "Calculation of the Force of Attraction of Disc and Rod-Shaped Ferroxdure Magnets," Matronics, No. 10, 173 - 180, (January, 1956).

101. "The Application of Ferroxdure for Premagnetizing Cores in Power Carrying Coils," Matronics, No. 9, 153 - 160, (June, 1955).

102. "Ignition Coils with Ferroxcube and Ferroxdure," Matronics, No. 9, 161 - 164, (June, 1955).

103. "Calculation of the Force of Attraction of Magnets of Ferroxdure Ceramic Material in the Form of Discs and Cylinders," Cienc. y. Téc., Vol. 124, 35 - 48, (August, 1957) (In Spanish).

104. "Ferrite Permanent Magnets," Cer. Age, Vol. 68, No. 4, 28 - 32, (October, 1956).

105. "Ceramic Magnet Production at Stackpole Carbon," Cer. Age, Vol. 72, No. 2, 22 - 26 and 46, (August, 1958).

106. "Oriented Crystals: Their Growth and Their Effects on Magnetic Properties," Gen. Elec. Rev., 53, 16 - 21, (August, 1950).

APPENDIX I

ORIENTING FIELDS

As discussed in Subsection C. 4, orienting fields of the order of $.707H_{an}$ (or $\frac{\sqrt{2}\,K_1}{M}$) were employed, where H_a and $\frac{K_1}{M}$ are values appropriate to the sample in preparation. It is the anisotropy field which permits crystallite orientation, and in fact the orienting torque per unit volume exerted on an individual crystallite is given by:

$$T_o = \frac{\delta f_k}{\delta \theta} \quad , \tag{I-1}$$

where T_o is the orienting torque,

θ is the angle between the direction of magnetization and the preferred axis of the crystal (c-axis for uniaxial materials),

and f_k is the anisotropy energy.

To first order this anisotropy energy is given by

$$f_k = K_1 \sin^2\theta \, . \tag{I-2}$$

Hence the torque is

$$T_o = 2K_1 \sin\theta\cos\theta = K_1 \sin 2\theta \, . \tag{I-3}$$

Thus the orienting torque varies directly with K_1 and is a maximum when $\theta = \pi/4$. Now the total magnetic energy will be given by

$$E = -MH_{ap}\cos(\phi - \theta) + K_1 \sin^2\theta, \tag{I-4}$$

where H_{ap} is the applied dc field and ϕ is the direction between the c-axis and the field (see Figure I-1). It is assumed that each crystallite is a single domain particle. The optimum orienting field is that value of H_{ap} that will cause M to be at $\theta = \pi/4$ and hence will exert a maximum orienting torque. We can find the equilibrium position of M by setting $\delta E/\delta\theta = 0$ thus,

$$\delta E/\delta\theta = -MH\sin(\phi - \theta) + 2K_1 \sin\theta\cos\theta = 0, \qquad (I\text{-}5)$$

or,

$$H = \frac{\frac{K_1}{M}\sin 2\theta}{\sin(\phi - \theta)} \quad . \qquad (I\text{-}6)$$

In a sample of material to be oriented the crystallites will have all possible orientations $0 \leq \phi \leq \pi$. (Either direction along a c-axis can, of course, be no further than $\pi/2$ from H_{ap}. The magnetization will, however, remain along a particular c direction until sufficient external field is applied to rotate the M vector through the hard direction. Thus we must consider ϕ as ranging up to $\phi = \pi$.) The problem then is to find the optimum orienting field, or the orienting field that will produce a maximum torque on all crystallites. This value will obviously vary from crystallite to crystallite depending on the value of ϕ for the particular crystallite. We have found (see equation (I-3)) that maximum torque is exerted when $\theta = \pi/4$ and in fact varies with θ as shown in Figure I-2. Thus for maximum torque on those crystallites with $\phi > \pi/4$ we can solve for the optimum orienting field as a function of ϕ, assuming $\theta = \pi/4$ (for maximum orienting torque). Thus we find:

$$H_{op} = \frac{K_1}{M} \quad \frac{1}{\sin(\phi - \pi/4)} \qquad (I\text{-}7)$$

This expression is plotted graphically in Figure I-3. For ϕ less than $\pi/4$ there is no optimum orienting field, and the bigger the better. For values of ϕ near $\pi/2$, however, an optimum field exists by virtue of the fact that if sufficiently large fields are applied, the magnetization vector may be rotated with respect to the c-axis to such an extent that $\theta = \pi/2$, and in this case no orienting torque is exerted (see Figure I-2).

The most reasonable orienting procedure is to initially apply an orienting field of approximately $H_a/\sqrt{2}$, thus exerting powerful torques on those crystallites whose c-axes lie far from the direction of the applied field. This field then presumably rotates these crystallites into approximate alignment. The field can next be raised to as high a value as possible to more precisely orient all crystallites. The sample is pressed while under the influence of this high field. All fields discussed here are internal fields, and demagnetizing factors appropriate to the shape being pressed should be taken into account when considering external applied fields.

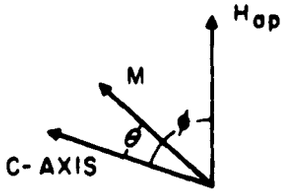

Figure I-1 Geometric Arrangement Considered in Deriving Optimum Orienting Field

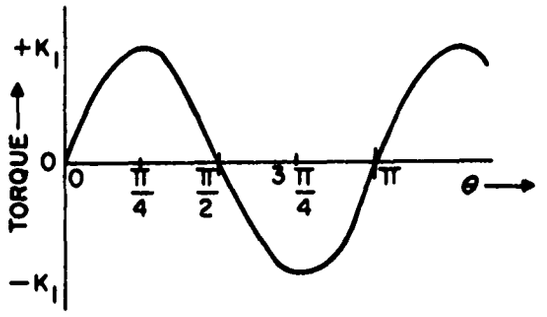

Figure I-2. Variation of Orienting Torque with Angle Between Magnetization and H_{ap}

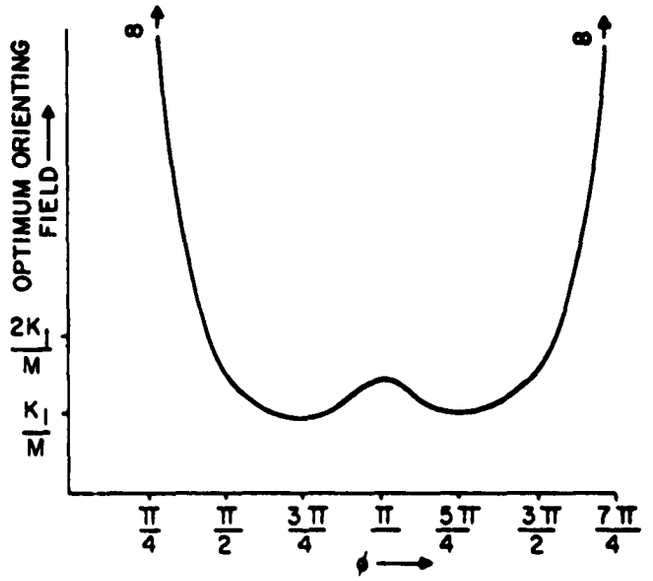

Figure I-3. Variation of Optimum Orienting Field with Angle between c-axis and H_{ap}